

**Apoptosis is a natural stimulus of IL-6R shedding
and contributes to the proinflammatory trans-
signalling function of neutrophils**

Dissertation
zur Erlangung des Doktorgrades
der Mathematisch-Naturwissenschaftlichen Fakultät
der Christian-Albrechts-Universität
zu Kiel

vorgelegt von

Athena Chalaris

Kiel, 2007

Referent: Prof. Dr. Rose-John

Korreferent: Prof. Dr. Roeder

Korreferent: Prof. Dr. Laskay

Tag der mündlichen Prüfung:

Zum Druck genehmigt:

Der Dekan

Table of Contents

1.	INTRODUCTION.....	1
1.1	The multifunctional cytokine IL-6	1
1.2	IL-6 type cytokine mediated signal transduction	2
1.3	The IL-6R.....	5
1.4	The soluble IL-6R in chronic inflammatory diseases.....	7
1.5	Generation of the soluble IL-6R.....	9
1.6	The tumor necrosis factor- α converting enzyme (TACE)	10
1.7	Apoptosis	13
2	AIM OF THIS STUDY	17
3	MATERIAL AND METHODS	18
3.1	Materials.....	18
3.1.1	Chemicals	18
3.1.2	Solutions and buffers	19
3.1.3	Bacterial media	23
3.1.4	Bacterial strains and cell lines	23
3.1.5	Cell culture growth media	24
3.1.6	Molecular weight markers.....	25
3.1.7	Plasmids	25
3.1.8	Primary Antibodies	26
3.1.9	Secondary antibody.....	29
3.1.10	Recombinant cytokines	29
3.2	Methods.....	30
3.2.1	Molecular biology.....	30
3.2.2	Protein-biochemical methods	34
3.2.3	Cell culture	36
3.2.4	Enzyme-linked immunosorbent assay (ELISA).....	39
3.2.5	Fluorescence-activated cell sorting (FACS)	40
3.2.6	Murine air pouch model of acute inflammation	41
3.2.7	Intraperitoneal injection	42
3.2.8	Statistical analysis.....	43
3.2.9	Animal treatment	43
3.2.10	Purification of antibody against the extracellular part of the human IL-6R.....	43
4	RESULTS	44

4.1	Production and purification of two monoclonal antibodies, raised against the ectodomain of the human IL-6R.....	44
4.2	The chemotherapeutic drug doxorubicin induces apoptosis in Ba/F3 [gp130/IL-6R] cells.....	46
4.3	Soluble IL-6R release during doxorubicin induced apoptosis of Ba/F3 [gp130/IL-6R] cells.....	49
4.4	Shedding of the IL-6R from the cell surface of apoptotic Ba/F3 [gp130/IL-6R] cells.	51
4.5	Shedding of the IL-6R during apoptosis is mediated by the metalloprotease TACE (ADAM17)	51
4.6	Ba/F3 [gp130/IL-6R] cells undergo apoptosis after cytokine deprivation	54
4.7	Shedding of the IL-6R after cytokine deprivation of Ba/F3 [gp130/IL-6R] cells.....	55
4.8	Extrinsic apoptotic pathways induced by Fas stimulation led to IL-6R shedding	57
4.9	Overexpression of dominant-negative ADAM17 suppresses IL-6R shedding during PMA stimulation and apoptosis.....	59
4.10	ADAM17 activation during apoptosis is caspase dependent.....	63
4.11	Apoptosis induced IL-6R shedding is PKC-, MAPK- and ROS-independent.....	64
4.12	IL-6R shedding is not required to terminate IL-6 induced STAT3 phosphorylation during apoptosis.....	69
4.13	Soluble IL-6R was released from apoptotic primary human neutrophils	71
4.14	The murine air pouch model of acute inflammation	75
4.15	Injection of neutralizing IL-6R antibodies led to impaired monocyte infiltration in the inflamed air pouch.....	77
4.16	“Trans-signalling” rather than “classic signalling” is important for monocytic infiltration into the inflamed air pouch	79
4.17	Leukocyte recruitment during acute inflammation in IL-6-deficient mice.....	81
5	DISCUSSION	84
5.1	Molecular basis of ADAM 17 activation during apoptosis	84
5.2	The physiologic role of IL-6R shedding during apoptosis	88
5.3	IL-6R shedding during neutrophil apoptosis: Implication during acute inflammation.....	90
5.4	Outlook	94

6	SUMMARY	95
7	ZUSAMMENFASSUNG	97
8	REFERENCES.....	99
9	APPENDIX.....	118
9.1	Vector maps.....	118
9.2	Oligonucleotides.....	119
9.3	Accession numbers	119
9.4	Abbreviations	120
9.5	Publications	125
9.6	Curriculum vitae	126

1 Introduction

1.1 The multifunctional cytokine IL-6

The pleiotropic cytokine Interleukin 6 (IL-6) was molecularly cloned in 1986 (1) and was originally identified as an antigen-nonspecific B-cell differentiation factor that activates B-cells to produce immunoglobulins (2). Today it is known that IL-6 provides a wide range of biological activities in immune regulation and it is secreted by various lymphoid cell types, such as T-cells, B-cells, macrophages and monocytes (3). Possessing autocrine, paracrine, and endocrine functions, it acts as a major regulator of the hepatic acute phase response by stimulating hepatocytes to produce C-reactive protein, fibrinogen and serum amyloid A (4). It induces growth of T-cells and differentiation of cytotoxic T-cells by enhancing the expression of IL-2 receptor and the production of IL-2 (5); further IL-6 induces differentiation of macrophages (6) and megakaryocytes (7). In addition, circulating IL-6 together with tumor necrosis factor α (TNF- α) and interleukin-1 (IL-1) cause fever and leukocytosis which is beneficial for pathogen elimination (8, 9).

Due to its potent ability to activate host immune response after infection, IL-6 expression is tightly regulated and the protein is almost not expressed under normal conditions. It is commonly produced at local tissue sites and is released in almost all situations of homeostatic perturbation, which include acute infection, trauma and endotoxaemia. IL-6 can also become chronically elevated, resulting in the prolonged activation of its biological activities. This dysregulation in IL-6 levels can then turn the initially beneficial responses into deleterious conditions.

Apart from lymphoid cells, IL-6 is produced also by various types of nonlymphoid cells, such as fibroblasts, keratinocytes, endothelial cells and several tumor cells (3). For instance, it has been shown that IL-6 levels are increased in the serum of patients suffering from colon carcinoma (10, 11). In addition, IL-6 has been identified as a growth factor for multiple myeloma cells (12) and renal cell carcinoma cells (13).

Generation of IL-6 deficient mice has been achieved by the insertion of a neomycin-resistance gene into the first coding exon of the IL-6 gene. Homozygous IL-6 knockout mice develop normally but show a severely compromised acute phase response after tissue damage or infection. They are impaired in controlling infection with facultative intracellular bacteria like *Listeria monocytogenes* and show compromised T-cell dependent antibody response (14).

Furthermore, IL-6 knockout mice are completely protected from collagen-induced arthritis, a mouse model for arthritis (15) and they are resistant to experimental autoimmune encephalomyelitis (EAE) induced by immunization with myelin oligodendrocyte glycoprotein (MOG), an animal model for the demyelinating disease multiple sclerosis (16). Taken together, the phenotype of the IL-6 knockout mice highlights that IL-6 is an important cytokine involved in regulation of host response after infection and that dysregulation of IL-6 contributes to several pathological conditions in various diseases like arthritis or multiple sclerosis.

1.2 IL-6 type cytokine mediated signal transduction

Apart from IL-6, the IL-6 family comprises IL-11, viral IL-6, IL-27, IL-31, neuropoietin (NP), ciliary neurotrophic factor (CNTF), cardiotrophin-1 (CT-1), oncostatin M (OSM), leukaemia inhibitory factor (LIF) and cardiotrophin-like cytokine (CLC), which all share the common signal transducer glycoprotein 130 (gp130) as part of their receptor complexes (17). All IL-6 type cytokines belong to the long chain four α -helix bundle class of proteins, consisting of four long α -helices termed A, B, C and D, which are arranged in an up-up-down-down topology (18). Each of the IL-6 type cytokines is characterized by a certain profile of receptor recruitment that in all cases involves at least one molecule of gp130. IL-6, IL-11 and CNTF first bind specifically to their nontransducing co-receptor, called α -chain, which leads to the recruitment and dimerization of the signalling subunits gp130 and LIFR β (19). IL-6 and IL-11 recruit two gp130 subunits and CNTF recruit one gp130 and one LIF receptor (LIFR β) subunit. LIF, CT-1, IL-27, IL-31, viral-IL-6 and OSM can directly interact with their signalling receptor subunits without requiring an α -receptor (20-22). The cytokine CLC can only bind to the signal transducing subunits in the presence of an additional soluble cytokine receptor. CLC first binds to the soluble CNTFR (sCNTFR) or to the cytokine-like factor-1 (CLF-1) which leads then to recruitment of one gp130 subunit and one LIFR β subunit (23, 24). Dimerization of the signal transducing chains gp130, LIFR β , WSX-1, gp130 like receptor (GPL) and OSM receptor (OSMR) brings the receptor associated tyrosine kinases, which belong to the Janus kinase (JAK) family, into close proximity leading to activation via inter- or intramolecular phosphorylation (25). There are six tyrosine residues in the intracellular part of human gp130 and at least five of the six cytoplasmic tyrosines are phosphorylated by the JAK kinases. Phosphorylation of the four distal tyrosines leads to recruitment and activation of the signal transducer and activator of transcription (STAT)

proteins (26). To-date, seven mammalian STAT genes have been cloned and it is described that in response to IL-6 there is potent activation of STAT3 and to a minor extent activation of STAT1 (27, 28). Immediately after tyrosine phosphorylation, STATs form homo- and heterodimers and translocate to the nucleus where they recognise DNA binding sites in the promoter of their target genes (29). STAT3 DNA binding sites were shown, for example in the promoters of acute phase genes, such as C-reactive protein (30), α_1 -antichymotrypsin (31), and lipopolysaccharide-binding protein (32), and in the promoters of transcription factors, such as Jun B (33), c-Fos (34), interferon regulatory factor-1 (IRF-1) (35) and CCAAT enhancer binding protein δ (C/ERB δ) (36).

In most systems the activation of STATs is transient. Inactivation of STATs is mediated by different pathways. One pathway is dephosphorylation of activated STATs by protein-phosphatases. It was shown that activated STAT1 molecules promptly enter the nucleus and later return quantitatively to the cytoplasm as non-phosphorylated molecules (37). Recently a protein inhibitor of activated STAT3, named PIAS3, has been discovered in various human tissues. PIAS3 co-immunoprecipitates with tyrosine-phosphorylated STAT3 and blocks DNA-binding as well as gene activation of activated STAT3 (38). Another mechanism to down-regulate the STAT pathway has been discovered with the cloning and identification of suppressor of cytokine signalling (SOCS) proteins. These proteins represent negative-feedback inhibitors, since their transcription is induced by IL-6 and LIF and since they inhibit tyrosine phosphorylation of gp130, STAT1 and STAT3 by directly interacting with the JAK kinases (39, 40).

In addition to the JAK-STAT signal transduction pathway, it is known that the Ras mitogen-activated protein (MAP) kinase pathway is also activated after IL-6 type cytokine stimulation. It has been shown that the Src homology protein 2 tyrosine phosphatase-2 (SHP-2) binds to phosphotyrosine-759 of gp130 (41) and leads via direct interaction with the adaptor protein growth factor receptor bound protein 2 (Grb2) to further activation of the Ras-Raf-MAPK pathway (42).

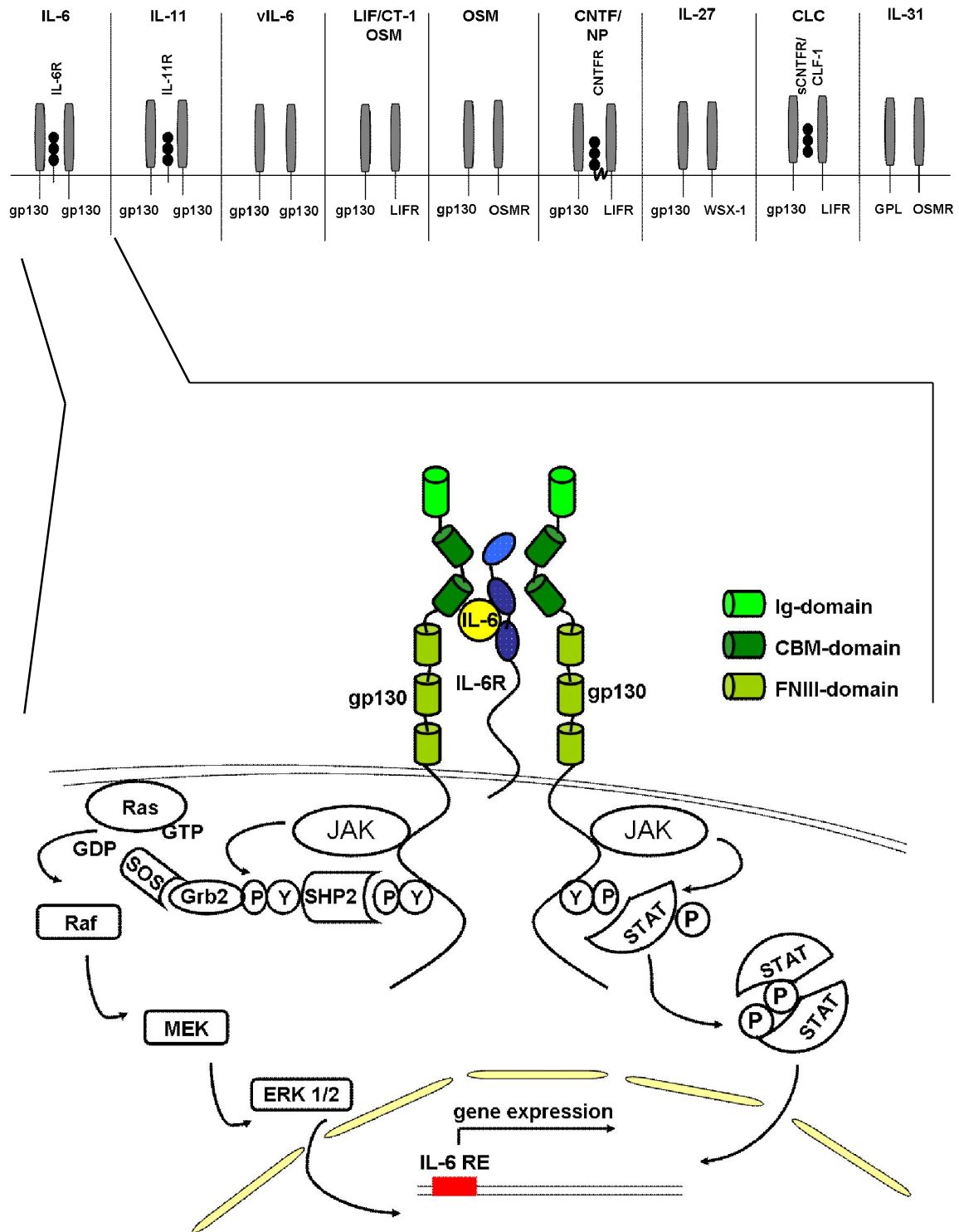


Figure 1: IL-6 family of cytokines and representation of the two major signal transduction pathways activated by IL-6.

OSM signals via a gp130 and LIFR β heterodimer or via a gp130 and OSMR heterodimer. Note: CNTFR is linked to the plasma membrane via a GPI-anchor.

Abbreviations: FNIII: fibronectin type III, CBM: cytokine binding module (modified FNIII-domains), Ig: immunoglobulin, IL-6 RE: interleukin-6 response element.

1.3 The IL-6R

The receptor complex mediating the biological activities of IL-6 consists of an 80 kDa IL-6 binding glycoprotein termed IL-6 receptor- α (IL-6R) and the signal transducer gp130. The high affinity complex of [IL-6/IL-6R] interacts on target cells with at least two molecules of gp130 and leads to activation of signal transduction pathways (Figure 1). Gp130 is ubiquitously expressed on all cell types whereas the expression of the type-I-transmembrane protein IL-6R is restricted to some lymphoid cells like monocytes, macrophages, neutrophils, B-cells, subpopulations of T-cells and non-lymphoid cells like hepatocytes (43). The expression pattern of the IL-6R determines which cell types are responsive to the cytokine IL-6, because cells that only express gp130 are unable to respond to IL-6.

The extracellular part of the IL-6R consists of one immunoglobulin-like domain (Ig-like domain) and two modified fibronectin-type III domains (FNIII-domains) which carry the cytokine binding motif tryptophan-serine-X-tryptophan-serine (W-S-X-S-W) and a set of four conserved tyrosine residues (44). IL-6 binding occurs between the two FNIII-domains whereas the Ig-like domain does not participate in cytokine binding. The FNIII-domains are followed by a long flexible stalk region, a transmembrane domain and a short intracellular domain which does not participate in signal transduction. Although the cytoplasmic part of the IL-6R is dispensable for receptor complex formation, it contains a tyrosine-based and a dileucine-type motif, which directs sorting of the IL-6R to the basolateral membrane of polarized cells (45).

Beyond the membrane bound IL-6R form there are also two soluble isoforms of this receptor detectable in several body fluids, which lack the cytoplasmic and transmembrane domains. These isoforms are generated by two distinct mechanisms involving both posttranscriptional and posttranslational processes (46). Soluble IL-6R (sIL-6R) was detected in the plasma of healthy individuals at concentrations about 25-35 ng/ml (47). The sIL-6R can bind to its ligand IL-6 with comparable affinity as the membrane-bound isoform (48, 49). The complex of [IL-6/sIL-6R] associates with gp130 and activates target cells which do not express the IL-6R. In contrast to other soluble receptors, such as the receptors for IL-1 or TNF- α , which are known to inhibit the effects of their ligands (50), sIL-6R acts agonistically on cells that express gp130. Activation of cells that only express gp130 *via* the [IL-6/sIL-6R] complex is called trans-signalling (50, 51) whereas activation of cells *via* the membrane-bound IL-6R in complex with IL-6 is called classic signalling (Figure 2).

The soluble IL-6R is generated by alternative splicing and ectodomain shedding. The differential mRNA splicing product codes for a reading frame shift and leads to the generation of a novel carboxy (COOH)- terminal protein sequence (GSRRRGSCGL), which has no influence on the biological properties of the sIL-6R in terms of ligand binding (52). Alternative spliced soluble cytokine receptors are described for many membrane-anchored proteins, like the LIFR, the epidermal growth factor (EGF) receptor and the CNTFR (50). Interestingly the second component of the IL-6 receptor complex, gp130, exists also in a soluble form (sgp130). Soluble gp130 is generated by alternative splicing (53) and there are relatively high circulating levels of sgp130 detectable in human blood (100-400ng/ml) (54). Since sgp130 binds the complex of [IL-6/sIL-6R] it has been concluded that this soluble cytokine receptor is a natural inhibitor of IL-6 trans-signalling (49, 55, 56).

Additionally, the soluble form of the IL-6R can also be produced by limited proteolysis of the membrane-anchored IL-6R resulting in the release of the ectodomain in the extracellular space and a short C-terminal fragment (CTF) remaining in the plasma membrane (53). The enzymes which are involved in the limited proteolysis of the IL-6R belong to the “A Disintegrin And Metalloproteinase Domain” (ADAM) family of metalloproteases. ADAM proteases are membrane anchored but also found as soluble proteins, and are characterized by the presence of a Zn²⁺- protease domain (57). Limited proteolysis of transmembrane proteins is also termed “shedding” and is a very important mechanism regulating and modulating cell signalling events mediated for example by TNF- α , IL-1R, L-Selectin, cadherins and amyloid precursor protein (APP) (58, 59).

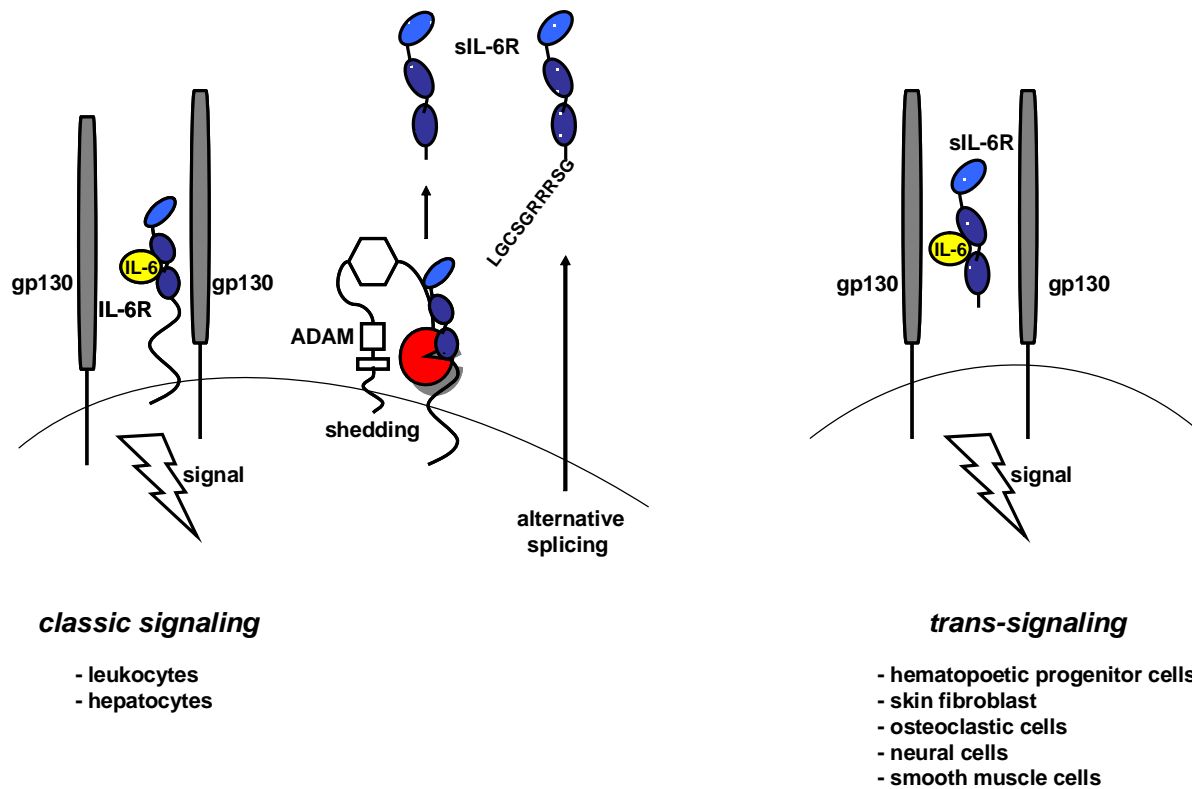


Figure 2: Classic signalling versus trans-signalling.

Cells that express both gp130 and the IL-6R are responsive to IL-6 (classic signalling). Cells that express only gp130 can be activated by the complex of [IL-6/sIL-6R]. Activation of such cells is termed trans-signalling. There are two mechanisms involved in sIL-6R generation. The soluble IL-6R can be generated by proteolytic cleavage. Members of the ADAM-protease family are involved in shedding of the IL-6R. Differential splicing leads to two distinct IL-6R mRNA transcripts: one encodes for the soluble IL-6R and the other for the membrane-anchored protein. Note: alternative splicing leads to a unique COOH-terminal sequence [GSRRRGSCGL].

1.4 The soluble IL-6R in chronic inflammatory diseases

The soluble isoforms of the IL-6R can be generated by alternative splicing or by proteolytic cleavage of the membrane-bound precursor from cells expressing the cognate receptor (Figure 2). There are several studies in which levels of the soluble IL-6R were measured during pathological conditions and in many cases there is a direct correlation between severity of the disease and elevated sIL-6R levels. Further, it has been shown that IL-6 trans-signalling rather than IL-6 classic signalling (60) is involved in the pathogenesis as well as in the persistence of these diseases.

Rheumatoid arthritis (RA) and juvenile rheumatoid arthritis (JRA) are inflammatory diseases characterized by destruction of bones and cartilage of affected joints mediated by dysregulation of inflammatory cytokines (61). IL-6 is one of these cytokines and its overproduction appears to be responsible for many clinical symptoms in RA. During RA there are not only elevated levels of the cytokine IL-6 detectable but also significant higher amounts of the sIL-6R (62, 63). Examination of IL-6 and sIL-6R concentrations in synovial fluid from arthritic patients showed that the extent of joint destruction correlates with the increased concentration of both proteins (64). Treatment of RA patients with a neutralizing humanized anti-IL-6R antibody leads to significant reduced disease symptoms like decreased serum CRP and fibrinogen levels and reduced thrombocytosis and hypoalbuminemia (65). Although the cellular origin of sIL-6R in arthritis remains unknown, it is assumed that sIL-6R is released by proteolytical cleavage from activated leukocytes, which infiltrate the joints (66).

Multiple myeloma is a malignant disorder caused by uncontrolled proliferation of plasma cells; patients suffering from this disease, show significantly elevated sIL-6R serum levels (67, 68). Again, the severity stage of multiple myeloma appears to correlate with circulating sIL-6R levels (69) and there are reports that physiological concentrations of sIL-6R increase the sensitivity of myeloma cells to IL-6 (70).

Crohn's disease (CD) is a chronic inflammatory condition of the gastrointestinal tract, where it has been shown that type-1 T-helper cells (TH₁-cells) are involved in disease manifestation. IL-6 trans-signalling contributes to CD by preventing T-cell apoptosis and elevated concentrations of both IL-6 and sIL-6R have been measured in patients suffering from this disease. IL-6 in combination with the sIL-6R leads to activation of STAT3 signalling and the upregulation of the anti-apoptotic proteins Bcl-2 and Bcl-X_L in mucosal T-cells (71). A neutralizing antibody against the IL-6R suppresses CD in various animal models by inducing apoptosis of lamina propria T-cells (72).

To determine the role of the sIL-6R *in vivo*, transgenic mice were constructed expressing either human IL-6 alone or together with human soluble IL-6R. Due to the observation that murine IL-6 is unable to bind the human IL-6R, trans-signalling mediated by the human soluble IL-6R is only taking place in the double transgenic mice (73). The phenotype of the IL-6/sIL-6R transgenic mice revealed increased hepatic and splenic hematopoiesis, hepatocellular hyperplasia and plasma cell proliferation. Major findings were also that transgenic expression of the sIL-6R makes animals more sensitive to the cytokine IL-6 and that the plasma half-life of IL-6 is significantly prolonged (74).

1.5 Generation of the soluble IL-6R

Although under several pathological conditions elevated levels of the sIL-6R have been described (75), there is still little understanding about the regulation of sIL-6R release. In many cases it is unclear whether the impact of the sIL-6R in various diseases depends on locally or systemic elevated sIL-6R levels.

Soluble IL-6R can be released from the cell surface by proteolytical cleavage of the membrane-anchored precursor protein. This process is referred to as “shedding”. Shedding of the IL-6R is strongly induced by phorbol ester e.g. PMA which are known to activate protein kinase C (PKC) (76). Shedding is completely inhibited in the presence of hydroxamic-acid based inhibitors, which potently inhibit metalloproteases. The IL-6R is a substrate of the metalloprotease ADAM10, which appears to be responsible for the constitutive shedding, and for ADAM17 also referred to as tumor necrosis factor- α converting enzyme (TACE), which is involved in stimulated shedding (77).

Besides of phorbol esters, there are also other stimuli described, which lead to enhanced ectodomain shedding of the IL-6R. It has been shown that the acute-phase protein CRP induces shedding of the IL-6R resulting in a threefold increase in sIL-6R levels after 30 to 60 minutes exposure on human neutrophils. Although, alternative mRNA splicing was excluded as mechanism involved in sIL-6R production after CRP stimulation, hydroxamate compounds had also only a minor effect suggesting that other proteases are involved in this process. Thus, CRP acts not only as an acute-phase reactant, but it contributes to formation of the agonistic sIL-6R/IL-6 complex (78). Indeed, CRP levels in several diseases have been found to correlate with those of sIL-6R (69). Interestingly, a study on the human osteoblast-like cell line MG63 revealed that the proinflammatory cytokines IL-1 β and TNF- α induce IL-6R shedding. This effect was not influenced by cycloheximide excluding de-novo protein synthesis but was markedly inhibited by hydroxamate compounds and transfection of TACE siRNA (79). Thus, not only the inflammatory mediator CRP has the potential to influence sIL-6R release but also IL-1 β and TNF- α , indicating that both cytokines are likely to increase sIL-6R levels *in vivo* which could lead to osteoclast-like cell formation in inflammatory conditions like rheumatoid arthritis.

Except of inflammatory mediators it was also shown that bacterial proteins have an impact on IL-6R shedding. The pore forming bacterial toxins Streptolysin O (SLO) and Hemolysin A (HlyA), which disturb membrane lipid asymmetry, were found to induce massive shedding of

IL-6R from transfected Cos-7 cells and human macrophages. Toxin-induced shedding was not sensitive to the PKC inhibitor staurosporin but was prevented by the hydroxamate TAPI (80). Interestingly, alteration of the plasma membrane composition by cellular cholesterol depletion also leads to enhanced IL-6R shedding. Again this stimulation was PKC-independent but hydroxamate sensitive (77).

The IL-6R is not only a target substrate for membrane-anchored metalloproteases belonging to the ADAM-family, but can also be cleaved by bacterial secreted proteases. Serralysins are metalloproteases, which are secreted by various pathogenic bacteria. Interestingly, *Serratia marcescens* metalloprotease (SMP) was found to release biological active sIL-6R from human monocytes. That effect was inhibitable with TAPI. The study revealed that the bacterial protease, cleaved the IL-6R at a site distinct from that utilized by the endogenous proteases (81). Further, it was demonstrated, that proteases belonging to the serine-family contribute to shedding of the IL-6R. Activated neutrophils, which infiltrate the site of tissue destruction, secrete high amounts of the serine proteases elastase and cathepsin G and it was shown that elastase is involved in sIL-2R release whereas cathepsin G selectively used the IL-6R as a substrate (82).

1.6 The tumor necrosis factor- α converting enzyme (TACE)

TACE was characterized and cloned in 1997 and was identified as the secretase responsible for releasing pro-TNF- α from the cell membrane (83, 84). Since then, the understanding of TACE biology has grown steadily and today many substrates for this protease have been identified. Among them are proteins, which play a pivotal role in cell development, differentiation, immune regulation and adhesion (Table 1).

Development and differentiation	Immune system	Other
TGF α (85)	pro-TNF- α (83)	APP (99)
EGF/HB-EGF (86)	TNFR1/II (92)	PrP ^c (100)
amphiregulin (87)	L-seectin (93)	MUC1 (101)
neuregulins (88)	IL-6R (77, 94)	Collagen XVII (102)
TrkA (89)	fractalkine (95)	
GHR (90)	IL-1RII (96)	
Notch (91)	M-CSF-R (97)	
	IL-15R (98)	

Table 1: TACE substrates.

Abbreviations: APP: amyloid precursor protein, EGF: epidermal growth factor, HB-EGF: heparin-binding EGF-like growth factor, GHR: growth hormone receptor, IL: interleukin, MUC1: mucin1, M-CSF-R: macrophage-colony stimulating factor-receptor, PrP^c: cellular prion protein, TGF: transforming growth factor, TNF: tumor necrosis factor, TrkA: neurothrophic tyrosine kinase type 1, TNFR: TNF receptor. Adopted from (103).

TACE belongs to a superfamily of zinc dependent proteases known as metzincins. Based on sequence and structural similarities, metzincins are grouped in four distinct subfamilies: the astacins, the matrix metalloproteinases (MMPs), the adamalysins (snake venom metalloproteinases and ADAMs) and the serralysins (bacterial proteases) (104). ADAMs are a family of metalloproteases with high sequence homology to the snake venom metalloproteinases (SVMPs) (105). The term ADAM stands for *A Disintegrin And Metalloproteinase*, which represents two key structural domains of this molecule. ADAMs are type-I transmembrane-proteins, which contain a prodomain as well as metalloprotease, disintegrin, cysteine-rich, EGF-like and cytoplasmic tail domains. ADAM17 (TACE), ADAM9 and ADAM10 (Kuzbanian) mediate the shedding of cell surface molecules and are called sheddases (106).

TACE is synthesized as a zymogen with the prodomain acting as an inhibitor of the protease activity *via* the cysteine switch mechanism. The free cysteine residue located in the prodomain coordinates with the zinc in the active site of the protease and prevents enzymatic activity (83). During TACE maturation the prodomain is removed. The furin cleavage site (R-V-K-R) localized between the pro and the catalytic domain is responsible for the generation of biologically active TACE (Figure 3). The metalloprotease domain contains the zinc-binding consensus motif H-E-X-G-H-X-X-G-X-X-H-D (104) involved in coordinating zinc with histidine residues and creating the active site of the enzyme. The function of the disintegrin, EGF-like and cysteine-rich domain of TACE is not well determined. The

cytoplasmic tail is likely to be a target for kinases because it contains putative MAPK-, PKC-, and casein kinaseII phosphorylation sites (107, 108).

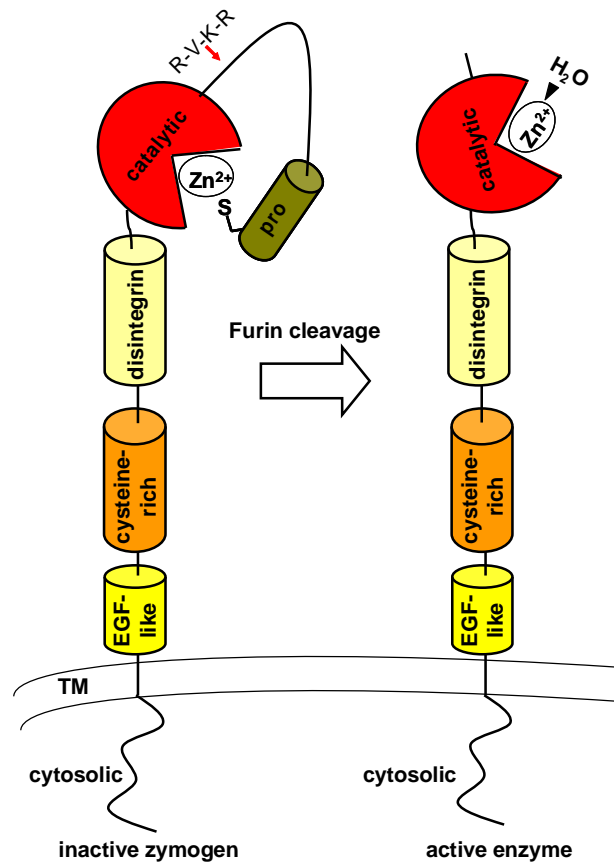


Figure 3: Schematic representation of the domain architecture of the ADAM metalloproteases.

All known ADAMs are expressed as inactive (latent) zymogens and require cleavage of a propeptide domain for activation. This propeptide contains a well-conserved cysteine which is involved in Zn^{2+} coordination and is responsible for the latency of the enzyme. After cleavage of the prodomain at the furin cleavage site (R-V-K-R), H_2O as the fourth ligand in Zn^{2+} coordination is recruited to the catalytic core and the enzyme is now present in its active form. Abbreviations: EGF: epidermal growth factor, S: sulfur, TM: transmembrane.

Although TACE is an important protein with various biological functions, which is underlined by the prematured death of mice lacking TACE activity ($TACE^{\Delta Zinc/\Delta Zinc}$ mice (83)) the activation mechanism of this enzyme remains largely unknown. Shedding of TACE substrates can be stimulated by PMA, a non-physiological stimulator of PKC indicating that phosphorylation of the cytoplasmic tail of TACE by PKC may be a potential regulatory mechanism. There are also studies, which show that activation of the MAP kinase pathway

leads to TACE activation by direct association and phosphorylation of the Erk kinase with the cytoplasmic domain of TACE (108). However, it has also been shown that a truncated TACE-construct lacking the whole cytoplasmic domain retains the ability to induce phorbol ester-stimulated shedding of various substrates suggesting that the cytoplasmic domain is dispensable for TACE activation (92).

In several studies it was demonstrated that cross-talk between G protein-coupled receptor (GPCR) and epidermal growth factor receptor (EGFR) requires TACE mediated cleavage of EGF-like growth factor precursors. TACE is involved in the cleavage of amphiregulin, HB-EGF, Epigen, Epiregulin and TGF α . (86). A recent study provides evidence that downstream activation of the PI3-kinase by GPCRs leads to recruitment of PDK1 to the plasma membrane where PDK1 binds and phosphorylates the cytoplasmic domain of TACE. This phosphorylation event leads to subsequent activation of TACE, which results in EGF-ligand precursors cleavage and EGFR activation (109). Further, it was shown that nitric oxide and reactive oxygen species (ROS) were involved in TACE activation. The proposed mechanism was that these compounds lead to oxidation of the cysteine, which is located in the inhibitory prodomain of TACE and participates in zinc coordination thereby resulting in releasing the active form of the enzyme (110). Interestingly, studies involving L-selectin shedding on human neutrophils demonstrate that some non-steroidal anti-inflammatory drugs (NSAIDs) are involved in TACE activation. Importantly, only NSAIDs, which had the potential to decrease cellular ATP levels induce L-selectin shedding, which leads to the hypothesis that TACE activation is prevented by an ATP-dependent mechanism (111). Recently it was shown that ADAM metalloproteases are activated during staurosporin- or camptothecin-induced apoptosis of epithelial cells thereby releasing the ectodomain of the cell adhesion molecule E-cadherin (112). However, the molecular mechanism leading to ADAM activation during apoptosis remains elusive.

1.7 Apoptosis

Apoptosis defines the programmed cell death, a process by which a cell dies in a regulated and organized fashion (113). As important as cell division, regulated cell death allows the organism to tightly control cell numbers and tissue size and to clear abnormal cells. Apoptosis is characterized by dramatic morphological and biochemical changes, which were distinct from the features observed in cells undergoing pathological, necrotic cell death (114). The typical features of cells dying apoptotically comprise nuclear condensation, intranucleosomal

DNA fragmentation, membrane blebbing, compaction of cytoplasmic organelles, decrease in cell volume and loss of plasma membrane phosphatidylserine (PS) asymmetry (115). PS externalization serves as a specific recruitment signal for phagocyte docking and subsequent engulfment and degradation of the apoptotic cell, preventing an inflammatory response (116).

Most of the morphological changes observed during programmed cell death are initiated by cysteine proteases that are activated specifically in apoptotic cells. These death proteases act as central executioners of the apoptotic pathway and are part of a large protein family known as the caspases (117). All known caspases possess an active-site cysteine and cleave substrates after an aspartic acid residue (Asp-X-X-X). However, the substrate specificity of different caspases is determined by the four residues amino-terminal to the cleavage site (118).

Caspases are highly conserved through evolution, and can be found from humans, to insects, nematodes and hydra (119, 120). Eliminating caspase activity, either through mutation or the use of small pharmacological inhibitors, has been shown to slow down or even prevent apoptosis (121).

As many enzymes, caspases are expressed constitutively as inert zymogens and consist of three domains: an amino-terminal prodomain, and the p20 and p10 domains. Both, the p10 and p20 domains, are found in the mature enzyme and in all caspases examined so far, the catalytic active enzyme is a heterotetramer containing two p20/p10 heterodimers (122). Most caspases are activated by proteolytic cleavage of the zymogen between the p20 and p10 domains and usually also between the prodomain and the p20 domain. Caspases are released in their active form by different mechanisms involving proteolytic cleavage of the zymogen, by previously activated caspase molecules, by autocatalytic cleavage or by association with regulating protein cofactors (122).

Initiator caspases are the first to be activated during programmed cell death and include caspase-2, -8, -9 and -10. These cleave and activate the effector caspases-3, -6 and -7, which are responsible for the digestion of many cytosolic and nuclear key proteins, such as the nuclear enzyme poly (ADPribose) polymerase (PARP), histone H1, lamin B, actin, fodrin, PKC δ and retinoblastoma protein (Rb). Cleavage of the effector caspase substrates leads finally to all typical biochemical and morphological changes observed in apoptotic cells (123-128).

Caspase activation during apoptosis occurs *via* two major pathways. The extrinsic pathway involves the binding of death ligands to cell surface receptors (e.g. CD95/Fas receptor or TNF receptor), which leads to recruitment of adaptor molecules and to formation of a death

inducing signalling complex (DISC) at the plasma membrane (129). Formation of the DISC leads to recruitment, oligomerization and activation of pro-caspase-8 by autocatalytic cleavage. Once activated, caspase-8 cleaves and activates the effector caspases, thereby inducing the cell death program.

The intrinsic pathway is initiated through the release of cytochrome *c* from the intermembrane space of mitochondria in response to apoptotic stimuli diverse as DNA-damage, UV irradiation or cytokine deprivation (130). Once translocated to the cytosol, cytochrome *c* binds to apoptosis protease activating factor-1 (APAF-1) and in the presence of ATP facilitates APAF-1 oligomerization and the recruitment of pro-caspase-9 (131). The formation of this caspase-activating complex is termed the apoptosome. Once bound to the apoptosome, caspase-9 is activated, and subsequently triggers a cascade of effector caspase activation and proteolysis, leading to apoptotic cell death (132).

Besides the caspases as major executioners, the family members of the Bcl-2 proteins represent the major regulatory molecules of programmed cell death. The cell death-regulating activity of the Bcl-2 proteins depend on their ability to modulate mitochondrial functions by regulating the release of pro-apoptotic factors like cytochrome *c* (133-135). Bcl-2 family members are divided into pro- and anti-apoptotic molecules. The family of pro-apoptotic Bcl-2 molecules comprises Bax, Bak, Bnip3, Nix/Bnip3L, Bid, Noxa, Puma and Bad whereas the family of anti-apoptotic molecules is smaller and comprises Bcl-X_L, Mcl-1, and Bcl-2 (136). Most of the Bcl-2 family members contain a transmembrane domain at their COOH-terminus, which is important for their targeting to intracellular membranes. Anti- and pro-apoptotic Bcl-2 proteins can be found in the cytosol, endoplasmic reticulum, mitochondria and nuclear envelope (137-139). The pro-apoptotic activity of Bcl-2 proteins is regulated by transcription and/or posttranslational modification. For example, Noxa and Puma are under p53-mediated transcriptional control and are upregulated in response to DNA-damage (140). Phosphorylated Bad is sequestered by 14-3-3 proteins under normal conditions, and growth factor deprivation leads to Bad dephosphorylation and activation (141). Bid is subjected to proteolytic cleavage by caspase-8, granzymeB or calpain and truncated Bid (tBid) translocates to the mitochondria, resulting in energetic failure and release of pro-apoptotic factors (142-144). The pro-apoptotic Bcl-2 protein Bax is localized under normal conditions in the cytosol. In response to death stimuli Bax undergoes a conformational change that triggers its translocation to and insertion into the outer mitochondrial membrane. This leads to permeabilization of the mitochondrial membrane and release of pro-apoptotic proteins. Bax function has been reported to be directly inhibited by Bcl-X_L and Mcl-1 (145). In contrast Bak

is always localized in the mitochondrial membrane as an integral protein and is maintained in an inactive conformation by anti-apoptotic Bcl-2 family proteins or by the type2 voltage-dependent anion channel (VDAC) (146, 147).

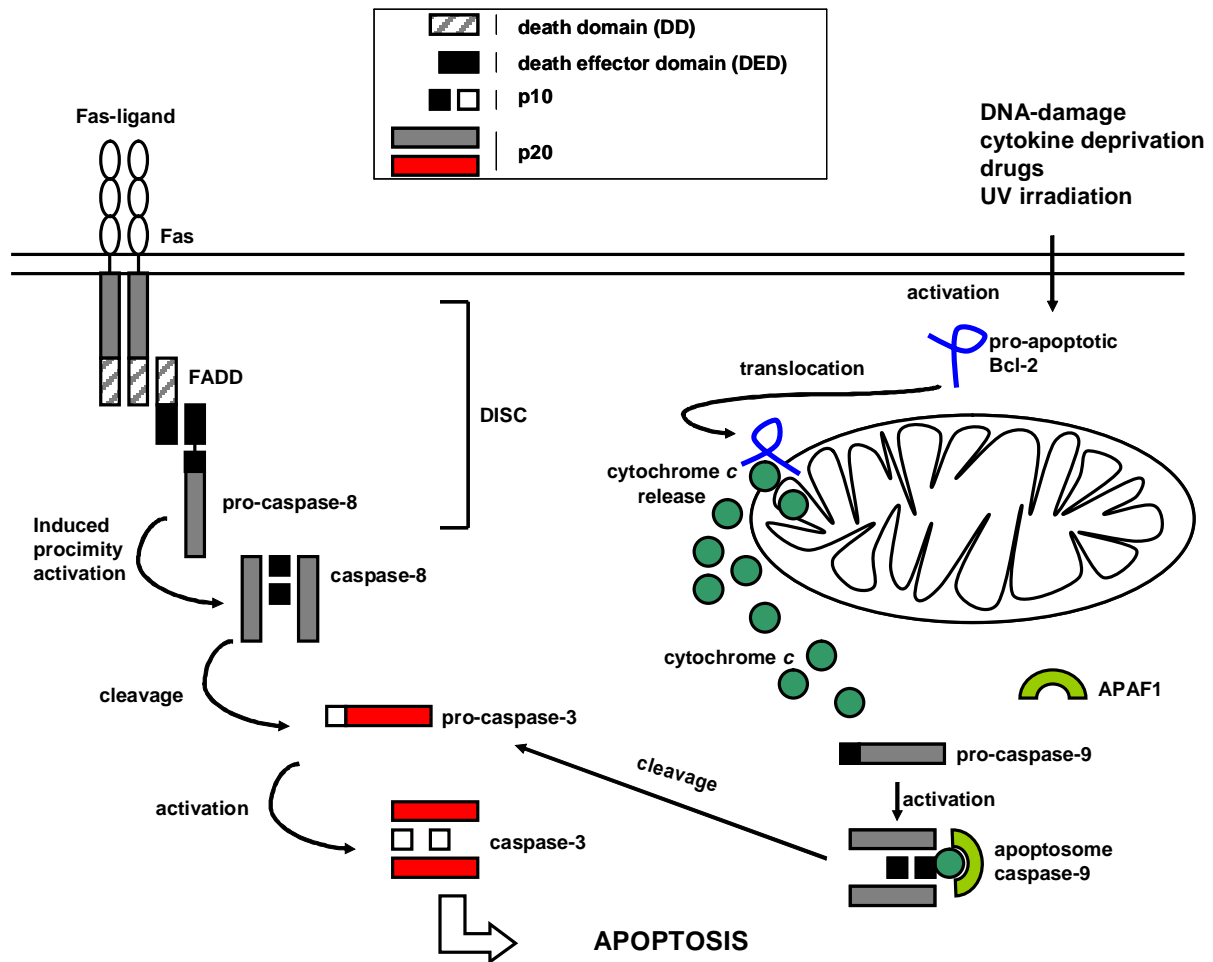


Figure 4: Intrinsic and extrinsic apoptotic pathways.

The death receptor pathway is triggered by members of the death receptor superfamily such as Fas and TNFR1. Binding of Fas-ligand (FasL) to Fas induces receptor clustering and formation of a death inducing signalling complex (DISC). This complex recruits, *via* the adaptor molecule FADD, multiple pro-caspase-8 molecules, resulting in caspase-8 activation through induced proximity. The intrinsic (mitochondrial) pathway is activated in response to different stimuli, such as DNA-damage and cytokine deprivation and leads to activation of pro-apoptotic members of the Bcl-2 family. Apoptotic signals activate the Bcl-2 proteins through proteolysis, dephosphorylation and several other mechanisms and target them to the mitochondria where they induce cytochrome *c* release.

2 Aim of this study

The soluble form of the IL-6R is generated by alternative splicing or by limited proteolysis (shedding). Importantly, elevated levels of soluble IL-6R were detected in body fluids of rheumatoid arthritis, multiple myeloma and Crohn's disease patients. Ectodomain shedding of the IL-6R can occur in a constitutive fashion mediated by ADAM10 activity or can be stimulated. Although the major protease, which is involved in stimulated IL-6R shedding was identified as ADAM17 (TACE), little is known about the physiological stimuli leading to generation of the sIL-6R during normal and pathological conditions. Unphysiologic activators of IL-6R ectodomain shedding are phorbol ester and cholesterol depleting agents, such as methyl- β -cyclodextrin.

The aim of this study was to identify physiologic stimuli leading to IL-6R shedding. Comparison of already described stimuli leading to generation of sIL-6R, like bacterial toxins, PKC activation and translocation to the plasma membrane, cholesterol depletion, and CRP-treatment, revealed that all of them trigger membrane alterations or perturbation. During apoptosis drastic membrane changes occur when phosphatidylserine is exposed to the exterior of the plasma membrane. Therefore it was reasonable to argue that apoptosis-induced membrane alterations might also lead to an induction of ectodomain shedding of the IL-6R.

To investigate if apoptosis is a natural stimulus of IL-6R shedding, intrinsic apoptotic pathways were induced in Ba/F3 [gp130/IL-6R] cells by doxorubicin treatment or cytokine deprivation. Moreover, extrinsic apoptosis was induced in the hepatocellular cell line HepG2 by Fas ligation. Studies on human neutrophils, which have been shown to express the IL-6R, should clarify if apoptosis-induced IL-6R shedding is promoted on primary cells and if the sIL-6R generated during programmed cell death facilitates IL-6 trans-signalling *in vivo*.

3 Material and Methods

3.1 Material

3.1.1 Chemicals

All chemicals were obtained from the following companies in p.a. quality:

Company	Chemicals
CarlRoth (Karlsruhe, Germany), Sigma-Aldrich (Deisenhofen, Germany), Merck (Darmstadt, Germany) Serva (Heidelberg, Germany)	buffer components
Sigma-Aldrich (Deisenhofen, Germany)	Doxorubicin, diphenyleiodonium chloride (DPI, NADPH-oxidase inhibitor), GF10920X (pan-PKC inhibitor), Gö6976 (Ca ²⁺ -dependent PKC inhibitor), cycloheximide, streptavidin coupled-agarose beads, SB202190 (p38-MAPK inhibitor), U0126 (Erk-MAPK inhibitor), 1,3-dimethyl-2-thiourea (DMTU, ROS-scavenger) and <i>n</i> -propyl-galleate (nPG, ROS-scavenger)
Calbiochem (Schwalbach am Taunus, Germany)	TAPI-2 (metalloprotease inhibitor), PMA, z-LEHD-FMK (caspase-9 inhibitor)
Bachem (Weil am Rein, Germany)	z-VAD-FMK (pan-caspase inhibitor), z-DEDV-FMK (caspase-3 inhibitor), z-IETD-FMK (caspase-8 inhibitor)
Glaxo-Smith Kline (Stevenage, United Kingdom)	GI254023X (ADAM10-inhibitor), GW280264X (ADAM10 and ADAM17 inhibitor), marimastat (metalloprotease inhibitor)

Restriction enzymes, molecular weight markers, Taq-polymerase, Pfu-Polymerase, T4-DNA-Ligase, Calf Intestine Alkaline Phosphatase (CIAP) and Reverse Transcriptase were obtained

from MBI Fermentas (St. Leon-Rot, Germany). Oligonucleotides were ordered from Metabion (München, Germany). All oligonucleotides used are listed in the appendix. Cell culture material was ordered from Sarstedt (Nürnbrecht, Germany). Cell culture media, Trypsin, FCS, L-glutamin and Penicillin/Streptomycin were obtained from PAA Laboratories (Pasching, Austria).

3.1.2 Solutions and buffers

Annexin V-binding buffer (FACS)	10 140 2.5 0.05	mM mM mM % (w/v)	HEPES, pH 7.4 NaCl CaCl ₂ Na ₃ Na
Blocking buffer (Western blot)	6	%	milk powder or BSA in TBS-T
Blotting buffer (Western blot)	25 192 20	mM mM % (v/v)	Tris-HCl, pH 8.3 glycine methanol
DNA-sample buffer (5x) (DNA-gels)	20 0.025	% (w/v) % (w/v)	glycerol in TBE buffer bromphenol blue
Destaining solution (protein gels)	10 40	% (v/v) % (v/v)	acetic acid methanol
Elution buffer (antibody purification)	0.5	M	glycine, pH 3.0

Material and Methods

FACS buffer	1	% (w/v)	BSA in PBS
<i>(FACS)</i>	0.05	% (w/v)	Na ₃ Na
Hypotonic lysis buffer	42	mM	KCl
<i>(cell lysis)</i>	10	mM	HEPES pH 7.4
	5	mM	MgCl ₂
	1	x	protease inhibitors
Lysis buffer	150	mM	NaCl
<i>(cell lysis)</i>	2	mM	EDTA
	50	mM	Tris-HCl, pH 7.4
	1	% (w/v)	Triton X-100
	1	% (w/v)	NP-40
	1	mM	Na ₃ VO ₄
	1	mM	NaF
	1	x	protease inhibitors
Neutralizing buffer	1	M	Tris-HCl, pH 11
<i>(antibody purification)</i>			
Phosphate buffered saline	150	mM	NaCl
<i>(PBS)</i>	8	mM	Na ₂ HPO ₄ , pH 7.4
	1.7	mM	NaH ₂ PO ₄ , pH 7.4
PBS-T	0.05	% (v/v)	Tween-20 in PBS

Material and Methods

Protease-inhibitors	COMPLETE™ pills, Roche (Mannheim, Germany). Resuspending 1 pill in 2 ml PBS results in a 25x stock solution		
Running gel 10 % (8 %) (<i>protein gels</i>)	7.74 ml (4.5 ml)		deionized water
	5.1 ml (5.1 ml)		1.5 M Tris, pH 8.8
	0.2 ml (0.2 ml)		10 % SDS
	6.6 ml (9.9 ml)		30 % Acrylamide-Bis 29:1
	200 µl (200 µl)		10 % APS
	20 µl (20 µl)		TEMED
S1 Buffer (<i>Miniprep</i>)	50 mM		Tris-HCl, pH 8.0
	10 mM		EDTA
	100 µg/ml		RNaseA
S2 Buffer (<i>Miniprep</i>)	200 mM		NaOH
	1 %		SDS
S3 Buffer (<i>Miniprep</i>)	2.8 M		KAc, pH 5.1
Sample-buffer (5X) (<i>protein-gels</i>)	10 % (w/v)		SDS
	5 % (w/v)		β-mercaptoethanol
	50 % (w/v)		glycerol
	0.13 % (w/v)		bromphenol blue
	312 mM		Tris-HCl, pH 6.8

Material and Methods

Sample-buffer (2x)	4	% (w/v)	SDS
<i>(protein-gels)</i>	20	% (w/v)	glycerol
	5	% (v/v)	β -mercaptoethanol
	0.13	% (w/v)	bromphenol blue
	125	mM	Tris-HCl, pH 6.8
SDS running buffer	25	mM	Tris-HCl, pH 8.3
<i>(protein-gels)</i>	192	mM	glycine
	0.1	% (w/v)	SDS
Stacking gel (4 %)	3.72	ml	deionized water
<i>(protein gels)</i>	0.625	ml	0.5 M Tris-HCl, pH 6.8
	0.05	ml	10 % SDS
	0.67	ml	30 % Acrylamid-Bis 29:1
	25	μ l	10 % APS
	7	μ l	TEMED
Coomassie staining solution	40	% (v/v)	ethanol
<i>(protein gels)</i>	10	% (v/v)	acetic acid
	0.1	% (w/v)	coomassie R250
Stripping solution	0.5	M	NaCl
<i>(Western blot)</i>	0.5	M	acetic acid
TBE (0.5x)	44.5	mM	boric-acid
<i>(agarose-gels)</i>	10	mM	EDTA, pH 8.0
	44.5	mM	Tris-HCl

Tris buffered saline (TBS)	10 mM	Tris-HCl, pH 8.0
	150 mM	NaCl

TBS-T	1 % (v/v)	Tween-20 in TBS
-------	-----------	-----------------

3.1.3 Bacterial media

LB-medium	10 g/l	Bacto-tryptone
	10 g/l	NaCl
	5 g/l	yeast extract

LB-agar	20 g/l	agar in LB-medium
---------	--------	-------------------

Media were autoclaved and 100 mg/l ampicillin or 25 mg/l kanamycin were supplemented prior to use.

3.1.4 Bacterial strains and cell lines

Ba/F3	murine peripheral blood pre-B-cell line (IL-3 dependent)
-------	--

Ba/F3 [gp130]	murine pre-B-cell line stably transfected with the human cDNA encoding gp130 (IL-3 or HIL-6 dependent) (148)
---------------	--

Ba/F3 [gp130/IL-6R]	murine pre-B-cell line stably transfected with the human cDNAs encoding gp130 and IL-6R (IL-3 or IL-6 dependent) (149)
---------------------	--

HepG2	human hepatocellular carcinoma cell line
-------	--

COS-7	African green monkey (<i>Cercopithecus aethiops</i>) kidney fibroblast-like cell line transformed with an origin defective mutant of SV40 which codes for wild type T antigen
Hybridoma [4-11]	fusion cell line of primary murine B-cells with the murine myelom cell line P3X63-Ag 8 635
Hybridoma [14-18]	fusion cell line of primary murine B-cells with the murine myelom cell line P3X63-Ag 8 635
<i>Escherichia coli</i> XL1-Blue	Stratagene
<i>Escherichia coli</i> DH5 α	Stratagene

3.1.5 Cell culture growth media

Ba/F 3 [gp130] medium	Dulbecco MEM (DMEM), high glucose (4.5g/l) supplemented with 10 % (v/v) fetal calf serum (FCS) 50 U/ml penicilline/streptomycine 10 ng/ml recombinant HIL-6
Ba/F 3 [gp130/IL-6R] medium	Dulbecco MEM (DMEM), high glucose (4.5g/l) supplemented with 10 % (v/v) fetal calf serum (FCS) 50 U/ml penicilline/streptomycine 10 ng/ml recombinant human IL-6
HepG2/COS-7 medium	Dulbecco MEM (DMEM), high glucose (4.5g/l) supplemented with 10 % (v/v) fetal calf serum (FCS) 50 U/ml penicilline/streptomycine

Hybridoma [4-11]/[14-18] medium	RPMI 1640 supplemented with
	10 % (v/v) fetal calf serum (FCS)
	200 mM L-glutamin
	50 U/ml penicilline/streptomycin
	0.07 % β -mercaptoethanol
	10 % conditioned J774-supernatant

Blood peripheral granulocyte medium	RPMI 1640 supplemented with
	10 % (v/v) fetal calf serum (FCS)
	200 mM L-glutamine
	50 μ M β -mercaptoethanol
	100 mM HEPES
	50 U/ml penicilline/streptomycin

3.1.6 Molecular weight markers

1kb DNA ladder	14 bands within the range from 150-10,000 bp (MBI Fermentas)
----------------	--

Protein ladder	5 μ l of the <i>Prestained Protein Molecular Weight Marker</i> (MBI Fermentas) were loaded on the SDS-PAGE gel. 5 bands within the range from 25-180 kDa
----------------	--

3.1.7 Plasmids

pESK	Donor vector (Gateway system); kanamycin-resistance
------	---

p409b	Mammalian expression vector for transfection; ampicilline-resistance
-------	--

pEGFP-N1 Mammalian expression plasmid encoding for the enhanced green fluorescent protein; kanamycin-resistance (Clontech)

3.1.8 Primary Antibodies

anti-c-myc mouse monoclonal antibody clone 9E10. Raised against the epitope EQKLISEEDLN.

Application:

IB: 10 % conditioned hybridoma supernatant (6 % milk powder in TBS)

anti-TACE rabbit polyclonal antibody derived from a peptide consisting of the C-terminus of TACE (Chemicon).

Application:

IB: dilution 1:5,000 (6 % milk powder in TBS)

anti-IL-6R (6.2) rabbit polyclonal antibody recognizing the extracellular stalk-region of the human IL-6R (150).

Application:

IP: dilution 1:1,000 (6 % milk powder in TBS)

anti-IL-6R (M-91) mouse monoclonal antibody raised against the extracellular part of the human IL-6R (Immunotech).

Application:

FACS: dilution 1:500 (FACS-buffer)

anti-IL-6R (14-18) mouse monoclonal antibody raised against the extracellular part of the human IL-6R (this work).

Application:

IB: dilution 1:5,000 (6 % milk powder in TBS)

- anti-caspase-3 rabbit polyclonal antibody raised against the residues surrounding the cleavage site of human caspase-3 (Cell signalling).
Application:
IB: dilution 1:2,000 (6 % milk powder in TBS-T)
- anti-PARP: rabbit monoclonal antibody which detects full-length PARP and the large fragment (89 kDa) produced by caspase cleavage (Cell signalling).
Application:
IB: dilution 1:2,000 (6 % milk powder in TBS-T)
- anti-PKC δ (C-20) rabbit polyclonal antibody raised against the C-terminus of human PKC δ (Santa Cruz).
Application:
IB: dilution 1:1,000 (6 % milk powder in TBS)
- anti- β -actin mouse monoclonal antibody raised against the N-terminus of β -actin (AC-15): (abCAM).
Application:
IB: dilution 1:5,000 (6 % milk powder in TBS)
- anti-STAT3: mouse monoclonal antibody which detects endogenous levels of total STAT3 protein (Cell Signalling).
Application:
IB: 1:2,000 (6 % milk powder in TBS-T)

- anti-Phospho-STAT3 rabbit monoclonal antibody which detects endogenous levels of STAT3 only when phosphoryated at tyrosine 705 (Cell signalling).
Application:
IB: 1:2,000 (6 % BSA in TBS-T)
- anti-Fas:
(CH-11) mouse monoclonal antibody (IgM) recognizing the human cell surface antigen Fas (Upstate).
Application:
Induction of apoptosis in HepG2 cells (25-100 ng/ml)
- anti-mIL-6R:
(D7715A7) rat monoclonal antibody raised against the extracellular part of the murine IL-6R (Biozol).
Application:
In vivo receptor blocking: 100 µg were injected intraperitoneally (i.p.) in C57Bl/6 mice
- anti-mIL-6R:
(MR-16-1) rat anti-mouse monoclonal antibody raised against the extracellular part of the murine IL-6R (Shugai pharmaceutical, kindly provided by Dr. M. Neurath).
Application:
In vivo receptor blocking: 100 µg were injected intraperitoneally (i.p.) in C57Bl/6 mice
- anti-Ly6G/Ly6C-:
FITC rat monoclonal antibody which reacts with a common epitope on Ly-6G and Ly-6C, previously known as the myeloid differentiation antigen Gr-1. The antibody recognizes granulocytes (neutrophils and eosinophils) and monocytes (BD Pharmingen).
Application:
FACS: 1:400 (FACS-buffer)

anti-F4/80-APC: rat monoclonal antibody which reacts with the mouse F4/80 antigen, a macrophage-restricted cell surface glycoprotein (CALTAG Laboratories/Invitrogen).

Application:

FACS: 1:400 (FACS-buffer)

3.1.9 Secondary antibody

All horseradish-coupled secondary antibodies were purchased from Amersham Bioscience (Buckinghamshire, United Kingdom) and used in a dilution of 1:10,000.

For fluorescence-activated cell sorting (FACS) analysis, the allophycocyanin-conjugated secondary antibody was obtained from Jackson Immuno Research Laboratories/Dianova (Hamburg, Germany) and used in a dilution of 1:100.

3.1.10 Recombinant cytokines

human IL-6 prepared and purified as described in (151).

Hyper-IL-6 The fusion protein of the human IL-6 and the human IL-6R, Hyper-IL-6 ; prepared and purified as described in (152).

sgp130-Fc kindly provided by Steffi Schnell (Biochemical Department, University of Kiel); was prepared and purified as described in (73).

3.2 Methods

3.2.1 Molecular biology

3.2.1.1 Transformation of bacteria

To 100 μ l competent *E.coli* XL1-*Blue* or DH5 α either 50-100 ng of plasmid DNA or 20 μ l of ligation mixture were added and incubated for 3 min on ice. After a heat shock (1 min, 42°C) an successive incubation on ice (3 min), 800 μ l of LB-medium were added to the bacteria and incubated at 37°C for 60 min. Cells were then centrifuged (6,000 x g, 1 min) and the supernatant removed. Cells were resuspendet in 100 μ l LB-medium and plated on LB-agar plates containing the appropriate antibiotics. Plates were incubated at 37°C overnight.

3.2.1.2 Plasmid isolation from 2 ml *E. coli* cultures (Minipreps, (153))

2 ml LB-medium supplemented with the appropriate antibiotic was inoculated with a single colony and incubated over night at 37°C with constant agitation. Cultures were pelleted by centrifugation (6,000 x g, 1 min) and resuspended in 100 μ l Buffer S1. For bacterial lysis the suspension was supplemented with 100 μ l Buffer S2 and incubated for 2-3 min at room temperature. Subsequent 100 μ l of Buffer S3 was added and the mixture was inverted until a homogenous suspension containing a white flocculate was formed. The bacterial lysate was cleared by centrifugation (16,000 x g, 15 min, and 4°C) and the resulting supernatant was transferred to a new reaction tube and supplemented with 900 μ l ice cold 100 % ethanol. After an incubation time of 30 min at -20°C the plasmid DNA was precipitated by centrifugation (16,000 x g, 15 min, 4°C) and washed once with ice cold 70 % ethanol. The DNA pellet was dried at room temperature for 30 min at 50°C and dissolved in 50 μ l Tris-HCl (10 mM, pH 8.0).

3.2.1.3 Plasmid isolation from 100 ml *E. coli* cultures (Midiprep)

For preparation of large quantities of DNA, the Macherey-Nagel Nucleo Bond Midiprep kit was used. A single colony was inoculated in 2 ml LB-medium and grown at 37°C for 8 hours with constant agitation. Afterwards, this culture was added to 100 ml LB-medium supplemented with the appropriate antibiotic and incubated at 37°C with constant agitation

over night. The culture was transferred into a 50 ml Falcon tube and the cells were pelleted by centrifugation (4,000 x g, 15 min, 4°C). The plasmid was isolated from the bacteria according to the manufactures protocol. Finally the DNA pellet was resuspended in 200 µl Tris-HCl (10 mM, pH 8.0) and the DNA concentration was determined.

3.2.1.4 Digestion of DNA (153)

For restriction, the DNA was incubated with an appropriate amount of restriction enzymes in the recommended buffer for 2-3 hours at 37°C. Restriction was terminated by addition of DNA sample buffer and applied on a agarose gel. If two enzymes were incompatible with each other, the DNA was digested successively with the enzymes. The DNA was purified between the two digestions using the PCR purification kit (Qiagen).

3.2.1.5 Dephosphorylation of Plasmid-DNA (154)

After enzymatic restriction the plasmid-DNA was dephosphorylated by directly addition of 1 U Calf Intestinal Alkaline Phosphatase (CIAP) to the restriction reaction. The dephosphorylation was carried out at 37 °C for 60 min.

3.2.1.6 Ligation of DNA-fragments

Ligation of DNA fragments was performed by mixing 50 ng vector with the five-fold molar excess of insert DNA. The DNA fragments were supplemented with 1 µl T4-ligase (MBI, Fermentas), 2 µl ligation buffer (10x) and were filled up to a final volume of 20 µl. The reaction was incubated for 1 hour at room temperature and was used directly for transformation in competent *E.coli* bacteria.

3.2.1.7 Polymerase chain reaction (PCR)

For amplification of the DNA fragment encoding the dominant negative variant of ADAM17 the PCR was performed in a 50 µl reaction mix in Stratagene PCR-cycler (Robocycler Gradient 96). The enzymes Taq-polymerase as well as Pfu-Polymerase and the appropriate buffers were obtained from MBI Fermentas. The following reaction mixture was used :

Template	2-10	ng
Forward-primer	10	pmol (appendix)
Reverse-primer	10	pmol (appendix)
Nucleotides (dNTPs)	10	mM each
PCR-buffer (10x)	5	μ l
Pfu/Taq-polymerase	1	U
ddH ₂ O	add	50 μ l

The PCR was performed with the following step gradient :

95°C	2 min		initial denaturation step
95°C	30 sec	} x35	denaturation
50°C	30 sec		primer annealing
72°C	1 min		elongation (1 min/1kb)
72°C	5 min		final elongation step

3.2.1.8 RT-PCR

RT-PCR is a PCR amplification of a product from the reverse transcription (RT) reaction, whereby a template mRNA is translated into a single-stranded cDNA. RevertAid M-MuLV Reverse Transcriptase from Fermentas was employed according to the manufacturer's instructions. The reactions were performed using oligo(dT) primer targeting the 3' poly(A) mRNA tail. The PCR settings were described above. The following reaction mixture was used:

RNA	2	μ g
Oligo (dT)	0.5	μ g
ddH ₂ O	5	μ l

The mixture was heated at 70°C for 5 min and then chilled on ice. The following components were added:

reaction buffer (5x)	4	µl
dNTPs	20	mM each
RevertAid M-MuLV RT	1	µl
ddH ₂ O	add	20 µl

The reaction mix was incubated at 37°C for 1 hour and afterwards the Reverse Transkriptase was heat inactivated at 75°C for 15 min. 2 µl of the resulting cDNA was used directly for the subsequent PCR.

3.2.1.9 DNA Gel-electrophoresis

DNA fragments were separated by horizontal electrophoresis chambers (BioRad) using agarose gels. Agarose gels were prepared by heating 1-2 % (w/v) agarose (Biozym) in 0.5 x TBE buffer, depending on the size of the DNA fragments, and the gels were supplemented with 0.05 % ethidium bromide. The samples were mixed with an appropriate amount of 6 x DNA sample buffer and loaded on the agarose gel. The gels were run at constant voltage (100 V) and finally documented using the Gel Doc 2000 UV-light documentation system (BioRad).

3.2.1.10 Extraction of DNA fragments from agarose gels

For isolation and purification of DNA fragments from agarose gels, ethidium bromide-stained gels were illuminated with UV-light and the appropriate DNA band was excised from the gel with a clean scalpel and transferred into a reaction tube. The fragment was isolated by using the QIAquick Gel Extraction Kit (Qiagen) following the manufacturer`s instructions.

3.2.1.11 Purification of DNA fragments

For purification of DNA fragments, the QIAquick PCR Purification Kit (Qiagen) was used according to the manufactures protocol.

3.2.1.12 Determination of DNA concentration

DNA concentration was determined spectroscopically using an Amersham-Pharmacia spectrometer. The absolute volume necessary for measurement was 50 µl. Concentration was determined by measuring the absorbance at 260 nm, 280 nm and 320 nm. Absorbance at 260

nm had to be higher than 0.1 but less than 0.7 for reliable determinations. A ratio of A_{260}/A_{280} between 1.8 and 2 monitored a sufficient purity of the DNA preparation.

3.2.1.13 DNA sequencing

DNA sequencing was performed by the company SeqLab, Göttingen. For preparation 0.7 μg of DNA and 20 pmol sequencing primer were diluted in 7 μl H_2O .

3.2.1.14 RNA Isolation

Total RNA from HepG2 cells (5×10^6 cells) was isolated with the NucleoSpin RNA II Kit (Macherey-Nagel) and the RNA concentration was determined by UV-spectrophotometry. The isolated RNA was used as template for the RT-PCR reaction where 2 μg of RNA was reverse transcribed in single stranded cDNA (3.2.1.7).

3.2.2 Protein-biochemical methods

3.2.2.1 SDS-polyacrylamide gel electrophoresis (155)

Separation of proteins was performed with a discontinuous SDS-polyacrylamide gel electrophoresis (SDS-PAGE) using the Mini-Protean III system (BioRad). The size of the running and stacking gel was as follows:

Running gel: height 4.5 cm, thickness 1.5 mm
 10 % or 15 % acrylamid solution

Stacking gel: height 1 cm, thickness 1.5 mm
 5 % acrylamid solution
 15 or 10-well combs

After complete polymerization of the gel, the chamber was assembled as described by the manufacturer's protocol. Up to 30 μl sample were loaded in the pockets and the gel was run at constant 80 V for 15 min and then at 140 V for the remainder. The gel run was stopped when

the bromphenol blue line reached the end of the gel. Gels were then either stained or subjected to Western blotting.

3.2.2.2 Coomassie-staining of polyacrylamide gels

After SDS-PAGE, the gels were stained in coomassie staining solution (30 min, RT) with constant agitation. The gels were then incubated in destaining solution until the background of the gel appeared nearly transparent.

3.2.2.3 Western Blot analysis

Proteins were transferred from the SDS-gel on a PVDF membrane (Amersham-Biosciences, Buckinghamshire, U.K.) using a MINI TRANSBLOT-apparatus (BioRad). The blotting sandwich was assembled as described in the manufactures protocol. Proteins were transferred electrophoretically at 4°C in Blotting-buffer at constant voltage (90 V, 120 min).

3.2.2.4 Immunochemical detection of proteins on PVDF membranes

After electrophoretic transfer, the membranes were removed from the sandwiches and placed with the protein-binding side up in plastic vessels. Membranes were immediately incubated with 20 ml blocking buffer for 1 hour at RT or overnight at 4°C. Afterwards, the primary antibody was added in the appropriate dilution either for 4 hours at RT or overnight at 4°C. The primary antibody was removed by washing the membrane 3 x 10 min with TBS-T. The appropriate secondary antibody was applied for 1 hour at RT and afterwards the membrane was washed again 6 x 10 min with TBS-T. Immunoreactive bands were visualized using the enhanced chemiluminescence detection system (Amersham-Biosciences, Buckinghamshire, U.K.). Therefore the membrane was soaked for 1 min in detection solution and afterwards placed between to transparent foils. The membrane was exposed to X-ray film (Amersham-Biosciences, Buckinghamshire, U.K.) or with the chemiluminescence kamara system LAS-1000 (Fujifilm, USA) for defined time periods.

3.2.2.5 Densitometric evaluation of band intensity

Densitometric evaluation of protein-band intensities was performed with digitized pictures. Band densities were quantified using the image processing software ImageJ (National Institute of Health, USA).

3.2.2.6 Determination of protein concentration (BCA)

The protein concentration of cell lysates was determined using the BCA kit (Pierce). Solution A and B were mixed (ratio 1:50) to give the BCA solution. 10 µl of the cell lysate were mixed with 200 µl BCA solution in microtiter plates and incubated for 30 min at 37°C. A BSA standard curve was co-incubated ranging from 3,000 µg/ml to 46 µg/ml. The extinction of the samples was determined at 568 nm in a microtiter plate reader (Tecan, Maennedorf, Switzerland).

3.2.3 Cell culture

3.2.3.1 Cultivation and transient transfection of the adherend cell line HepG2

HepG2 cells were obtained from the American Type Culture Collection (Rockville, MD/Manassa, VA) and were cultivated at 37°C, 5 % CO₂ and 90 % relative humidity in dishes (10 cm diameter) with 10 ml culture medium. Cells were passaged when they were confluent (usually after 3-4 days). Medium was removed and cells were detached by incubation with 3 ml Trypsin/EDTA (PAA Laboratories) for 5 min at 37°C. Cells were centrifuged (1,000 x g) and the pellet was resuspended in 10 ml fresh medium. Cells were split 1:10 for maintenance or seeded in dishes (10 cm diameter, 3 x 10⁶ cells) for transfection.

HepG2 cells were transfected using DEAE-Dextran. Before transfection, the culture medium was replaced to 75 µM chloroquin-containing culture medium. For one 1 culture dish (10 cm diameter), 5 µg of the appropriate plasmid DNA was thoroughly mixed with 435 µl Chloroquin-containing medium and 65 µl DEAE-Dextran (4 mg/ml). The mixture was dropwise added to the cells followed by 4-6 hours incubation at 37°C. Then the culture medium was removed and the cells were treated with medium containing 10 % DMSO for 7 min at room temperature. Subsequently the cells were washed with PBS and new medium was added. The next day, the medium was exchanged again.

3.2.3.2 Cultivation of suspension cell lines

Ba/F3 and hybridoma cells were grown continuously in suspension culture and were maintained at 37°C, 5 % CO₂ and 90 % relative humidity in dishes (10 cm diameter) with 10 ml culture medium. For subcultivation the cells were spun down (800 x g, 5 min, RT) and the

resulting cell pellet was resuspended in 10 ml fresh medium. Ba/F3 cells were split 1:100 whereas the Hybridoma cells were split 1:10 for maintenance.

For production of the human IL-6R antibodies 4-11 and 14-18, the hybridoma cells were seeded in dishes (10 cm diameter) at a density of 1×10^6 cells/ml Hybridoma Express medium (PAA Laboratories) supplemented with 2 mM L-glutamin. After 5 days the cells were spun down ($3,000 \times g$, 30 min, 4°C), the supernatant containing the produced antibodies was transferred into a new collection tube and was finally stored at -80°C .

3.2.3.3 Cell lysis

After stimulation of HepG2 cells, the culture medium was removed and the cells were washed twice with ice cold PBS and placed on ice. Cells were scraped of the wells, transferred into a 1.5 ml eppendorf tube and resuspended in chilled lysis buffer ($100 \mu\text{l}$ lysis buffer/ 0.5×10^6 cells). Cells were lysed for 1 hour at 4°C with constant agitation. Debris was removed by centrifugation ($16,000 \times g$, 15 min, 4°C) and the supernatant was stored at -20°C .

Suspension cells were spun down ($1,000 \times g$, 5 min RT) and the resulting cell pellet was washed twice with ice cold PBS before resuspension in lysis buffer ($100 \mu\text{l}$ lysis buffer/ 1×10^6 cells).

3.2.3.4 Surface biotinylation of transfected HepG2 cells

48 hours after transfection, HepG2 cells were washed twice with ice cold PBS and placed on ice. Surface proteins were biotinylated by incubating the cells with 0.1 mg/ml Sulfo-NHS-LC-biotin (Pierce, Rockford, IL, USA) in PBS for 30 min at 4°C . Biotinylation was terminated by addition of a 20 mM glycine solution in PBS for 10 min at 4°C . Afterwards the cells were washed 5 times with ice cold PBS and finally scraped of the wells, transferred into a 1.5 ml eppendorf tube and resuspended in chilled lysis buffer ($100 \mu\text{l}$ lysis buffer/ 0.5×10^6 cells). Cells were lysed for 1 hour at 4°C with constant agitation. Debris was removed by centrifugation ($16,000 \times g$, 15 min, 4°C) and the supernatant was diluted 1:5 with PBS. Biotinylated surface localized proteins were precipitated with $30 \mu\text{l}$ streptavidin-coupled agarose beads (Sigma-Aldrich, Deisenhofen, Germany) at 4°C overnight with constant agitation. Agarose beads were pelleted by centrifugation ($1,800 \times g$) and washed twice with PBS. Precipitated proteins were solubilised by addition of $60 \mu\text{l}$ SDS-sample buffer (2 x) to the agarose beads. Proteins were separated by SDS-PAGE for further Western blot analysis

3.2.3.5 Preparation of cytosolic and membrane fractions

48 hours after transfection 5×10^6 HepG2 cells were washed twice with ice cold PBS, scraped of the wells and resuspended in 300 μ l hypotonic lysis buffer for 60 min at 4°C. Afterwards the cell suspension was passaged several times through a 22-gauge needle and centrifuged (500 x g, 10 min, 4°C) to remove remaining cells and debris. The resulting post-nuclear supernatant was centrifuged again (100,000 x g, 1 h, 4°C). After centrifugation the supernatant represent the cytosolic fraction and was transferred into a new collection tube. The membrane pellet was resuspended in 100 μ l lysis buffer and incubated on ice for 60 min. The lysate was centrifuged again (16,000 x g, 15 min, 4°C) and the resulting supernatant represent the membrane fraction. Both, cytosolic and membrane fractions, were stored at -20°C.

3.2.3.6 Induction of cellular apoptosis and immunoprecipitation of the sIL-6R

Ba/F3 [gp130/IL-6R] cells were washed 3 times with PBS and seeded out at a density of 1×10^6 cells/ml. Apoptosis was induced by addition of 500 ng/ml doxorubicin or cytokine withdrawal.

HepG2 cells transfected with the p409-huIL-6R plasmid were seeded out 24 hours after transfection at a density of 3×10^5 cells/ml in a six-well plate. For induction of apoptosis, HepG2 cells were treated with 100 μ M cycloheximide (CHX) for 120 min prior to stimulation with 500 ng/ml of the anti-Fas antibody (CH-11). All other inhibitors were added 30 min prior anti-Fas stimulation.

Freshly isolated neutrophils were seeded out at a density of 5×10^6 cells/ml and treated with UV (200,000 μ J/cm²) or anti-Fas (500 ng/ml) and were incubated for 6 hours at 37°C.

After induction of apoptosis the supernatant was removed and centrifuged for 5 min at 16,000 x g at 4°C to remove cell debris. The cleared supernatant was transferred into a new collection tube and supplemented with 2 μ l of the polyclonal IL-6R antiserum 6.2 (150) and 30 μ l of protein A-coupled agarose beads (Amersham-Biosciences Buckinghamshire, U.K.). The sIL-6R was precipitated over night under constant agitation at 4°C and afterwards the beads were washed twice with PBS. Proteins were eluted from the beads with 2x SDS sample buffer (10 min, 95°C)

3.2.3.7 Isolation of human peripheral blood granulocytes (PMNs)

Peripheral blood was collected by venipuncture from healthy adult volunteers. Approval was obtained from the University Hospital Schleswig-Holstein institutional review board for these studies. Informed consent was provided according to the Declaration of Helsinki. 5 ml anticoagulated blood (lithium heparin) was layered onto a histopaque gradient consisting of two layers: 2 ml lymphocyte separation medium (PAA Laboratories, Pasching, Austria) on the top and 5 ml histopaque 1119 (Sigma-Aldrich, Deisenhofen, Germany) at the bottom prior to centrifugation at 800 x g for 20 min at room temperature. The granulocyte rich layer of histopaque 1119 was collected and washed once in PBS. The PMN pellet was resuspended in 2 ml RPMI 1640 medium and further fractionated on a discontinuous percoll (Amersham-Biosciences Buckinghamshire, U.K.) gradient consisting of layers, 2 ml each, with densities of 1.105 g/ml (85 %), 1.100 g/ml (80 %), 1.093 g/ml (75 %), 1.087 g/ml (70 %), 1.081 g/ml (65 %) percoll. After centrifugation for 20 min at 800 x g, the interface between the 80 % and 85 % percoll layers was collected and washed twice in PBS. PMN purity was more than 95 % as assessed by size and granularity on flow cytometry.

Isolated PMNs were counted with a Neubauer cell-counter chamber and seeded out at a density of 5×10^6 cells/ml in RPMI 1640 medium (3.1.5) prior stimulation.

3.2.4 Enzyme-linked immunosorbent assay (ELISA)

1. To determine the concentration of different antigens the two antibody “sandwich” ELISA method was used. First, the capture antibody was coated to a microtitre plate (Greiner Microlon, Solingen, Germany). After blocking, antigen is added and allowed to complex with the bound antibody. Unbound products were removed by extensive washing, and a biotinylated detection antibody was added. Finally subsequent addition of streptavidin-horseradish peroxidase (Roche, Mannheim, Germany) and peroxidase substrate (Roche, Mannheim, Germany) led to a calorimetric reaction which allowed the quantitation by measuring the amount of bound detection antibody. To determine the absolute amount of antigen in the samples a purified antigen standard was used. The following general protocol was used: 50 µl of coating antibody-solution was added to each well and incubated at RT over night; the wells were washed three times with PBS-T; 200 µl of blocking buffer was added to saturate the remaining protein binding sites on the microtiter plate for 2 hours at room temperature; the wells were washed three times with PBS-T; 50 µl of antigen solution (mostly conditioned supernatants) or purified antigen standard were added to each well for 2 hours at

RT. The samples were diluted in PBS supplemented with 1 % BSA; the wells were washed three times with PBS-T; 50 µl of detection antibody solution was added to each well incubated at RT for 2 hours; the wells were washed three times with PBS-T; 100 µl of streptavidin-horseradish peroxidase solution (1: 5,000 in PBS supplemented with 1 % BSA) was added and incubated for 45 min at RT; the wells were washed three times with PBS-T; 75 µl of the peroxidase substrate BM blue POD (Roche) was added for approximately 20 min and the reaction was stopped by addition of 75 µl 1.8 M H₂SO₄; the wells were washed three times with PBS-T; Optical densities at 450 nm were measured on an ELISA plate reader (SLT Rainbow; Tecan, Maennedorf, Switzerland).

Antigen	Capture antibody	Blocking buffer	Detection antibody
human soluble IL-6R	MAB 227 (R&D-Systems) Working concentration: 1 µg/ml	PBS supplemented with 1 % BSA and 5 % sucrose	BAF 227 (R&D-Systems) Working concentration: 50 ng/ml

The soluble gp130 ELISA kit as well as the murine IL-6 ELISA kit were purchased from R&D systems and were used according to the manufactures protocol.

3.2.5 Fluorescence-activated cell sorting (FACS)

3.2.5.1 Flow cytometry analysis of cell surface proteins

Ba/F3 [gp130/IL-6R] cells were washed twice with FACS-buffer and then incubated with 1 µg/ml anti-IL-6R antibody M91 for 60 min on ice. After a single wash in FACS-buffer, cells were incubated with the allophycocyanin-conjugated goat anti-mouse antibody for 60 min on ice. Cells were washed once, resuspended in 500 µl FACS buffer, and analyzed by flow cytometry (FACS-Canto; Becton Dickinson, Heidelberg, Germany). All centrifugation steps were performed at 1,000 x g for 5 min at 4°C.

To analyze the different cell populations in the lavage fluid of carrageenan-challenged mice, cells were counted with a Neubauer cell-counter chamber and washed twice with FACS-buffer. 2 x 10⁵ cells were used for flow cytometry analysis. To block Fc-receptors on

neutrophils and macrophages the cell suspension was incubated for 5 min with Mouse BD Fc Block CD 16/32 mAB (1:500 diluted in FACS-buffer). Afterwards the cells were spun down (1,000 x g, 5 min, 4°C) and resuspended in FACS-buffer containing the fluorescence-coupled antibodies against Ly6G/Ly6C and F4/80 for 60 min on ice protected from direct light. The cells were subsequently washed and resuspended in 500 µl FACS-buffer and analyzed by flow cytometry.

3.2.5.2 Flow cytometry analysis of phosphatidylserine

Annexin V preferentially binds phosphatidylserine and can be used as a specific early indicator of apoptosis. The annexin V/propidium iodide staining kit (BD Bioscience, Heidelberg, Germany) was used according to the manufacturer's instructions. Briefly, 3×10^5 cells were spun down and washed twice in annexin V-binding buffer. Afterwards the cells were incubated in 100 µl annexin V-binding buffer containing 2 µl FITC-conjugated annexin V for 15 min at room temperature protected from light. Finally 400 µl annexin V-binding buffer was directly added to the cell suspension and the cells were analyzed within 10 min by flow cytometry.

3.2.5.3 Flow cytometry analysis of nucleosomal DNA fragments

10^6 Ba/F3 [gp130/IL-6R] cells were washed twice with PBS and subsequently fixed with chilled 70 % methanol for at least 1 hour on ice. Afterwards the cells were washed twice with chilled PBS and resuspended finally in 1 ml PBS supplemented with 1 mg/ml RNase (30 min, 37°C). After two washing steps the cell suspension was supplemented with 500 µl PBS containing 1 mg/ml propidium iodide incubated for 5 min at room temperature and finally analyzed by flow cytometry.

3.2.6 Murine air pouch model of acute inflammation

Animals used throughout the air pouch experiments were 8-10 weeks old male C57Bl/6 wild type mice and IL-6 knock-out mice (C57Bl/6 IL-6^{-/-}) obtained from Charles River Laboratories (Sulzfeld, Germany). The air pouch model of local inflammation was performed according to Edwards et al. (156). Mice were anesthetized with ether and subcutaneous dorsal pouches were generated by injection of 6 ml sterile air. After three days the pouches were reinjected with 4 ml of air. On day 6, 1 ml of a suspension of 1 % Carrageenan (Sigma-

Aldrich, Deisenhofen, Germany) in sterile PBS (PAA Laboratories, Pasching, Austria) was injected into the cavity. Carrageenan is composed of mainly sulfated polysaccharides, which are generally extracted from seaweed. Injection of Carrageenan into air pouches of rats and mice is a well established disease model of acute, local inflammation (156-158).

Three days after Carrageenan challenge, mice were sacrificed and the pouches were washed with 3 ml ice-cold PBS. Exudates were collected and the volume was recorded. Total cell numbers were counted with a Neubauer cell-counter chamber. The remaining lavage fluid was centrifuged at 16,000 x g for 10 min at 4°C, and the supernatant was stored at -80°C until analyzed by ELISA.

Aliquots of the exudate containing 2×10^5 cells were used for flow cytometry analysis, whereby the mABs Ly6GC (BD Pharmingen), F4/80 (Caltag), were employed to count infiltrating neutrophils and monocytes.

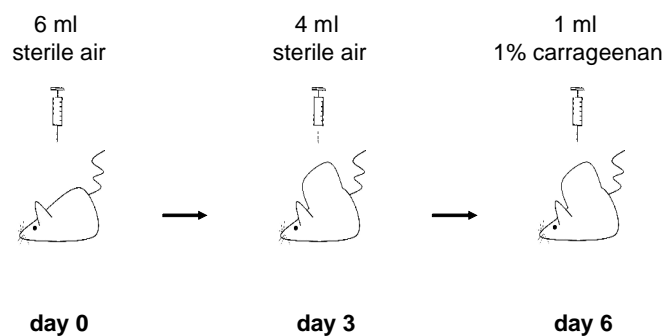


Figure 5: Air pouch model of acute inflammation.

Schematic representation of the air pouch time schedule. At different time points after Carrageenan injection the pouch was washed with 3 ml PBS and the exudate was analyzed by FACS or ELISA.

3.2.7 Intraperitoneal injection

400 μ l sterile PBS or 400 μ l sterile PBS containing either purified neutralizing anti-murine IL-6R antibody or recombinant soluble gp130-Fc were injected into the peritoneal cavity of an ether anesthetized mouse. Both components were injected i.p. 6 hours before carrageenan challenge. Solutions were prepared and loaded under a sterile fume hood. Intraperitoneal injection was performed using a 1 ml syringe in combination with a 27 gauge needle.

3.2.8 Statistical analysis

Data are expressed as mean values \pm SD; 3-5 mice were used per experimental group. Statistical analysis was performed by using a Student's unpaired *t* test (<http://www.physics.csbsju.edu/stats/t-test.html>). A p-value below 0.05 was considered statistically significant.

3.2.9 Animal treatment

Procedures involving animals and their care were conducted in conformity with national and international laws according to home office approved project license 66-6/06 from 9/15/2006. Mice were maintained in a 12 hours light-dark cycle under standard conditions and were provided with food and water ad libitum. All mice were maintained under barrier conditions and were pathogen free as assessed by regular microbiological screening. The animals were kept at $21^{\circ}\text{C} \pm 2^{\circ}\text{C}$ and $60\% \pm 5\%$ humidity in individually ventilated cages (IVC).

3.2.10 Purification of antibodies against the extracellular part of the human IL-6R

The murine hybridoma cell lines 4-11 and 14-18, producing monoclonal antibodies against the extracellular part of the human IL-6R, were generated by Hans Lange (Department of General and Thoracic Surgery, University Hospital Schleswig-Holstein).

The secreted antibodies were purified from culture supernatant by affinity chromatography with a protein A-sepharose column (Amersham). The protein A-sepharose column was washed once with 50 ml degassed PBS. The antibody containing hybridoma cell culture supernatant (1,000 ml) was sterile filtered and degassed. Afterwards the culture supernatant was applied to the column. This was followed by a washing step with 150 ml PBS. The bound antibody was eluted from the column with 20 ml elution buffer, pH 3.0 and fractions of approximately 1,800 μl were collected. Each fraction was neutralized by addition of 200 μl neutralizing buffer, pH 11. Each fraction (10 μl) was analyzed on a 15 % SDS-PAGE gel under reducing conditions stained with coomassie solution. The fractions which contain the antibody were pooled and loaded onto a NAP column (Pharmacia, Uppsala, Sweden) to change the buffer to PBS. Protein concentration was determined spectrophotometrically at 280 nm.

4 Results

4.1 Production and purification of two monoclonal antibodies, raised against the ectodomain of the human IL-6R

BALB/c mice were immunized with recombinant human soluble IL-6R in order to obtain monoclonal antibodies. Immunization of mice and generation of immortalized B-cells, which produce large amounts of monoclonal antibodies (hybridoma cells), was performed by Hans Lange (Department of General and Thoracic Surgery, University Hospital Schleswig-Holstein). The fusion of primary murine spleenocytes with the myeloma cell line P3X63-Ag 8 635 led to generation of 57 antibody producing hybridoma cell clones. The cell culture supernatants, containing the secreted antibodies, were collected and antigen recognition was tested by Western blotting. Western blot analysis of purified Hyper-IL-6 (Figure 6A, B) and lysates of COS-7 cells transfected with the human IL-6R (Figure 6C) revealed that several clones produced antibodies which recognize the immunogen (apparent molecular size of 80 kDa). Two cell lines (4-11 and 14-18) were selected for further studies based on their ability to secrete highly specific antibodies, which are able to detect the human IL-6R (Figure 6B, C).

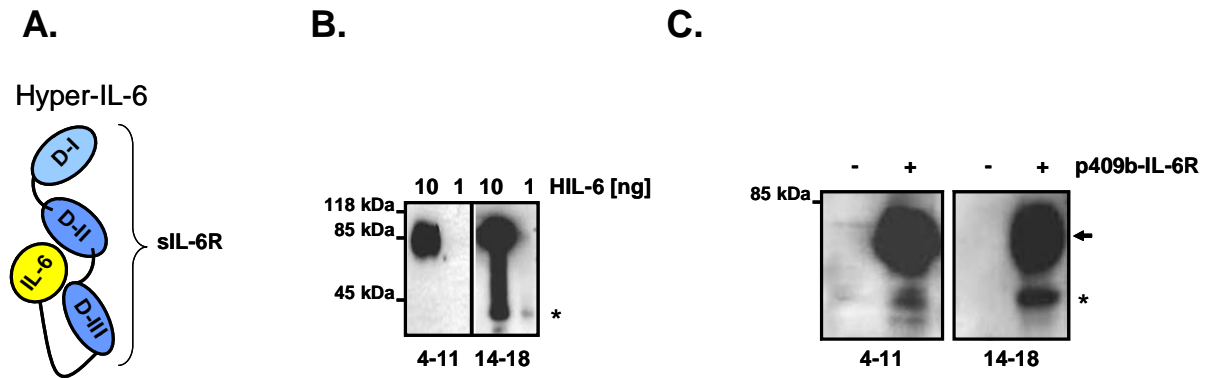


Figure 6: Immunochemical detection of the human IL-6R with monoclonal antibodies produced by the hybridoma clones 4-11 and 14-18.

A. The designer cytokine, Hyper-IL-6. Hyper-IL-6 is a fusion protein built up of human IL-6 and the human sIL-6R connected via a flexible peptide linker (159, 160).

B. Hyper-IL-6 (HIL-6) was subjected to SDS-PAGE and transferred to PVDF membrane after separation. The fusion protein was detected by the hybridoma supernatants 4-11 and 14-18 (1:500) and the anti mouse IgG-HRP secondary antibody (1:10,000) (* degradation product).

C. COS-7 cells were transiently transfected with the eukaryotic expression vector p409b-IL-6R and lysed after 48 h. The immunochemical detection of the IL-6R was performed as in Figure 6B. To exclude unspecific binding untransfected COS-7 cells were used as negative control. Molecular weights are present on the left. The mature IL-6R protein is marked by an arrow and the immature protein (probably not entire glycosylated) is marked by an asterisk.

For purification of the anti-IL-6R antibodies *via* affinity chromatography, cell culture supernatants of the two hybridoma clones were harvested and collected in two independent pools of 500 ml each. The two pools were successively applied to a Protein A-sepharose column. After washing, the bound antibodies were eluted using an acidic glycine buffer. All eluate fractions were subjected to SDS-PAGE and stained with coomassie-blue. After purification two predominant bands of approximately 50 kDa and 25 kDa, representing the heavy and light chain of the purified antibodies, were detected in the coomassie stained gels.

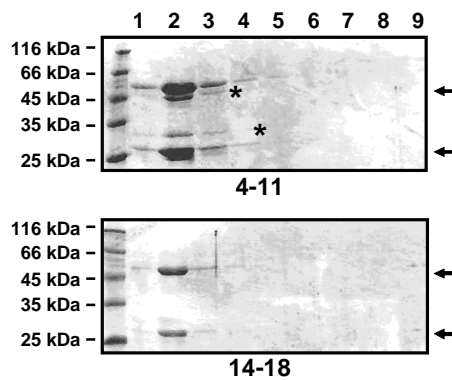


Figure 7: Purification of the α -IL-6R antibodies 4-11 and 14-18.

1,000 ml of supernatants produced by the hybridoma clones 4-11 and 14-18 were applied to a Protein A-sepharose column. The antibodies bound to the column were eluted with 20 ml acidic glycine buffer. The 9 eluate fractions were analyzed by SDS-PAGE and subsequent coomassie-blue staining. The two predominant bands visible in the coomassie-blue stained gel represent the heavy (50 kDa) and light (25 kDa) chain of the purified

antibodies (arrows). The purified antibody 4-11 contained two unspecific proteins (*) which probably represent degradation products. Molecular weights are present on the left.

The first four eluate fractions were pooled and the buffer was exchanged to 3.5 ml PBS. Afterwards the protein concentration in the samples was determined by UV spectroscopy at 280 nm and the values were 1 mg/ml for the anti-IL-6R 4-11 antibody and 0.25 mg/ml for the anti-IL-6R 14-18 antibody.

The anti-IL-6R antibody 14-18 was used throughout this study for detection of the human IL-6R by Western blotting.

4.2 The chemotherapeutic drug doxorubicin induces apoptosis in Ba/F3 [gp130/IL-6R] cells.

Pre-B cells stably transfected with the cDNA for the human IL-6R and the human gp130 were treated with the chemotherapeutic drug doxorubicin. Doxorubicin causes intrinsic cell death by irreversibly inhibition of DNA topoisomerase II, activation of p53 protein and formation of reactive oxygen species. Doxorubicin induces apoptosis in Ba/F3 [gp130/IL-6R] cells in a dose and time dependent manner (Figure 8). Apoptosis was assessed by annexin V-staining. Annexin V is a phospholipid-binding protein with a high specificity and affinity to phosphatidylserine (PS) which is exposed to the outer leaflet of the plasma membrane on cells undergoing apoptosis. Necrotic cells exhibit membrane permeabilization and will also bind annexin V. To distinguish between viable, early apoptotic and necrotic or late apoptotic cells propidium iodide was used. Propidium iodide does not penetrate the plasma membrane and therefore is excluded from viable and early apoptotic cells. Late apoptotic and necrotic cells

were stained with both annexin V and propidium iodide due to the final disintegration of the cell.

Ba/F3 [gp130/IL-6R] cells were exposed to increasing concentrations of doxorubicin and analyzed by flow cytometry after 15 hours treatment. The lowest dose of 100 ng/ml doxorubicin caused apoptotic cell death in 75 % of the cells. Higher concentrations caused a dose-dependent decrease in the number of viable cells (Figure 8A). Similarly, a time-dependent increase in apoptosis was observed when Ba/F3 [gp130/IL-6R] cells were treated with 500 ng/ml doxorubicin for the time periods of 2, 4 and 8 hours (Figure 8B). Except of phosphatidylserin exposure doxorubicin-induced apoptosis was accompanied by cleavage of the caspase-3 substrate PKC δ . Considerable cleavage of the full length PKC δ to its active form could be observed after 6 hours of doxorubicin treatment (Figure 8C).

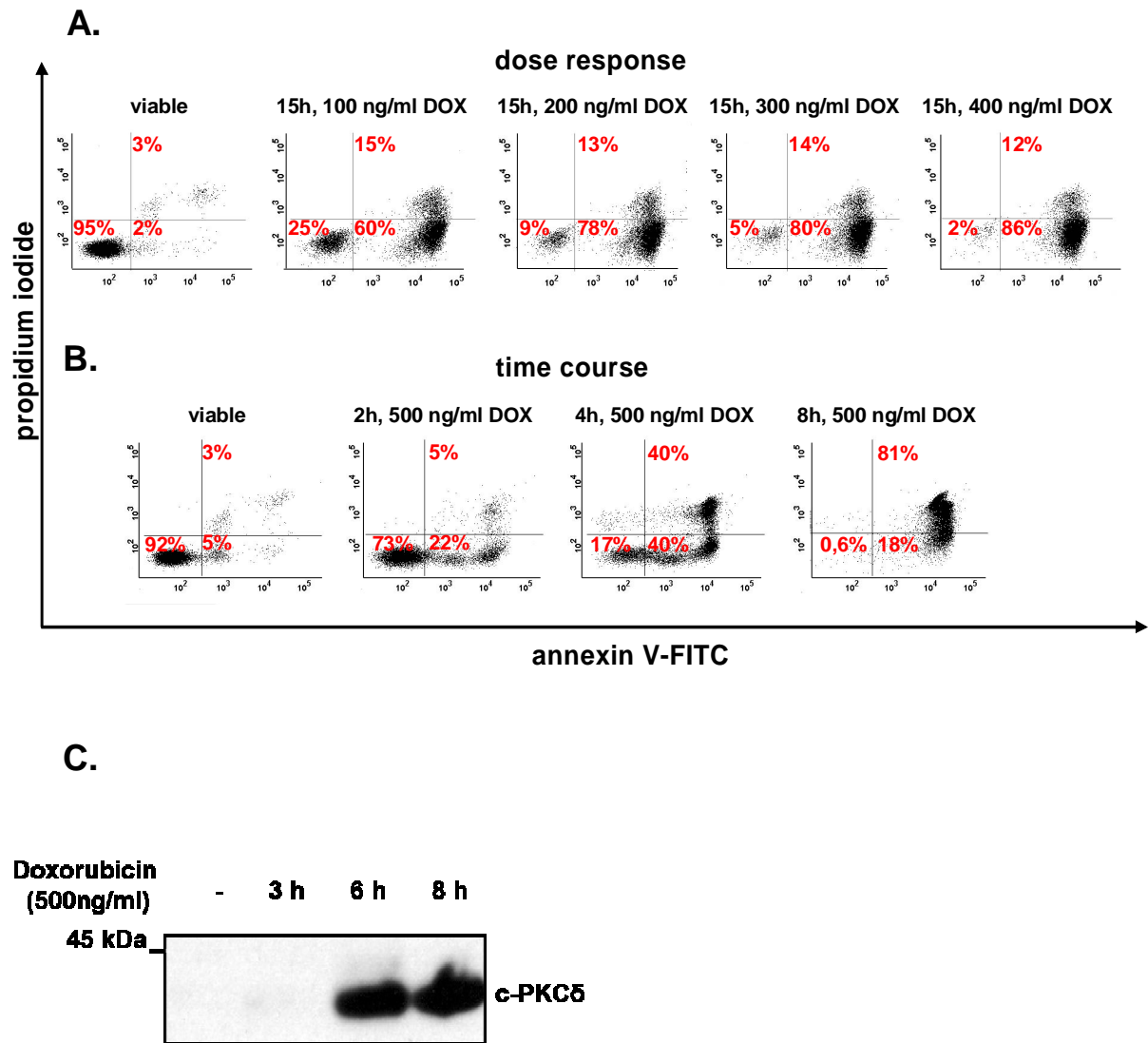


Figure 8: Doxorubicin induced apoptosis of Ba/F3 [gp130/IL-6R] cells in a dose- and time-dependent manner.

A. Dose-dependent increase of apoptotic cells was observed when Ba/F3 [gp130/IL-6R] cells were treated with increasing concentrations of doxorubicin (DOX) (100, 200, 300 and 400 ng/ml) for 15 hours and apoptosis was measured using annexin V-FITC/propidium iodide staining and flow cytometry.

B. A time-dependent increase in apoptotic and late apoptotic Ba/F3 [gp130/IL-6R] cells was observed when cells were treated with doxorubicin (500 ng/ml) for the indicated time periods (2, 4 and 8 hours) before measurement of apoptosis. Annexin V-FITC staining is represented on the x-axis and propidium iodide staining on the y-axis. The percentage of viable (lower left quadrant), apoptotic (lower right quadrant) and late apoptotic (upper right quadrant) cells are indicated.

C. When Ba/F3 [gp130/IL-6R] cells were treated with doxorubicin (500 ng/ml), induction of apoptosis was accompanied by a time dependent (6 and 8 hours) cleavage of the caspase-3 substrate PKC δ as demonstrated by immunoblotting (c-PKC δ : cleaved-PKC δ).

4.3 Soluble IL-6R release during doxorubicin-induced apoptosis of Ba/F3 [gp130/IL-6R] cells

Ba/F3 [gp130/IL-6R] cells underwent apoptosis after treatment with the chemotherapeutic drug doxorubicin. To investigate the fate of the IL-6R during programmed cell death, supernatants and lysates of Ba/F3 [gp130/IL-6R] cells were examined by Western blot analysis upon induction of apoptosis. Apoptosis was induced for different time points with 500 ng/ml doxorubicin. In immunoprecipitation experiments with antibodies directed against the extracellular domain of the IL-6R, increasing amounts of the 65 kDa IL-6R ectodomain were precipitated from cell culture supernatants of apoptotic cells with time after doxorubicin treatment. While an increase of the soluble form of the IL-6R (sIL-6R) was detectable after 4 hours of doxorubicin treatment the amount of cellular IL-6R decreased in the lysates (Figure 9A, B). As positive control, Ba/F3 [gp130/IL-6R] cells were treated for 2 hours with PMA, a well-known inducer of IL-6R shedding (Figure 9B).

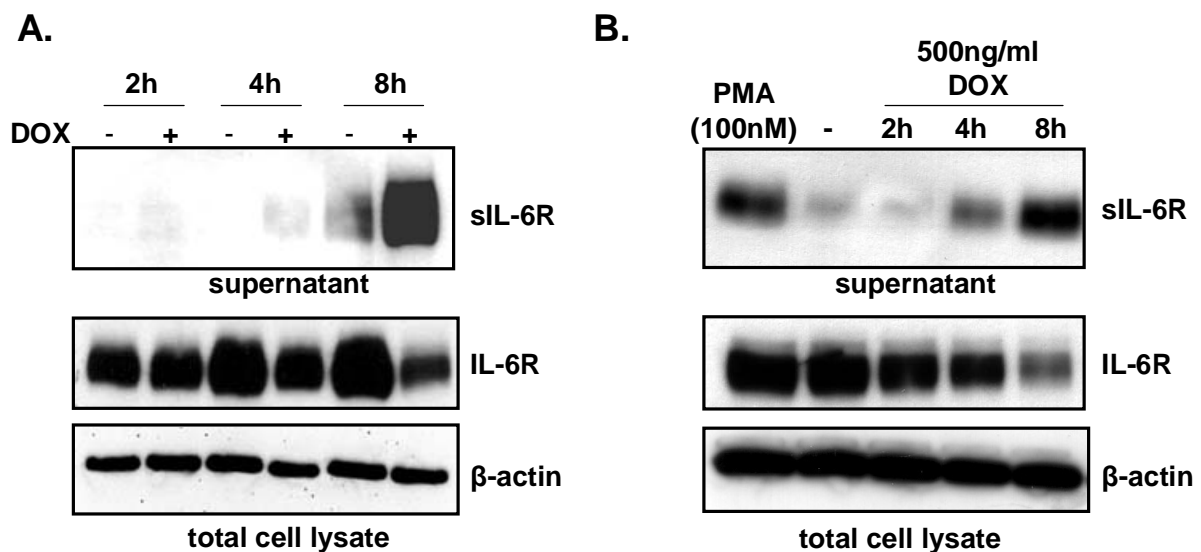


Figure 9: Time dependent release of the IL-6R from doxorubicin treated Ba/F3 [gp130/IL-6R] cells.

A. Ba/F3 [gp130/IL-6R] cells were treated for 2, 4 and 8 hours with 500 ng/ml doxorubicin (DOX). Soluble IL-6R was immunoprecipitated from conditioned media using the polyclonal α -IL-6R serum 6.2 and subsequently visualized by Western blot analysis using the α -IL-6R mAB 14-18. Reciprocal Western blot analysis of cell lysates was performed using 14-18 mAB and α - β -actin mAB, which was used as a loading control.

B. Ba/F3 [gp130/IL-6R] cells were treated for 2, 4 and 8 hours with 500 ng/ml doxorubicin (DOX) or 2 hours with the phorbol ester PMA (100 nM). Western blot analysis was performed as described in A.

Non-apoptotic as well as early and late stage apoptotic Ba/F3 [gp130/IL-6R] cells were identified using flow cytometry in combination with annexin V and propidium iodide. To monitor IL-6R cell surface expression during apoptosis, doxorubicin treated Ba/F3 [gp130/IL-6R] cells were stained additionally with the anti-IL-6R antibody M91. After 6 hours of doxorubicin treatment three populations were detectable in the annexin V/propidium iodide-staining: the annexin V-negative/propidium iodide-negative cell population representing the viable cells, the annexin V-positive/propidium iodide-negative cell population representing the early apoptotic cells and the annexin V-positive/propidium iodide-positive cell population representing the late apoptotic cells (Figure 10, left). The three populations were gated separately and IL-6R surface expression was measured for each population (Figure 10, right). Examining the IL-6R levels revealed that its surface expression was decreased in annexin V-positive and annexin V/propidium iodide double-positive cells. Early as well as late apoptotic cells showed similar IL-6R cell surface decrease indicating that loss of IL-6R surface expression is an early apoptotic event.

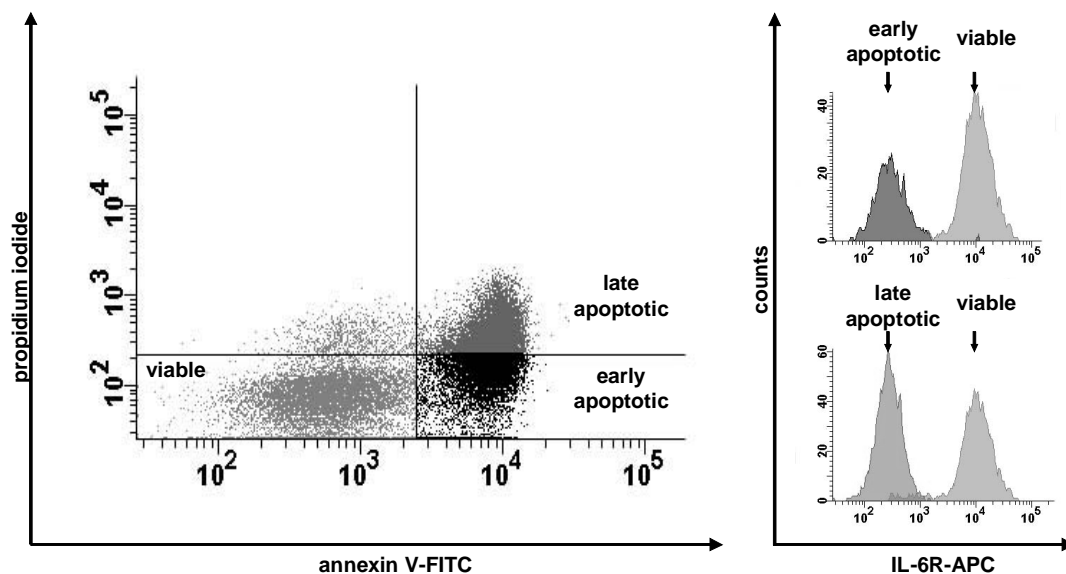


Figure 10: Loss of cell surface IL-6R during early stages of doxorubicin-induced apoptosis in Ba/F3 [gp130/IL-6R] cells.

Ba/F3 [gp130/IL-6R] cells were treated for 6 hours with doxorubicin and multiparameter FACS staining was performed with propidium iodide, annexin V-FITC and the α -IL-6R M-91 mAb. Annexin V-FITC staining is represented on the x-axis and propidium iodide staining on the y-axis of the dot plot (left). The three cell populations (viable, early apoptotic and late apoptotic) are indicated. Each population was gated and IL-6R cell surface expression was monitored on the histogram (right). IL-6R cell surface expression is represented on the x-axis.

4.4 Shedding of the IL-6R from the cell surface of apoptotic Ba/F3 [gp130/IL-6R] cells.

Doxorubicin treatment of Ba/F3 [gp130/IL-6R] cells led to enhanced sIL-6R release and to downregulation of membrane-bound IL-6R on the cell surface. To examine whether this events occurred through ectodomain shedding of the membrane-bound IL-6R, Ba/F3 [gp130/IL-6R] cells were stimulated with doxorubicin in the presence of the hydroxamic acid-based inhibitor marimastat. Marimastat is a broad-spectrum metalloprotease inhibitor (active against both matrix metalloproteases and ADAM proteases), which has been shown to abrogate proteolysis of several ADAM10 and ADAM17 substrates (77). Cotreatment of the doxorubicin-treated Ba/F3 [gp130/IL-6R] cells with marimastat completely blocked generation of the soluble IL-6R indicating that the IL-6R is shed from the cell surface during apoptosis by metalloprotease activity (Figure 11). Marimastat did not prevent programmed cell death as judged by annexin V-staining (Figure 12).

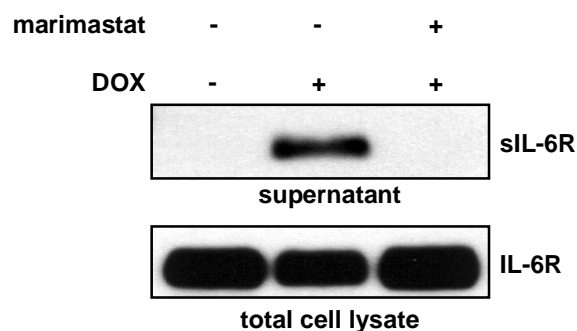


Figure 11: Doxorubicin treatment induced metalloproteinase mediated shedding of the IL-6R in Ba/F3 [gp130/IL-6R] cells.

Exposure of Ba/F3 [gp130/IL-6R] cells to 500 ng/ml doxorubicin (DOX) for 8 hours resulted in metalloproteolytic release of sIL-6R into the supernatant as shown by complete inhibition of the release by marimastat (10 μ M). Marimastat

was added to the cells 15 minutes prior doxorubicin stimulation. Western blot analysis was used as outlined in Figure 9 to monitor levels of sIL-6R and IL-6R.

4.5 Shedding of the IL-6R during apoptosis is mediated by the metalloprotease TACE (ADAM17)

It was previously described that shedding of the IL-6R after PMA treatment or cholesterol depletion was mediated by the metalloprotease ADAM17 and to a lesser extent by ADAM10 (77). To identify the sheddase which is responsible for apoptosis-induced IL-6R shedding two

further hydroxamate-based metalloprotease inhibitors were used. The inhibitor GW280264X (GW) has the ability to potently block the activity of ADAM10 and ADAM17, whereas GI254023X (GI) inhibits ADAM10 100-fold better than ADAM17 (161) (Table 2).

Compound	IC ₅₀ (nM)		Selectivity ADAM10 potency/ ADAM17 potency ^{a)}
	ADAM17	ADAM10	
GI254023X	541	5.3	102
GW280264X	8.0	11.5	1.4

Table 2: Potency of the compounds GW280264X and GI254023X for inhibition of recombinant ADAM17 and ADAM10 ectodomain.

The inhibitor concentration leading to half maximal inhibition (IC₅₀) of recombinant TACE or ADAM10 ^(a) Potency is defined as 1/IC₅₀). The 2 compounds differ in their capacity to block the activities of the two metalloproteinases ADAM17 (TACE) and ADAM10. The compound GW280264X potently blocked both recombinant enzymes. The Compound GI254023X, however, possessed comparable inhibitory potency for ADAM10 and blocked TACE with more than 100-fold reduced potency. Adopted from (162).

The two inhibitors were tested for their ability to block IL-6R shedding during apoptosis. As control, Ba/F3 [gp130/IL-6R] cells were treated with PMA, a well known inducer of ADAM17-mediated IL-6R shedding. As shown in Figure 12, the ADAM10/ADAM17-specific inhibitor GW280264X blocked the cleavage in unstimulated, PMA-stimulated as well as in doxorubicin-treated cells. The selective ADAM10 inhibitor blocked the constitutive cleavage of the IL-6R but hardly affected the cleavage of PMA and doxorubicin-treated cells. Thus the inhibitor profile indicated that the constitutive shedding of the IL-6R is mediated by ADAM10 whereas the PMA- and doxorubicin-inducible cleavage is mediated by ADAM17 activity in Ba/F3 [gp130/IL-6R] cells. Both metalloprotease inhibitors did not interfere with the progression of apoptosis as judged by annexin V-staining (Figure 12).

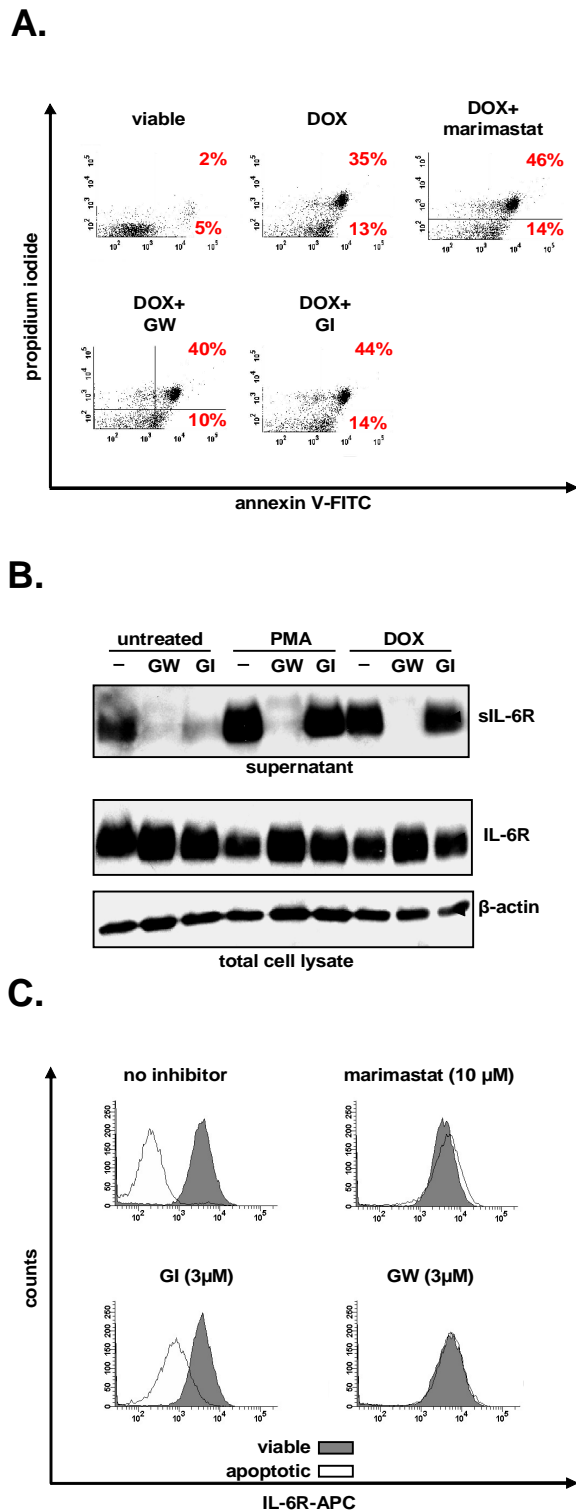


Figure 12: The metalloprotease inhibitor GW280264X prevented the proteolytic cleavage of the IL-6R during doxorubicin treatment.

A. Ba/F3 [gp130/IL-6R] cells were treated for 8 hours with 500 ng/ml doxorubicin (DOX) in presence of 10 μ M marimastat, 3 μ M GW280264X (GW) and 3 μ M GI254023X (GI). FACS staining was performed with propidium iodide and annexin V-FITC to monitor apoptosis. The percentage of viable (lower left quadrant), apoptotic (lower right quadrant) and late apoptotic (upper right quadrant) cells are indicated.

B. Ba/F3 [gp130/IL-6R] cells were treated for 8 hours with 500 ng/ml doxorubicin (DOX) or for 2 hours with 100 nM PMA in the presence or absence of the metalloprotease inhibitors GW280264X (GW, 3 μ M) and GI254023X (GI, 3 μ M). Inhibitors were added 15 minutes prior to stimulation. Western blot analysis was used as outlined in Figure 9 to monitor levels of sIL-6R, IL-6R and β -actin.

C. Flow cytometric analysis of the IL-6R from doxorubicin treated Ba/F3 [gp130/IL-6R] cells. The cells were treated with the metalloprotease inhibitors GI254023X (GI, 3 μ M), GW280264X (GW, 3 μ M) and marimastat (10 μ M) in the presence or absence of 500 ng/ml doxorubicin. The cells were harvested after 8 hours incubation, stained with the α -IL-6R antibody M91 (1 μ g/ml) and subsequent analyzed by flow cytometry. The analysis showed that apoptotic cells lost cell surface expression of the IL-6R. The level of IL-6R surface expression was

similar in doxorubicin-treated cells and in viable cells when metalloprotease activity was blocked with the broad-spectrum metalloprotease and the combined ADAM17/ADAM10 inhibitors but not with the specific ADAM10 inhibitor.

4.6 Ba/F3 [gp130/IL-6R] cells undergo apoptosis after cytokine deprivation

Ba/F3 cells are dependent on IL-3 for their survival and proliferation. Ba/F3 cells stably transfected with the cDNA coding for human gp130 and IL-6R respond additionally to the cytokine IL-6. Both cytokines, IL-3 and IL-6, induce the expression of genes for promotion of cell growth and prevention of apoptosis. Thus, Ba/F3 cells are dependent on their respective cytokines for growth and undergo apoptosis upon cytokine deprivation. Cytokine withdrawal was used as a physiological stimulus to trigger intrinsic programmed cell death which is associated with loss of mitochondrial membrane potential, release of cytochrome *c* into the cytosol as well as activation of caspases. Ba/F3 [gp130/IL-6R] cells were cultured in the presence of IL-6 or IL-3. 12 hours after IL-6 or IL-3 withdrawal, Ba/F3 [gp130/IL-6R] cells began to undergo apoptosis as judged by annexin V/propidium iodide-staining or nucleosomal DNA fragmentation analysis (Figure 13). 24 hours cultivation in absence of IL-3, led to complete degradation of the nuclear DNA in nucleosomal fragments (Figure 13, SubG1-peak) and 24 hours of IL-6 deprivation led to approximately 40% annexin V-positive Ba/F3 [gp130/IL-6R] cells.

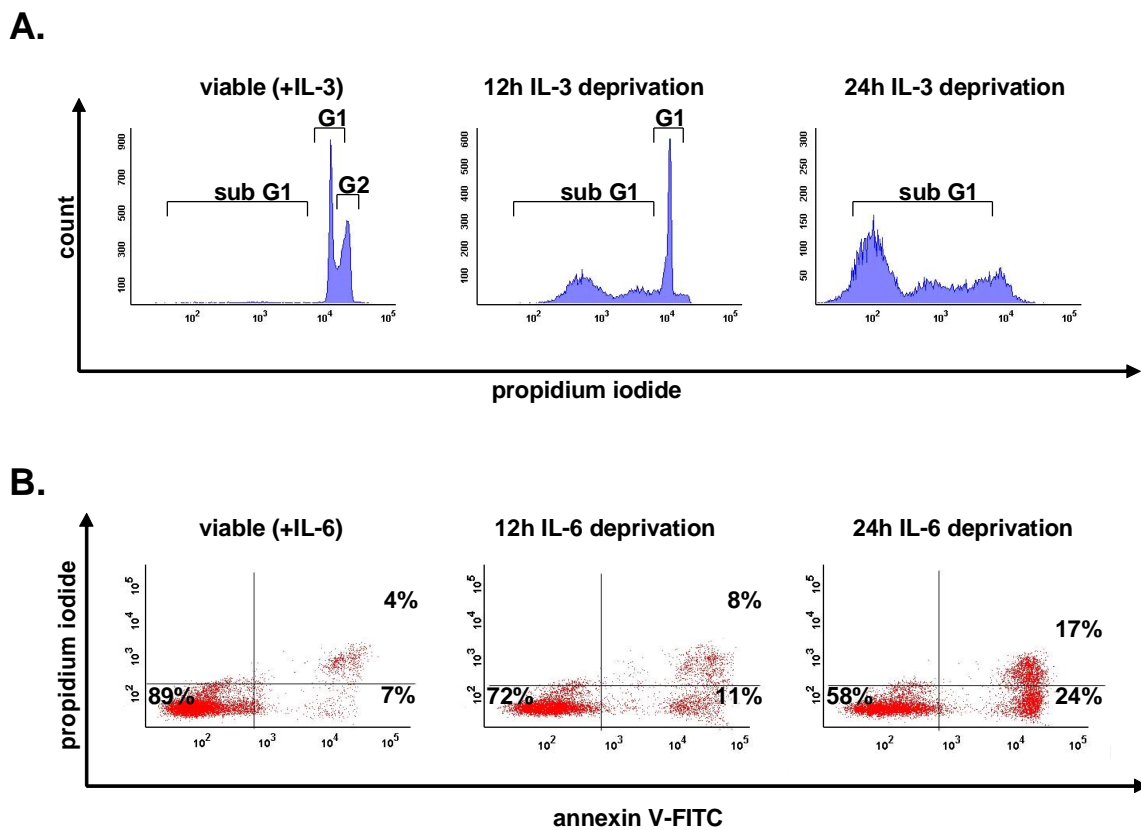


Figure 13: Cytokine deprivation of Ba/F3 [gp130/IL-6R] cells induced apoptosis.

A. Ba/F3 [gp130/IL-6R] cells were cultured for 3 weeks in IL-3 containing cultivation medium. The cells were washed 3 times with PBS and cytokine deprived for the indicated time periods. Afterwards the cells were permeabilized with 70 % methanol and stained with propidium iodide prior analysis by flow cytometry. Viable cells showed no detectable DNA laddering. After 12 and 24 hours of IL-3 deprivation, apoptotic cells were detected in the ‘sub-G1 peak’.

B. Ba/F3 [gp130/IL-6R] cells were cultured for 3 weeks in IL-6 supplemented cultivation medium. The cells were washed 3 times with PBS and cytokine deprived for the indicated time periods. Annexin V-FITC/propidium iodide-staining was performed as described in Figure 8.

4.7 Shedding of the IL-6R after cytokine deprivation of Ba/F3 [gp130/IL-6R] cells

Apoptosis induced by doxorubicin treatment led to enhanced IL-6R shedding. To investigate whether a different apoptotic stimulus has the same impact on the proteolytic cleavage of the IL-6R, Ba/F3 [gp130/IL-6R] cells were cytokine deprived for different time periods. Generation of the soluble IL-6R as well as the membrane-bound form was monitored by

Western blot and flow cytometry analysis. As depicted in Figure 14, intrinsic apoptosis following cytokine withdrawal induced shedding of the IL-6R. In line with data from doxorubicin-treated Ba/F3 [gp130/IL-6R] cells, ectodomain shedding after cytokine deprivation was completely inhibited by marimastat (pan-metalloprotease inhibitor) and almost completely by the ADAM10/ADAM17-specific inhibitor GW280264X but not by the ADAM10-specific inhibitor GI254023X.

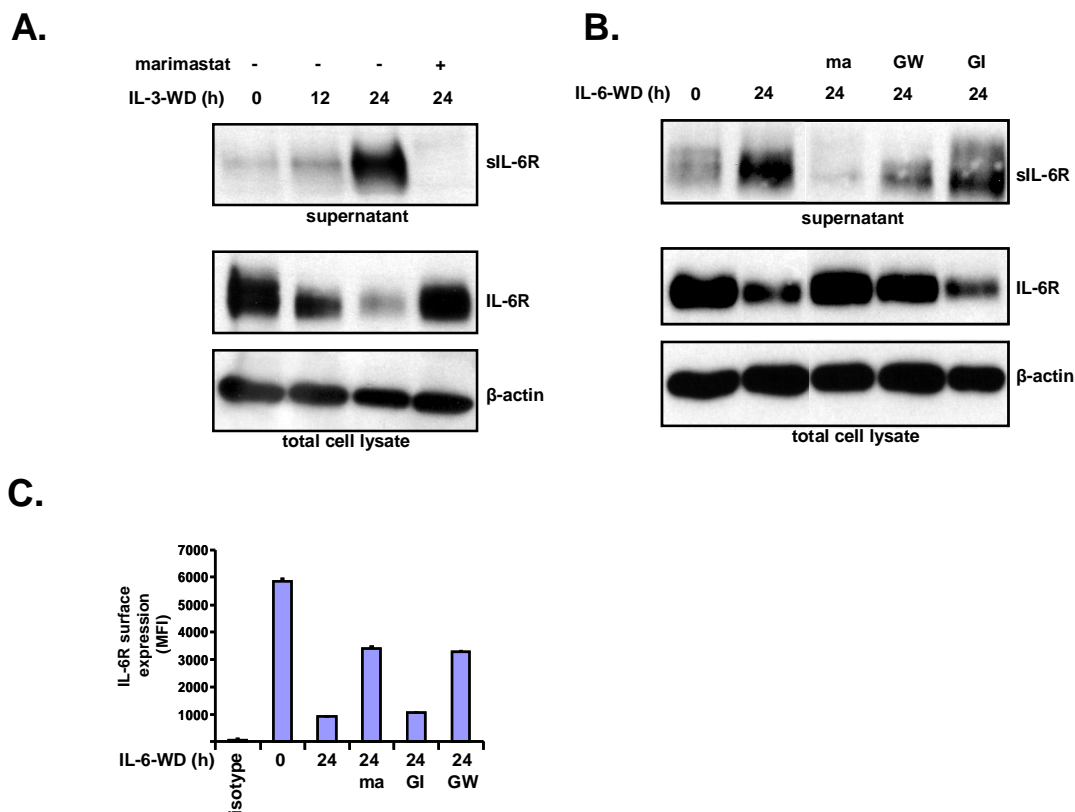


Figure 14: Cytokine withdrawal-induced apoptosis led to ectodomain shedding of the IL-6R.

A. IL-3 dependent Ba/F3 [gp130/IL-6R] cell were washed 3 times and cultured for 12 and 24 hours in cytokine-free medium to induce apoptosis. Control cells were maintained over the 24-hour period in the presence of IL-3 (IL-3-WD, 0h). Marimastat (10 μ M) was added as indicated. Lysates and immunoprecipitated supernatants were subjected to SDS-PAGE and analyzed by Western blot with the α -IL-6R antibody 14-18.

B. IL-6 dependent Ba/F3 [gp130/IL-6R] cell were treated and analyzed as described in panel A. The metalloprotease inhibitors marimastat (ma, 10 μ M), GW280264X (GW, 3 μ M) and GI254023X (GI, 3 μ M) were added as indicated.

C. IL-6 dependent Ba/F3 [gp130/IL-6R] cells were treated and analyzed as described in panel A and B. Cells were washed and stained with the α -IL-6R antibody M91 and analyzed by flow cytometry. The isotype control staining was performed with viable cells incubated with a monoclonal IgG1 antibody. Cell surface expression of the IL-6R is depicted in mean fluorescence intensity (MFI) units on the y-axis.

4.8 Extrinsic apoptotic pathways induced by Fas stimulation led to IL-6R shedding

Doxorubicin stimulation as well as cytokine withdrawal led to induction of the intrinsic apoptotic pathway in Ba/F3 [gp130/IL-6R] cells which was accompanied by shedding of the IL-6R from the cell surface. To investigate whether shedding of the IL-6R is stimulated during extrinsic apoptosis, further studies were performed with the human hepatocellular carcinoma cell line HepG2.

Fas has been shown to trigger apoptosis by binding to its natural ligand (FasL) or to specific anti-Fas agonistic antibodies. HepG2 cells were resistant to FasL or anti-Fas treatment, but were rendered susceptible in the presence of cycloheximide (CHX) an inhibitor of protein translation. The cytotoxicity induced by anti-Fas/CHX was accompanied by cleavage of several caspase substrates like PKC δ and PARP, indicating apoptotic death of HepG2 cells (Figure 15A). Although HepG2 cells express endogenously the IL-6R, the protein levels were not sufficient to perform Western blot analysis. Therefore HepG2 cells were transiently transfected with an expression plasmid coding for the human IL-6R throughout this study. Western blot analysis of apoptotic HepG2 cells revealed that the levels of cellular IL-6R were reduced after anti-Fas/CHX treatment but not after CHX or anti-Fas treatment alone. The cleavage product of PKC δ (cleaved PKC δ) was also only detectable during the combined anti-Fas/CHX treatment, indicating that neither CHX nor anti-Fas had the ability to induce apoptosis when incubated separately (Figure 15A). Western blot analysis of cell culture supernatants revealed that anti-Fas/CHX treatment led to increased sIL-6R release compared to control cells (Figure 15B, lane 1 and 2). Release of the sIL-6R after anti-Fas/CHX treatment was comparable with PMA-induced sIL-6R release. Cellular IL-6R levels decreased after PMA/CHX or anti-Fas/CHX treatment, indicating that IL-6R was shed from the cell surface.

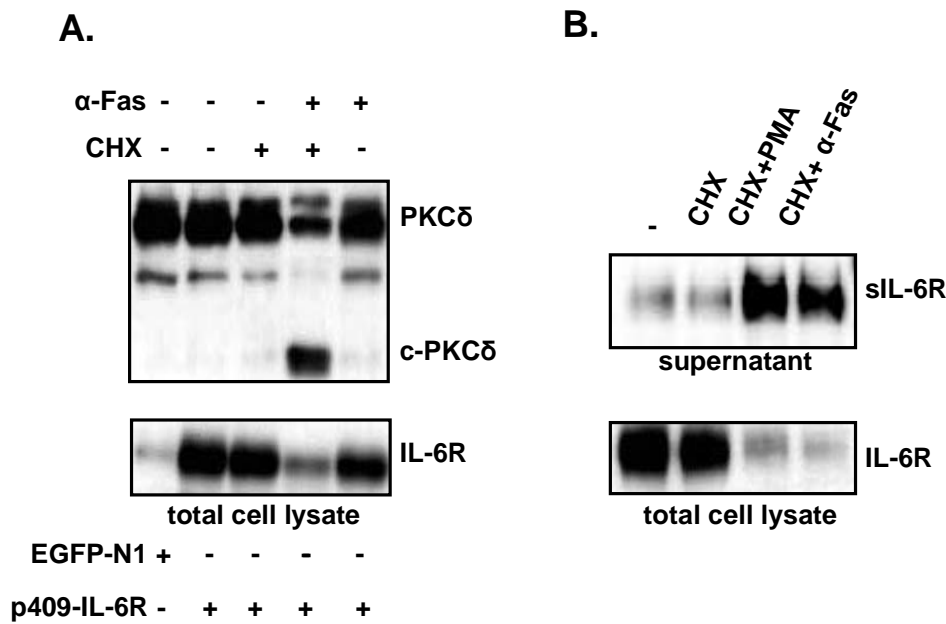


Figure 15: Soluble IL-6R release after induction of extrinsic apoptosis by agonistic Fas antibodies.

A. HepG2 cells were transiently transfected with expression plasmids encoding the human IL-6R or a control marker protein EGFP. Cells were treated with cycloheximide (CHX, 100 μ M), agonistic α -Fas antibody CH-11 (α -Fas, 500 ng/ml) or a combination of cycloheximide and agonistic α -Fas antibody CH-11 for 6 hours. Cell lysates were prepared and Western blot analysis of IL-6R and the caspase-3 substrate PKC δ was performed (c-PKC δ : cleaved-PKC δ). Apoptosis visualized by the appearance of c-PKC δ was only detectable in the cells which were treated with cycloheximide in combination with α -Fas.

B. HepG2 cells were transfected with p409-IL-6R expression plasmid and treated with CHX (100 μ M, 6 hours), CHX (100 μ M, 6 hours) + PMA (100 nM added directly to the supernatants after 4 hours cycloheximide treatment) or CHX (100 μ M, 6 hours) + α -Fas antibody CH-11 (500 ng/ml, 6 hours). After stimulation the soluble IL-6R was precipitated from the supernatant and lysates were prepared from the cell pellets. IL-6R and sIL-6R were subsequently visualized by Western blot analysis.

Inhibitor studies were performed to test whether the formation of sIL-6R during Fas-induced apoptosis was mediated by metalloprotease activity. The presence of the broad-spectrum metalloprotease inhibitor TAPI-2 markedly blocked formation of sIL-6R. Fas-induced IL-6R shedding was also blocked in the presence of the combined ADAM10/ADAM17 (GW280264X) inhibitor but not in the presence of the selective ADAM10 (GI254023X) inhibitor. In line with the data of apoptotic Ba/F3 [gp130/IL-6R] cells, Fas-induced IL-6R shedding was mediated by the metalloprotease ADAM17. Since PARP cleavage was not inhibited, blockade of the sheddases did not interfere with the progression of apoptosis (Figure 16).

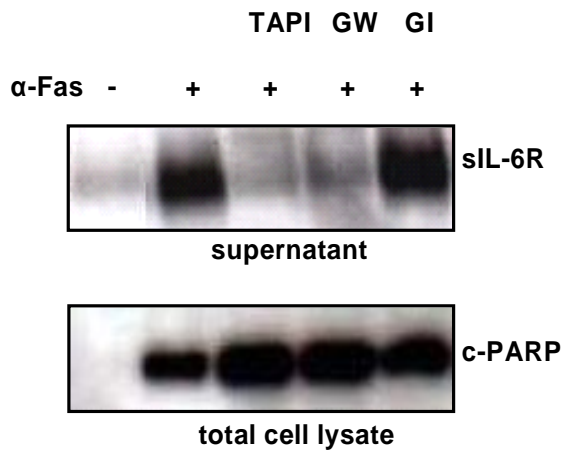


Figure 16: TAPI and GW280264X inhibited shedding of the IL-6R extracellular domain during Fas-induced apoptosis.

TAPI-2 (100 μ M), GW280264X (GW, 3 μ M) and GI254023X (GI, 3 μ M) were added to HepG2 cells (transfected with the p409-IL-6R plasmid) 15 minutes prior induction of apoptosis by Fas stimulation. Apoptosis was induced as described in Figure 15. After 6 hours of agonistic α -Fas/CHX treatment the sIL-6R was immunoprecipitated from the cell

culture supernatants and analyzed by Western blotting with α -IL-6R 14-18 antibody. Lysates of treated cells were also analyzed by Western blotting with α -PARP antibody (c-PARP: cleaved PARP). Shedding of the IL-6R was inhibited in presence of TAPI-2 and GW280264X. The metalloprotease inhibitors did not interfere with the apoptotic program since the caspase substrate PARP, which is cleaved only during programmed cell death, was present in the cleaved form in presence as well as in absence of the metalloprotease inhibitors (lane 2-5).

4.9 Overexpression of dominant-negative ADAM17 suppresses IL-6R shedding during PMA stimulation and apoptosis

It has been shown that transfection of a deletion mutant of human ADAM17 lacking the prodomain and catalytic domain results in inhibition of the proteolytic release of TNF- α and TNF receptor II. This deletion mutant has been postulated to act as a dominant-negative inhibitor for endogenous TACE activity (163). The cDNA encoding for the dominant-negative ADAM17 was amplified from reverse transcribed HepG2 RNA. The amplified cDNA encoded the disintegrin, transmembrane and cytoplasmic tail regions of ADAM17. The ADAM17 PCR-Product (encoding for amino acids S 474 to C 824) was cloned into the spIL-6/pESL vector (Rabe B., Department of Biochemistry, University Kiel, unpublished results) and subsequent subcloned into the mammalian expression vector p409b which drives the expression of a the dominant-negative TACE N-terminally fused to the signal peptide of human IL-6 and C-terminally to the c-myc as well as the his tag. This mutant was referred to as DN-ADAM17.

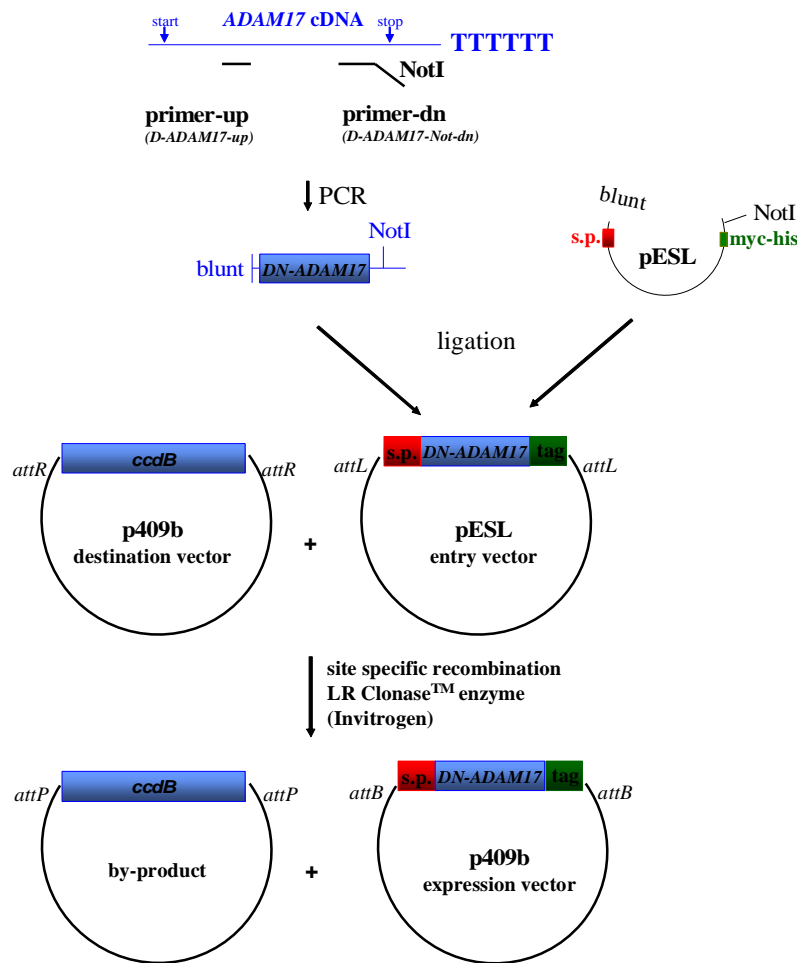


Figure 17: Cloning scheme for the vectors pESL-DN-ADAM17 and p409b-DN-ADAM17.

Total RNA was isolated from HepG2 cells and the mRNA was subsequently reverse transcribed into cDNA using an oligo dT-Primer. The transcript encoding for the mutant ADAM17 (DN-ADAM17) was amplified with the primers *D-ADAM17-up* and *D-ADAM17-Not-dn* (sequences are listed in the appendix) and the resulting PCR product was cloned in the entry vector pESL between the sequence encoding for the signal peptide of IL-6 (s.p.) and the sequence encoding for a c-myc and a his tag. To transfer the insert into the expression vector p409b (destination

vector) the Gateway® technology (Invitrogen) was used, which is based on the bacteriophage lambda site-specific recombination system. The recombination occurred between the site-specific *att* sites. The *attL* sites encoded by the pESL vector served as the binding site for the recombination protein mix LR-Clonase™ and the recombination occurred between the *attL* (entry vector) and the *attR* (destination vector, p409b) to give to *attB* sites. The presence of the *ccdB* gene allows negative selection of the destination vector after recombination (by-product). The CcdB protein interferes with *E.coli* DNA gyrase, thereby inhibiting growth of most *E.coli* strains. When recombination occurs (between the destination vector and the entry vector) the *ccdB* gene is replaced by the gene of interest.

The DN-ADAM17-p409b plasmid was transiently transfected in HepG2 cells and membrane localization of DN-ADAM17 was monitored by preparation of membrane fractions. Cell surface expression was monitored by surface biotinylation experiments. DN-ADAM17 was detected by Western blot analysis in the membrane fraction of transfected HepG2 cells whereas endogenous levels of ADAM17 were detectable in the membrane fraction of DN-ADAM17 overexpressing as well as in control HepG2 cells (Figure 18A). To further analyze

the localization of DN-ADAM17 protein, surface biotinylation of transfected HepG2 cells was performed. Western blot analysis of streptavidin-precipitated lysates prepared from surface-labeled cells revealed that DN-ADAM17 is located on the plasma membrane (Figure 18B).

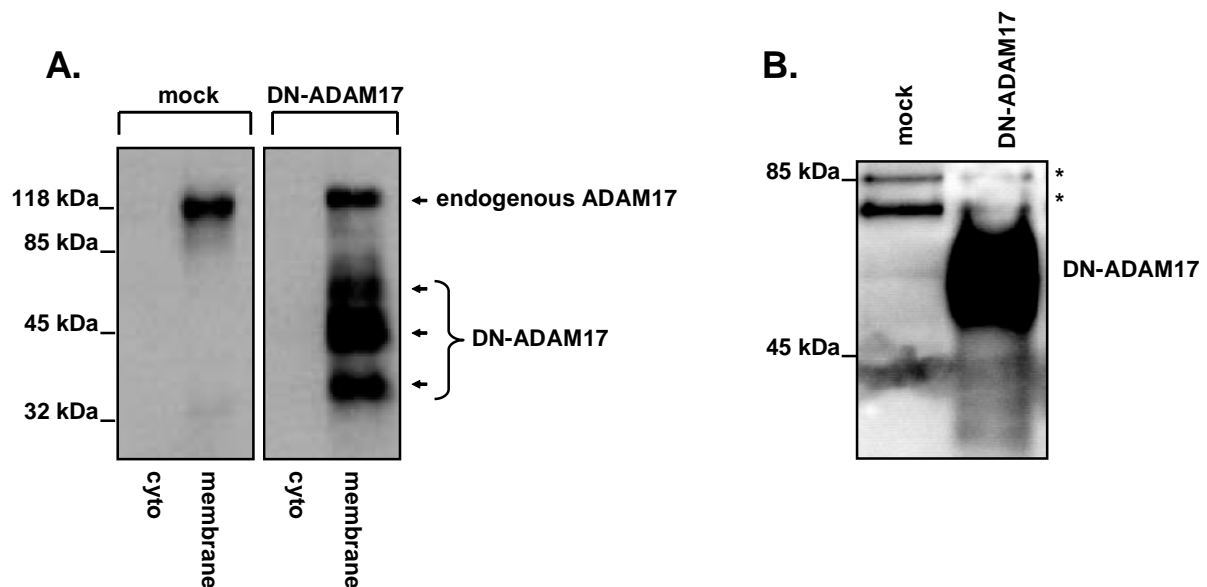


Figure 18: Membrane localization and surface expression of DN-ADAM17.

A. Membrane and cytosolic fractions were prepared from mock as well as from DN-ADAM17 expressing HepG2 cells. Protein concentrations were determined and 10 μ g total protein was loaded on a SDS-gel. Subsequent Western blot analysis with α -ADAM17 antibody raised against the C-terminus of human ADAM17 revealed that both endogenous ADAM17 and DN-ADAM17 were located in the membrane fraction. Several bands, probably representing different glycosylation isoforms, were detected in the membrane fraction of DN-ADAM17 overexpressing HepG2 cells.

B. Transiently transfected HepG2 cells with empty vector (mock, p409b) or with p409b/DN-ADAM17 were surface-biotinylated with Sulfo-NHS-Biotin. Surface-labeled cells were lysed, and the lysates were precipitated with streptavidin-coated agarose beads. The precipitated surface proteins were subjected to SDS-PAGE and transferred onto a PVDF membrane for Western blotting. With antibodies against the c-myc tag DN-ADAM17 was visualized (* unspecific band).

Given the information that DN-ADAM17 is expressed and probably transferred to the cell surface double transfected HepG2 cells were used for further studies. HepG2 cells were transfected with a plasmid coding for the human IL-6R in presence or absence of DN-ADAM17. IL-6R secretion into the culture supernatant was quantified by a specific IL-6R

“sandwich”-ELISA. HepG2 cells which expressed only the IL-6R produced on average 4 ng/ml sIL-6R. PMA as well as doxorubicin treatment led to 2-3 fold increase of secreted IL-6R. Cotransfection of the DN-ADAM17 mutant did not interfere with constitutive sIL-6R release (Figure 19A). However the stimulated sIL-6R release after PMA as well as anti-Fas treatment was reduced by 31 % and 28 % respectively, supporting the view that ADAM17 is responsible for stimulated IL-6R shedding (Figure 19A, B). IL-6R shedding was not reduced to background level after cotransfection of DN-ADAM-17. This might be explained by the fact that the amount of the mutant ADAM17 did not largely exceed the amount of endogenous ADAM17 (Figure 18A).

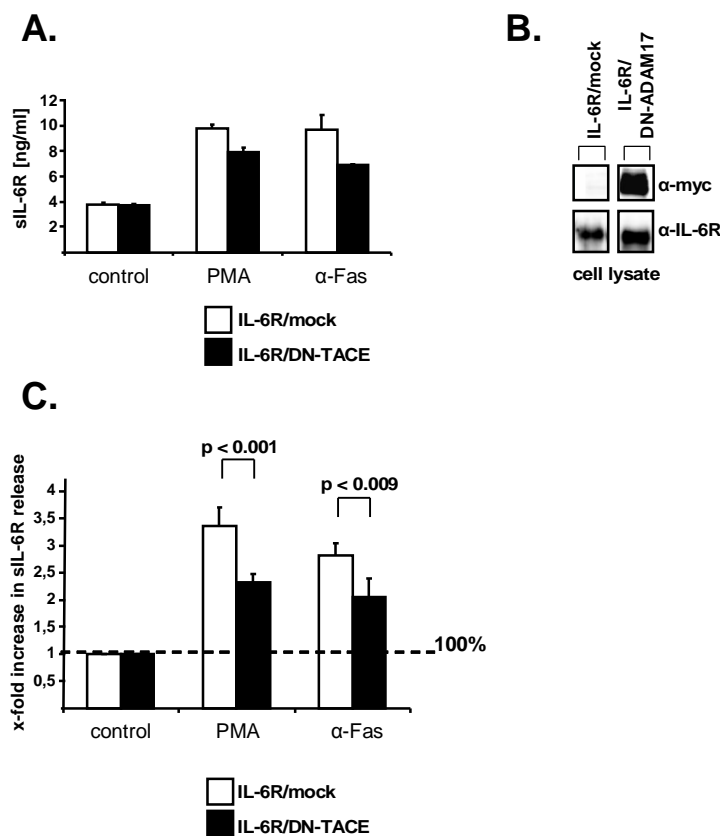


Figure 19: Effect of DN-ADAM17 on IL-6R shedding after PMA as well as α -Fas treatment.

A. HepG2 cells were transiently transfected with IL-6R cDNA alone (white bars, 1 μ g p409b-IL-6R, 9 μ g p409b) or with DN-ADAM17 cDNA (black bars, 1 μ g p409b-IL-6R, 9 μ g p409b-DN-ADAM17). Afterwards the cells were stimulated with CHX (100 μ M, 6 hours) with CHX (100 μ M, 6 hours)+ PMA (100 nM added directly to the supernatant after 4 hours CHX treatment) or CHX (100 μ M, 6 hours) + α -Fas antibody CH-11 (500 ng/ml, 6 hours). After stimulation soluble IL-6R-protein amounts were quantified using the sIL-6R specific ELISA. Cotransfection of DN-ADAM17 did not interfere with baseline shedding but reduced PMA as well as α -Fas stimulated shedding.

B. HepG2 cells were transiently transfected with IL-6R cDNA alone (white bars, 1 μ g p409b-IL-6R, 9 μ g p409b) or with DN-ADAM17 cDNA (black bars, 1 μ g p409b-IL-6R, 9 μ g p409b-DN-ADAM17). 48 hours after transfection the cells were lysed and Western blot analysis was performed to monitor DN-ADAM17 expression with the α -c-myc antibody. The α -IL-6R antibody 14-18 was used to visualize amounts of IL-6R.

C. HepG2 cells were transiently transfected and stimulated as described in A. The sIL-6R protein in the culture media was quantified using the IL-6R ELISA. The fold increase of the sIL-6R is expressed as percentage of baseline shedding which was set to 1 (100 %). Values represent the mean \pm SD from 3 independent experiments. The P values were determined using the Student’s T test.

4.10 ADAM17 activation during apoptosis is caspase dependent

Caspases are major intracellular effectors of intrinsic and extrinsic apoptosis. To establish a link between caspase activation and IL-6R shedding, zVAD-fmk (pan-caspase inhibitor) was applied 30 minutes prior anti-Fas/CHX treatment. HepG2 cells were stimulated to undergo apoptosis by Fas ligation in the presence of zVAD-fmk. Inclusion of zVAD-fmk prevented apoptosis and inhibited the processing of the caspase substrates PARP and PKC δ (Figure 20). At the same time, shedding of the IL-6R was completely abrogated, indicating that caspase activation was required for ADAM17 activation.

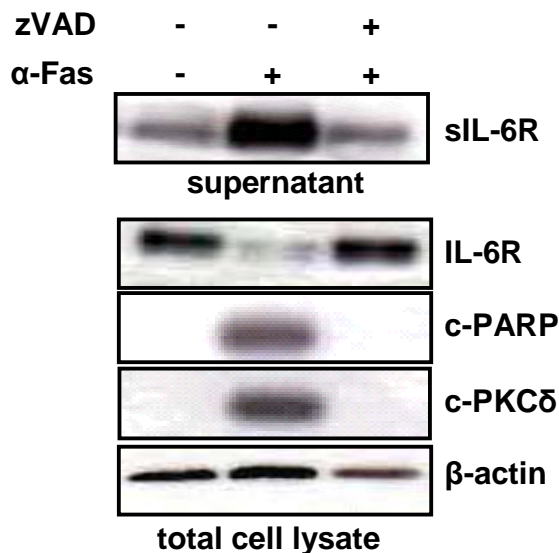


Figure 20: The pan-caspase inhibitor zVAD-fmk decreased α -Fas-induced shedding of the IL-6R.

HepG2 cells were transiently transfected with p409b-IL-6R plasmid and stimulated with α -Fas (500 ng/ml)/CHX (100 μ M) to undergo apoptosis. Control cells were treated with CHX (100 μ M). The pan-caspase inhibitor zVAD-fmk was added as indicated at a concentration of 100 μ M 30 minutes before exposure of the cells to α -Fas/CHX. After 6 hours of incubation the cell culture media as well as the cell pellets were harvested. The sIL-6R was immunoprecipitated

from the supernatants as described in Figure 9. The lysates were directly used for analysis of following proteins: IL-6R, cleaved PAPP (c-PARP), cleaved PKC δ (c-PKC δ) and β -actin (loading control).

To further investigate if a special caspase isoform was involved in regulating IL-6R shedding during apoptosis, more specific inhibitors for the initiator caspase-8, caspase-9, and for the effector caspase-3 were used. Apoptosis was induced in HepG2 cells by Fas ligation in presence of the different inhibitors. None of the isoform-specific caspase-inhibitors tested led to appreciable blockade of IL-6R shedding during apoptosis. However, combined inhibition of caspase-8 and -9 reduced IL-6R release, and further multiple inhibition of caspase-3, -8 and -9 completely abolished apoptosis-induced IL-6R shedding (Figure 21).

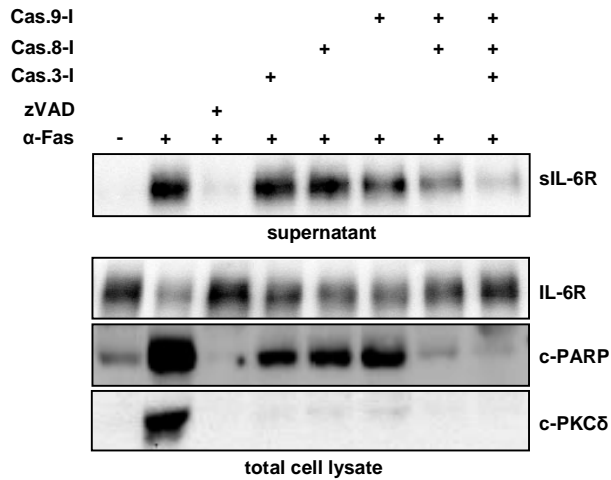
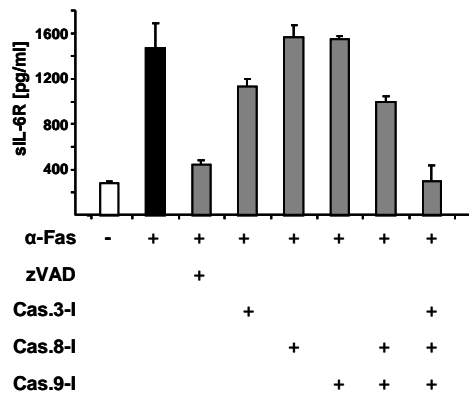
A.**B.**

Figure 21: Combined inhibition of caspase-8, -9 and -3 led to reduction of α -Fas-induced IL-6R shedding.

A. HepG2 cells overexpressing the IL-6R were stimulated with α -Fas (500 ng/ml)/CHX (100 μ M) in presence of 100 μ M zVAD-fmk (pan-caspase inhibitor, lane 3), 100 μ M zDEDV-fmk (caspase-3 inhibitor, lane 4), 100 μ M zIETD-fmk (caspase-8 inhibitor, lane 5), 100 μ M zLEHD-fmk (caspase-9 inhibitor, lane 6), zIETD-fmk + zLEHD-fmk (50 μ M each, lane 7) or zDEDV-fmk + zIETD-fmk + zLEHD-fmk (33 μ M each, lane 8). Control cells were incubated only with 100 μ M CHX (lane 1). The caspase inhibitors were added 30 minutes prior α -Fas/CHX stimulation. After 6 hours incubation period the sIL-6R-protein was precipitated from the culture supernatant and visualized by Western blotting using the α -IL-6R antibody 14-18. The cells were lysed and also subjected to Western blot analysis as described in Figure 9.

B. HepG2 cells were treated as described in A. and culture media were analyzed in triplicates with the sIL-6R ELISA.

4.11 Apoptosis-induced IL-6R shedding is PKC-, MAPK- and ROS-independent

Using specific metalloprotease inhibitors as well as a dominant-negative ADAM17 variant, the metalloprotease ADAM17 was identified as sheddase which mediated IL-6R shedding during apoptosis. From the fact that treatment of HepG2 cells with the protein biosynthesis inhibitor cycloheximide did not affect IL-6R shedding, enhanced ADAM17 protein synthesis

during apoptosis was excluded. To analyze if pre-existing ADAM17 molecules were activated during apoptosis HepG2 cells were incubated with anti-Fas antibody for 2, 4 and 6 hours. Afterwards the cells were lysed and ADAM17 was immunoprecipitated from the cell lysate by using an ADAM17 specific antibody directed against the C-terminus of the protein. Western blot analysis of the precipitated lysates revealed that in control cells ADAM17 was mainly present in the proform. After induction of apoptosis there was a time dependent decrease of the ADAM17 unprocessed proform and at the same time an increase in the active mature form detectable (Figure 22).

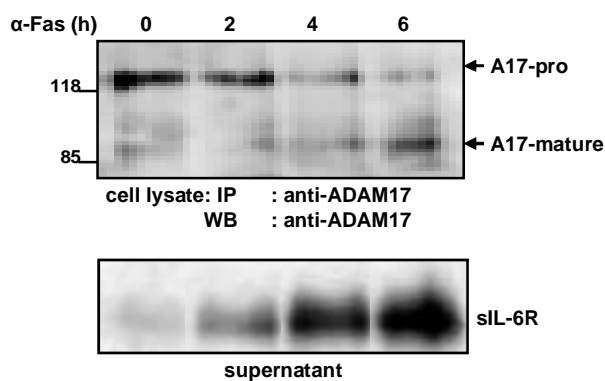


Figure 22: Activation of pre-existing ADAM17 molecules during Fas-induced apoptosis.

HepG2 cells were stimulated with 500 ng/ml α -Fas antibody (CH-11) and CHX (100 μ M) for the indicated time periods. The control cells (0 hours, α -Fas) were treated only with cycloheximide for 6 hours. The cell culture supernatants were collected and sIL-6R was precipitated as

described above. The cell pellets were lysed in 100 μ l lysis buffer containing 2 % detergent. Afterwards the lysate was diluted 1:10 with PBS (containing protease inhibitors) and supplemented with 3 μ g α -ADAM17 antibody (Chemicon) and 50 μ l Protein A-Sepharose. After an incubation period of 16 hours, the Protein A-Sepharose beads were washed and protein complexes were suspended in 60 μ l Lämmli-buffer. 20 μ l were loaded onto a SDS-Gel. The subsequent Western blot analysis was performed with the α -ADAM17 antibody (Chemicon).

To investigate the molecular mechanism which led to apoptosis-induced ADAM17 activation and subsequent IL-6R shedding, already described activators of metalloproteases were analyzed. The phorbol ester PMA, a well-known activator of PKC, has been shown to facilitate the shedding of several cell-surface receptors among them also the IL-6R (Figure 9, 15, 20). The PKC family consists of 11 isoenzymes, which can be subdivided into three groups. The conventional PKCs (α , β _I, β _{II}, γ) depend on Ca^{2+} and are activated by diacylglycerol or the analogon PMA. The novel PKCs (δ , ϵ , η , θ) are also activated by diacylglycerol but are Ca^{2+} - independent. Finally, the atypical PKCs (ζ and λ) are Ca^{2+} - independent and do not respond to diacylglycerol (164-166). During apoptosis PKC δ is activated by caspase-3

cleavage (Figure 8, 15, 20). It has been reported that proteolytic activation of PKC δ contributes to certain features of the apoptotic phenotype, like nuclear fragmentation (127) (167) To investigate if a member of the PKC family was involved in ADAM17 activation during apoptosis, HepG2 cells were stimulated to undergo apoptosis by anti-Fas treatment in the presence of the PKC inhibitors GF109203X (pan-PKC inhibitor) and Gö6976 (conventional PKC inhibitor). As control, HepG2 cells were stimulated with PMA, a well known activator of PKCs. Both inhibitors effectively blocked PMA-induced IL-6R shedding indicating that PMA led to activation of a conventional PKC family member, which subsequent mediate the activation of ADAM17. Contrary to PMA-induced shedding, Fas-induced shedding could not be blocked by any of the PKC inhibitors, suggesting that upon apoptosis induction, ADAM17 was activated in a PKC-independent manner. Inhibition of PKCs did not inhibit caspase-3 cleavage and activation, since PKCs are believed to act downstream of caspase-3.

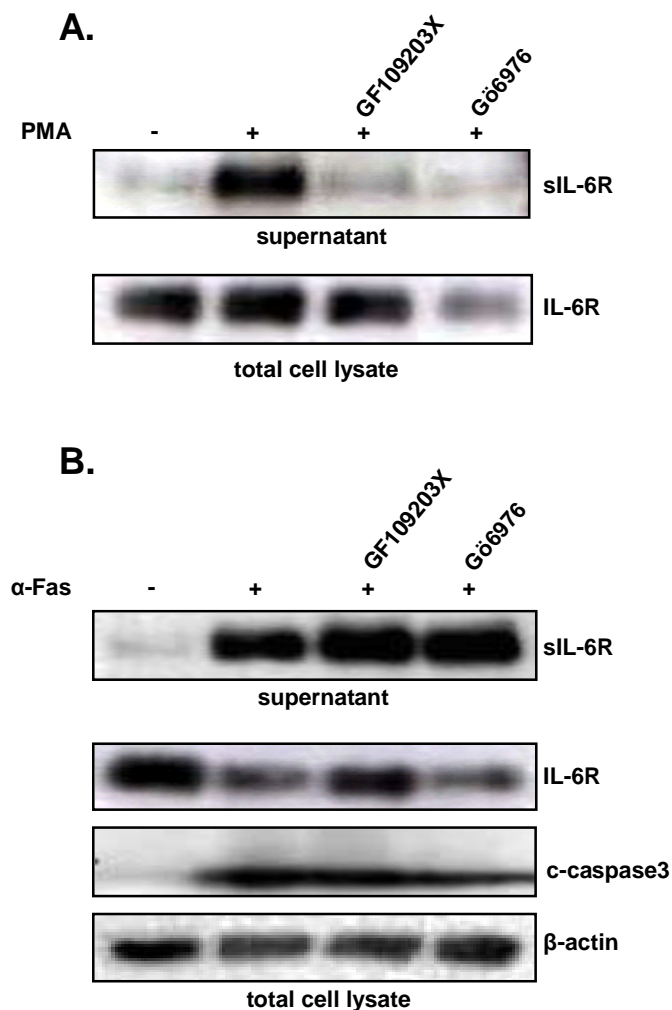


Figure 23: Apoptosis-induced shedding of the IL-6R was PKC independent.

A. HepG2 cells overexpressing the IL-6R were incubated with PMA (100 nM) for 2 hours. The pan-PKC inhibitor GF109203X (5 μ M) as well as the conventional PKC inhibitor Gö6976 (1 μ M) were added 15 minutes prior PMA stimulation as indicated. The sIL-6R was immunoprecipitated from the cell culture supernatants as described in Figure 9. The cells were lysed and the lysate was subjected to SDS-PAGE. Western blot analysis was performed with the α -IL-6R antibody 14-18.

B. HepG2 cells overexpressing the IL-6R were incubated with α -Fas (500 ng/ml)/CHX (100 μ M) for 6 hours. Control cells (lane 1) were incubated with CHX (100 μ M) alone. Inhibitors were added as described in A. Western blot analysis was also performed as described in A (c-caspase-3, cleaved caspase-3).

Besides of PKCs it has been postulated that PMA-induced ADAM17 activation is mediated by serine/threonine kinases belonging to the mitogen-activated protein kinase (MAPK)-family. During the last years accumulating studies have informed the view that the MAPKs Erk and p38 mediate most of the shedding-activation signals triggered by growth factors, stress and commonly used non-physiological drugs (168, 169). Phosphorylation of the cytoplasmic tail of ADAM17 (threonine₇₃₅) by the MAP kinase Erk was associated with subsequent ADAM17 activation (89). Osmotic stress-induced ADAM17 activation (e.g. sorbitol) can be mediated via the MEK/Erk pathway or the p38-MAPK pathway. It has been shown that osmotic stress-mediated HB-EGF shedding is controlled by p38 activity implicating that p38-MAPK is an upstream activator of ADAM metalloproteases (170). Thus MAPK pathways participate in regulating ADAM-mediated ectodomain shedding of various substrates.

To test whether p38- or Erk-MAPKs were upstream regulators of apoptosis-induced IL-6R shedding, transiently transfected HepG2 cells were stimulated to undergo apoptosis by Fas ligation in presence of the p38 inhibitor SB202190 or the Erk inhibitor U0126. Apoptosis-induced IL-6R shedding was unaffected in the presence of both inhibitors suggesting that MAPK pathways were not involved in ADAM17 activation during programmed cell death.

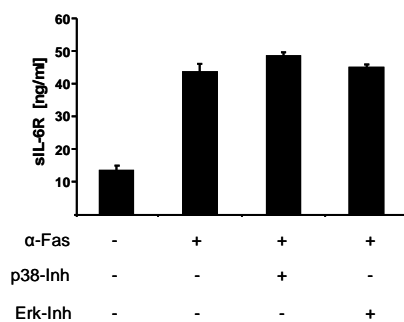


Figure 24: Apoptosis-induced shedding was p38- and Erk-MAPK independent.

Transiently transfected HepG2 cells with the expression plasmid p409b-IL-6R were incubated with CHX (100 μM, 6 hours, bar 1) or with CHX (100 μM)/α-Fas (500 ng/ml, 6 hours, bar 2) to undergo apoptosis. The p38-MAPK inhibitor SB202190 (10 μM) as well as the Erk-MAPK inhibitor U0126 (5 μM) were added as indicated 15 minutes prior α-Fas treatment. The cell culture

supernatants were collected and analyzed with the specific sIL-6R ELISA. The standard deviation was determined from triplicate values.

Reactive oxygen species (ROS, e.g. H₂O₂) have been shown to activate ADAM17. The proposed mechanism was that ROS mediate the release of the inhibitory N-terminal prodomain which masks the catalytic domain of the enzyme. ROS attack the cysteine

sulfhydryl moiety of the ADAM17 prodomain and release it from coordination with the catalytic zinc of the metalloprotease domain, thus activating TACE.

Activation of the Fas receptor results in signal transduction pathways which lead to cytochrome *c* release and ROS formation. Although the major biological process leading to oxygen-derived generation of ROS is electron transport associated with mitochondrial membranes, the membrane-bound NADPH oxidase appeared to play a role in production of ROS in conjunction with apoptosis. The NADPH oxidase consists of several components and all of them have been detected in HepG2 cells (171, 172). To test whether the production of ROS is involved in ADAM17 activation and subsequent shedding of the IL-6R during apoptosis, the flavine oxidase inhibitor DPI and the ROS-scavengers 1,3-dimethyl-2-thiourea (DMTU) and *n*-propyl-gallete (nPG) were used. HepG2 cells were stimulated to undergo apoptosis by Fas treatment in presence of the NADPH oxidase inhibitor or the ROS-scavengers. Anti-Fas treatment led to a three fold increase of sIL-6R in the cell culture supernatants. This effect could not be blocked by DPI or the combined treatment of DMTU/nPG suggesting that reactive oxygen species were not involved in the signal transduction leading to ADAM17 activation after induction of apoptosis.

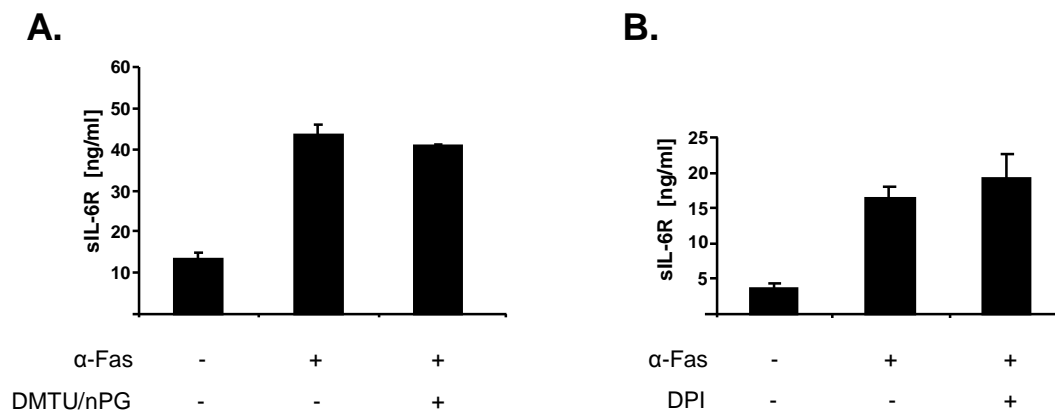


Figure 25: The NADPH oxidase inhibitor DPI as well as the ROS-scavengers DMTU and nPG did not inhibit sIL-6R release from α -Fas treated cells.

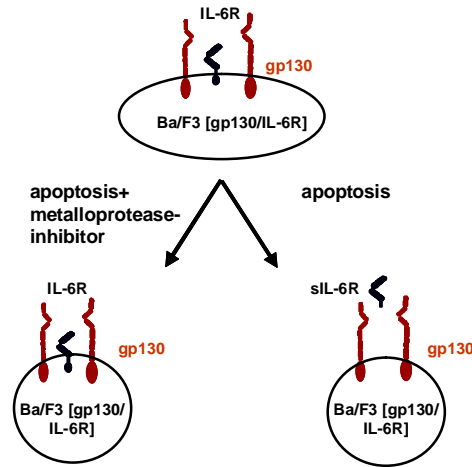
A. HepG2 cells were treated with α -Fas (500 ng/ml)/CHX (100 μ M) for 6 hours in the presence or absence of the ROS-scavengers DMTU (20 mM) and nPG (100 μ M). ROS-scavengers were added 30 minutes prior α -Fas stimulation. The cell culture supernatants were collected and analyzed with the specific sIL-6R ELISA. The standard deviation was determined from triplicate values.

B. HepG2 cells were treated with α -Fas (500 ng/ml)/CHX (100 μ M) for 6 hours in the presence or absence of the NADPH inhibitor DPI (10 μ M). DPI was added 30 minutes prior α -Fas stimulation. The cell culture supernatants were collected and analyzed as described in A.

4.12 IL-6R shedding is not required to terminate IL-6-induced STAT3 phosphorylation during apoptosis

IL-6 mediated signal transduction involves first binding of the α -chain IL-6R and subsequent recruitment of two gp130 subunits. The signals which are transmitted into the cells by gp130 lead to induction of pro-survival pathways. It is known for example that Bcl-X_L and Bcl-2, which represent anti-apoptotic members of the Bcl-family, are target genes for the activated transcription factor STAT3. Shedding of the IL-6R during apoptosis resulted in diminished cell surface expression of the receptor. Without the α -chain, cells become unresponsive to IL-6. To investigate if apoptosis-induced shedding of the IL-6R is required to terminate IL-6-induced signal transduction, Ba/F3 [gp130/IL-6R] cells were used. The cells were treated with doxorubicin for 2 hours, 4 hours and 6 hours and subsequently stimulated for 10 minutes with IL-6 to induce STAT3 phosphorylation. Upon induction of apoptosis, the cells become less susceptible to IL-6 stimulation as indicated by decreasing STAT3 phosphorylation after 4 and 6 hours. Surprisingly, blocking IL-6R shedding during apoptosis by the broad-spectrum metalloprotease inhibitor marimastat, did not increase the amount of phosphorylated STAT3, indicating that the role of IL-6R shedding is not termination of STAT3 activation.

A.



B.

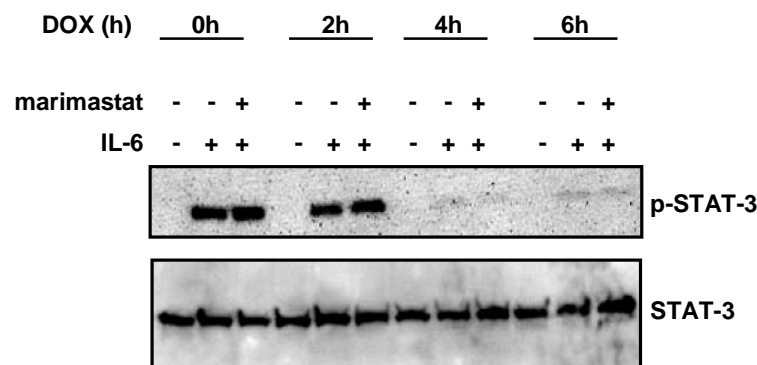


Figure 26: STAT3 phosphorylation was abrogated during apoptosis.

A. Schematic representation of the experiment described in B. Ba/F3 [gp130/IL-6R] cells were stimulated to undergo apoptosis by doxorubicin treatment. During apoptosis the IL-6R is shed from the cell surface and the cells become unresponsive to IL-6. Induction of apoptosis in presence of the metalloprotease inhibitor marimastat, abrogated shedding and rescued IL-6R cell surface expression.

B. Ba/F3 [gp130/IL-6R] cells were washed 3 times and incubated for 0, 2, 4 and 6 hours with 500 ng/ml doxorubicin, in serum-free medium and in the absence of IL-6. The metalloprotease inhibitor

marimastat was added as indicated to prevent IL-6R shedding at a concentration of 10 μ M. After the induction period, the cells were centrifuged and resuspended in medium containing IL-6 (200 ng/ml) or without IL-6 as control for 10 min. The cells were immediately lysed and the proteins were immunoblotted with α -p-STAT3 antibody. Reprobing with an α -STAT3 specific antibody ensured comparable protein loading.

Apoptotic cells did not respond to IL-6 stimulation even when IL-6R shedding was prevented by metalloprotease inhibition. Upon induction of apoptosis gp130 mediated STAT3 activation was abrogated by different molecular mechanism than IL-6R shedding. Furthermore it was analyzed if the sIL-6R generated during apoptosis can bind IL-6 and activate surrounding cells via trans-signalling. HepG2 cells overexpressing the IL-6R were stimulated to undergo apoptosis by anti-Fas treatment in presence or absence of the pan-caspase inhibitor zVAD-fmk. The conditioned supernatants were harvested and supplemented with recombinant IL-6, to allow formation of [sIL-6R/IL-6] complexes. Afterwards Ba/F3 cells overexpressing the

human gp130 were stimulated with the conditioned supernatants. Ba/F3 [gp130] cells can induce STAT3 phosphorylation only following stimulation with IL-6 in the presence of the sIL-6R. As shown in Figure 27, only conditioned supernatants from apoptotic HepG2 cells induced STAT3 phosphorylation in Ba/F3 [gp130] cells, indicating that the sIL-6R generated during apoptosis is biologically active and can promote IL-6 trans-signalling.

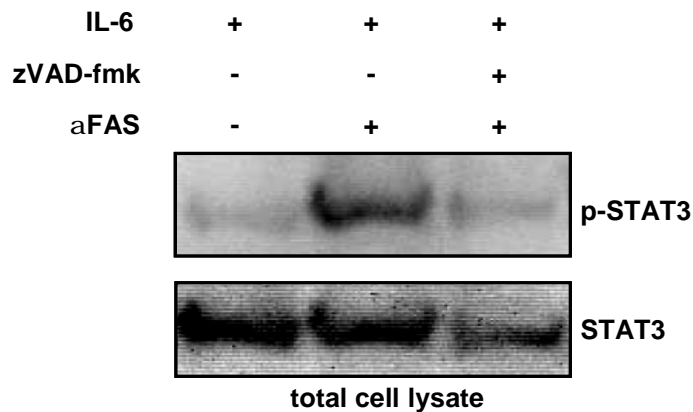


Figure 27: The sIL-6R generated during apoptosis was biological active. HepG2 cells were transfected with p409b-IL-6R and subsequent treated with CHX (100 μ M, control), α -Fas (500 ng/ml)/CHX (100 μ M) or α -Fas/CHX + zVAD-fmk (100 μ M). The supernatants were harvested and supplemented with 200 ng/ml recombinant human IL-6. After an incubation period of 30 min, the

supernatants were used to stimulate Ba/F3 [gp130] cells for 10 min. Afterwards the Ba/F3 [gp130] cells were spun down (13,000 rpm, 30sec, 4°C), the supernatant was discarded and the cell pellet was frozen in liquid nitrogen. Then the cell pellet was resuspended in 100 μ l 2x Lämmli buffer and 20 μ l were loaded on a SDS-gel. Western blot analysis was performed as described in Figure 26B.

4.13 Soluble IL-6R was released from apoptotic primary human neutrophils

To place these studies in a more physiological context apoptosis was induced in primary human neutrophils. In previous studies it was shown that human neutrophils express constitutively both, IL-6R mRNA and the mature protein (173, 174). Additionally it was shown that expression of the IL-6R on the cell surface of neutrophils was reduced after fMLP or PMA treatment. This loss correlated with a decrease in surface L-selectin expression, suggesting that the IL-6R was shed from neutrophils upon stimulation (174).

Human neutrophils were isolated from blood of healthy donors and apoptosis was subsequently induced by Fas stimulation, UV irradiation or doxorubicin treatment. Fas stimulation and UV treatment induced apoptosis of neutrophils with 45 % and 90 % of the

cells being annexin V-positive after 6 hours. Doxorubicin did not induce apoptosis in primary human neutrophils since there were no annexin V-positive cells detectable after treatment (Figure 28A). Western blot analysis of the cell culture media from apoptotic cells revealed increasing amounts of the IL-6R ectodomain compared to the control cells.

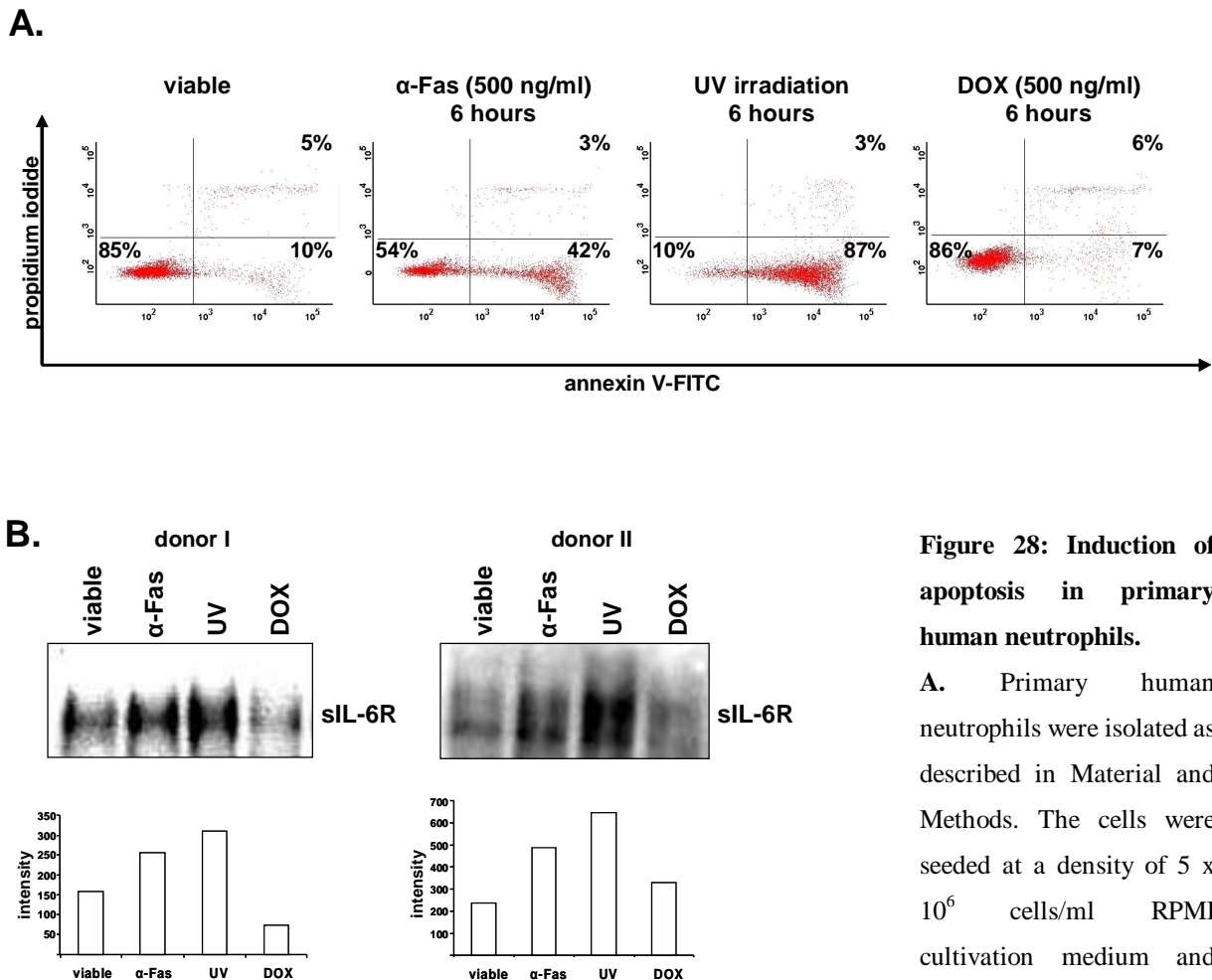


Figure 28: Induction of apoptosis in primary human neutrophils.

A. Primary human neutrophils were isolated as described in Material and Methods. The cells were seeded at a density of 5×10^6 cells/ml RPMI cultivation medium and apoptosis was induced as indicated. For UV

treatment the cells were exposed to $200,000 \mu\text{J}/\text{cm}^2$ UV and subsequent incubated at 37°C for 6 hours. The agonistic α -Fas antibody CH-11 (500 ng/ml) as well as doxorubicin (DOX) were added directly to the cultivation medium. Apoptosis was measured using annexin V-FITC/propidium iodide staining and flow cytometry. Annexin V-FITC staining is represented on the x-axis and propidium iodide-staining on the y-axis. The percentage of viable (lower left quadrant), apoptotic (lower right quadrant) and late apoptotic (upper right quadrant) cells are indicated.

B. Neutrophils were treated as described in panel A and the culture supernatants were immunoprecipitated with the polyclonal 6.2 α -IL-6R serum. The precipitated proteins were subjected to SDS-PAGE and Western blot analysis was performed with the α -IL-6R 14-18 antibody. Lower panel in B. shows intensities of the bands determined by densitometric quantification (Image J, NIH).

For further experiments primary human neutrophils were UV irradiated since this method led to high amounts of early apoptotic cells. Neutrophils were isolated from three different donors and apoptosis was induced in presence of the pan-metalloprotease inhibitor TAPI-2, the combined ADAM10/ADAM17 (GW) inhibitor and the selective ADAM10 (GI) inhibitor. Cell culture supernatants were prepared 6 hours after UV irradiation, and the levels of sIL-6R were assessed by Western blotting. To monitor apoptosis neutrophils were stained additionally with annexin V-FITC and propidium iodide and analyzed by flow cytometry (Table 3). As indicated in Figure 29, sIL-6R was shed from apoptotic neutrophils after UV irradiation to a larger extent than from untreated (viable) cells. The generation of sIL-6R during apoptosis was inhibited by TAPI-2 and by GW280264X but not by GI254023X. These data indicate that also in primary human neutrophils ADAM17, and not ADAM10, was responsible for the shedding of the IL-6R during apoptosis.

	viable neutrophils	early apoptotic neutrophils	late apoptotic neutrophils
untreated control	91%	7%	0.4%
UV irradiation	6%	93%	0.4%
UV irradiation in presence of TAPI (10 μ M)	4%	94%	1.4%
UV irradiation in presence of GW280264X (3 μ M)	8%	91%	0.5%
UV irradiation in presence of GI254023X (3 μ M)	6%	94%	0.6%

Table 3: Neutrophil apoptosis was not altered in the presence of different metalloprotease inhibitors.

Primary human neutrophils were UV irradiated (200,000 μ J/cm²) and afterwards incubated for 6 hours at 37°C. The cells were spun down and stained with annexin V-FITC/propidium iodide to monitor apoptosis. Via flow cytometry the viable (annexin V-negative/propidium iodide-negative), early apoptotic (annexin V-positive/propidium iodide-negative) and late apoptotic (annexin V-positive/propidium iodide-positive) cell populations were determined.

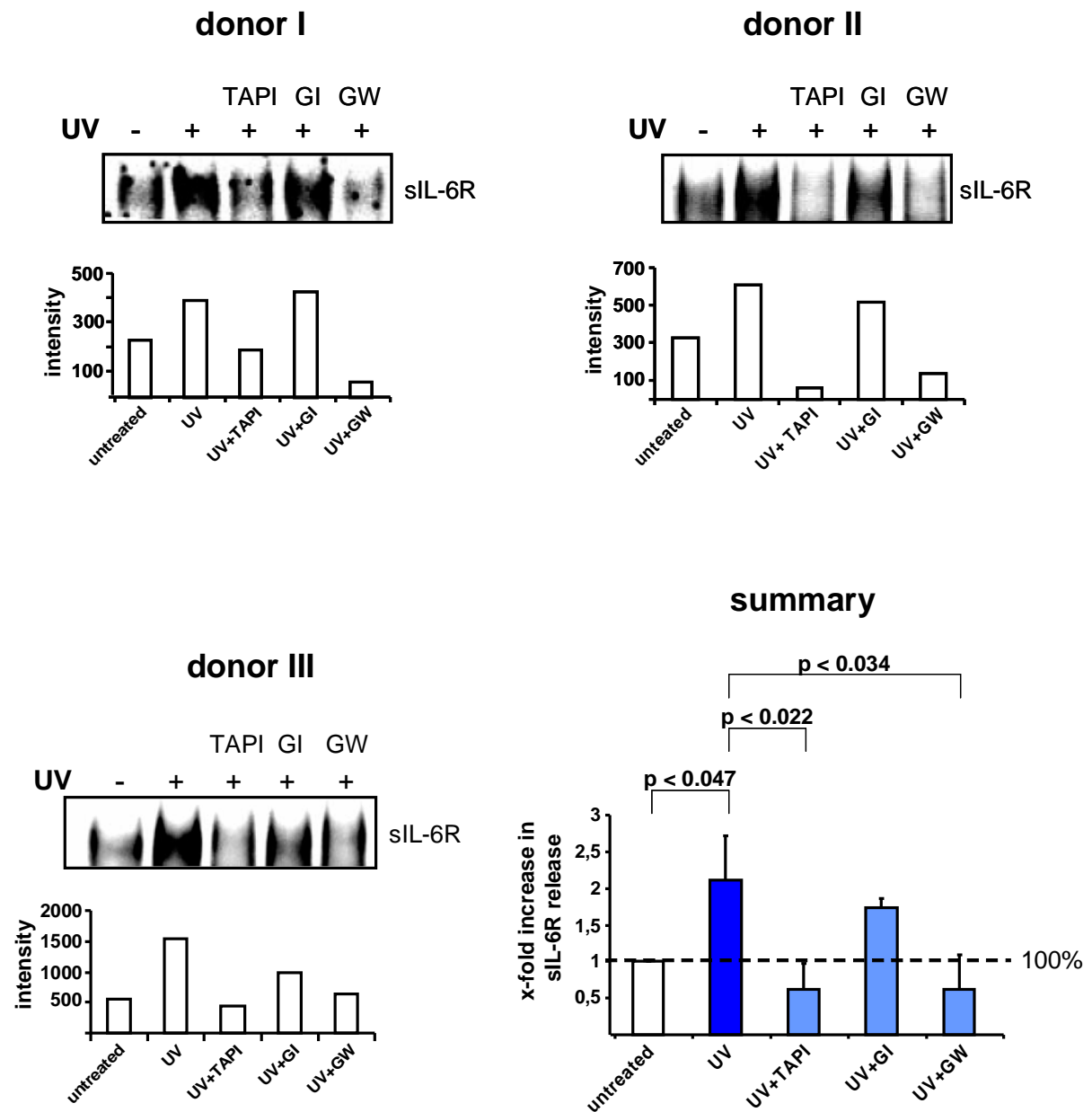


Figure 29: IL-6R was shed from apoptotic human neutrophils.

Neutrophils were isolated from three healthy donors and apoptosis was induced by UV irradiation. The metalloprotease inhibitors TAPI-2 (10 μ M), GW280264X (GW, 3 μ M) and GI254023X (GI, 3 μ M) were added as indicated 15 minutes prior UV irradiation. Soluble IL-6R was immunoprecipitated from the cell culture supernatant and subsequently analyzed by Western blotting. The lower panels show intensities of the protein bands determined by densitometric quantification. The intensities of the sIL-6R protein band of the three experiments were summarized and expressed as a percentage of the control (set to 100 %). The P values were determined using the Student's T test.

Apoptosis of Fas stimulated neutrophils could be prevented by the addition of the caspase-3 inhibitor zDEDV-fmk but not by recombinant IL-6 or the fusion protein HIL-6 (sIL-6/IL-6R, (152)), again indicating that the role of IL-6R-shedding is not to render the cells unresponsive to IL-6 but to induce IL-6 trans-signalling in neighbouring non-apoptotic cells.

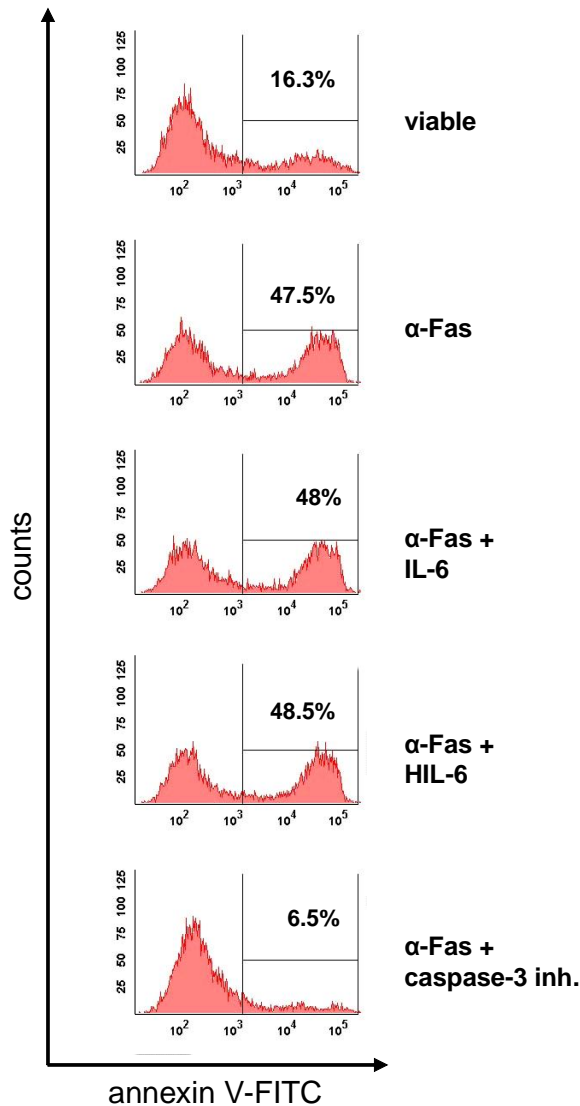


Figure 30: Apoptosis of neutrophils was not prevented by IL-6 or HIL-6.

Peripheral blood neutrophils were isolated as described in Materials and Methods and were stimulated with 500 ng/ml agonistic α -Fas antibody CH-11 and incubated for 7 hours in RPMI-medium. Recombinant human IL-6 (10 ng/ml), recombinant human Hyper-IL-6 (fusion protein of IL-6/IL-6R, 10 ng/ml) and the caspase-3 inhibitor zDEDV-fmk (100 μ M) were added to the culture medium together with the α -Fas antibody as indicated. To monitor apoptosis the cells were stained with annexin V-FITC and analyzed by flow cytometry. Annexin V-FITC fluorescence intensity is represented on the x-axis.

4.14 The murine air pouch model of acute inflammation

Induction of apoptosis in human neutrophils led to enhanced shedding of the IL-6R. Neutrophils, which release the IL-6R, play a dominant role in host defence. To investigate the role of IL-6R shedding *in vivo* a mouse model of inflammation was used where neutrophils infiltrate the inflamed area as first host defence reaction. Because neutrophils represent a short-lived cell population, they undergo apoptosis during resolution of inflammation and the

host defence is carried over by monocytes, which represent the second cell population infiltrating the inflamed area. Thus, resolution of the neutrophil infiltrate is associated with a subsequent recruitment of mononuclear cells (175). It has been described previously that neutralization of the IL-6R reduced the infiltration of immune cells in the murine carrageenan air pouch model of acute inflammation, but it was not demonstrated whether this reduction affected neutrophilic or mononuclear phagocytic cells (176). To demonstrate the importance of IL-6R signalling during acute inflammation and to discriminate between the neutrophilic and mononuclear cell population, the mouse air pouch model of acute inflammation was used. The air pouch model of acute inflammation described by Sedgwick *et al* (157) consists of a subcutaneous injection of air on the back of mice. This procedure results in the formation of an air pouch with lining cells morphologically and functionally similar to the synovium. The non-inflamed cavity is lined by a thin layer of fibroblasts and macrophage-like cells. The injection of the irritant carrageenan (a sulphated polysaccharide obtained from the alga *Chondrus crispus*) induces a local inflammatory response and the pouch serves as a reservoir of cells and mediators in the fluid that accumulate locally. The kinetic of leukocyte recruitment during carrageenan-induced inflammation in the air pouch was analyzed in previous studies. 24 hours after carrageenan injection most of the leukocytes which were recruited into the air pouch were polymorphonuclear leukocytes (PMN, neutrophils). The cell population changed from 48 hours after treatment to a prevalence of mononuclear leukocytes (monocytes, macrophages) (177).

Air pouches were formed on the dorsal skin of 8 to 10-week old male C57Bl/6 wildtype mice and 6 hours before carrageenan injection neutralizing anti-murine IL-6R antibodies (to inhibit classic signalling and trans-signalling) or recombinant soluble sgp130-Fc protein (to inhibit only trans-signalling) were administered. The mice were sacrificed 72 hours after induction of the acute inflammation and total cell numbers, cell numbers of neutrophils and mononuclear phagocytes as well as inflammatory mediators were determined. Figure 31 gives a schematic overview of the time schedule used in the air pouch experiments.

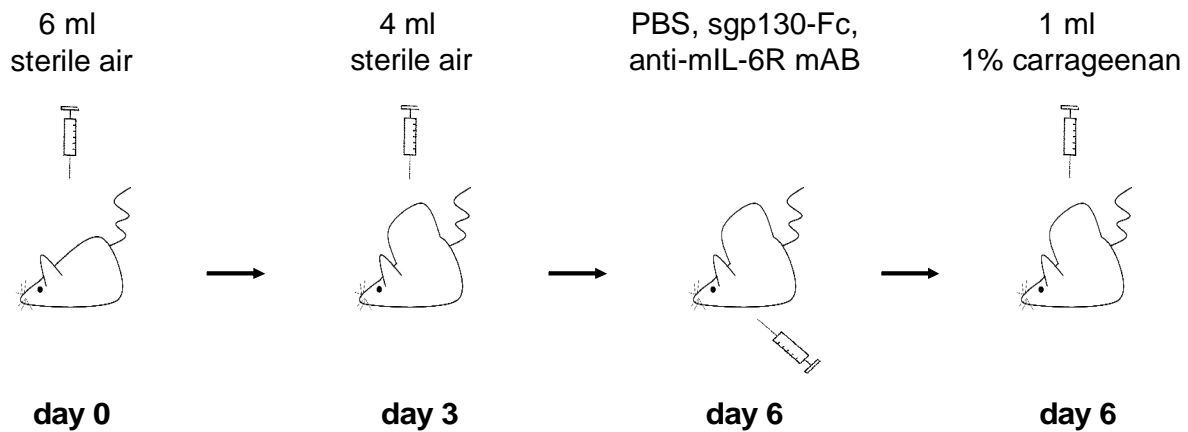


Figure 31: Time schedule of the air pouch experiments.

Air pouches were formed on the back of C57Bl/6 wildtype mice by injection of 6 ml sterile air. On day three the pouches were reinjected with 4 ml of sterile air. On day six the mice were challenged with neutralizing antibodies raised against the murine IL-6R or sgp130-Fc intraperitoneally and after 6 hours 1 ml of 1 % carrageenan (dissolved in PBS) was injected into the pouch. 72 hours after carrageenan injection the animals were sacrificed and the pouches were washed with 3 ml ice cold PBS to obtain the pouch lavage.

4.15 Injection of neutralizing IL-6R antibodies led to impaired monocyte infiltration in the inflamed air pouch

Two different neutralizing antibodies raised against the murine IL-6R were administered in 8 to 10 week old male C57Bl/6 wildtype mice before carrageenan injection. A group of five mice was challenged with PBS as control, five mice were challenged with 100 μ g anti-mouse IL-6R (clone D7715A7, diluted in PBS) and finally five mice were challenged with 100 μ g anti-mouse IL-6R (clone MR-16-1, diluted in PBS). Both antibodies were used in previous studies to block signal transduction mediated by the IL-6R (178-180) and were administered by intraperitoneal (i.p.) injection. 6 hours after the i.p. injection the mice were challenged with 1 % carrageenan solution to induce an inflammatory response. After 72 hours the mice were sacrificed, the pouches were washed with 3 ml PBS and the lavage fluid was analyzed in terms of cell numbers and inflammatory mediators. Total cell numbers were recorded and additionally cell numbers of neutrophils and monocytes were determined by flow cytometry. The numbers of total infiltrating cells in the inflamed air pouch was significantly reduced in the anti-IL-6R antibody-treated mice to approximately 10×10^6 cells/air pouch compared to the PBS-treated mice (20×10^6 cells/air pouch) indicating that IL-6 mediated signal

transduction was important for leukocyte recruitment. Neutrophil infiltration was measured by flow cytometry with the use of anti-Ly6G antibody, a marker for neutrophils. Compared to PBS injection as a control, anti-IL-6R antibody injection slightly decreased the numbers of infiltrating neutrophils into the air pouch but not to significant levels. In terms of infiltrating monocytes there were significant differences observed between the PBS control group and the anti-IL-6R antibody challenged group. Flow cytometry analysis using the anti-F4/80 antibody revealed that administration of anti-IL-6R antibodies led to inhibition of monocyte infiltration into the air pouch. These results indicated that blocking IL-6R signalling suppresses events upstream of monocyte infiltration.

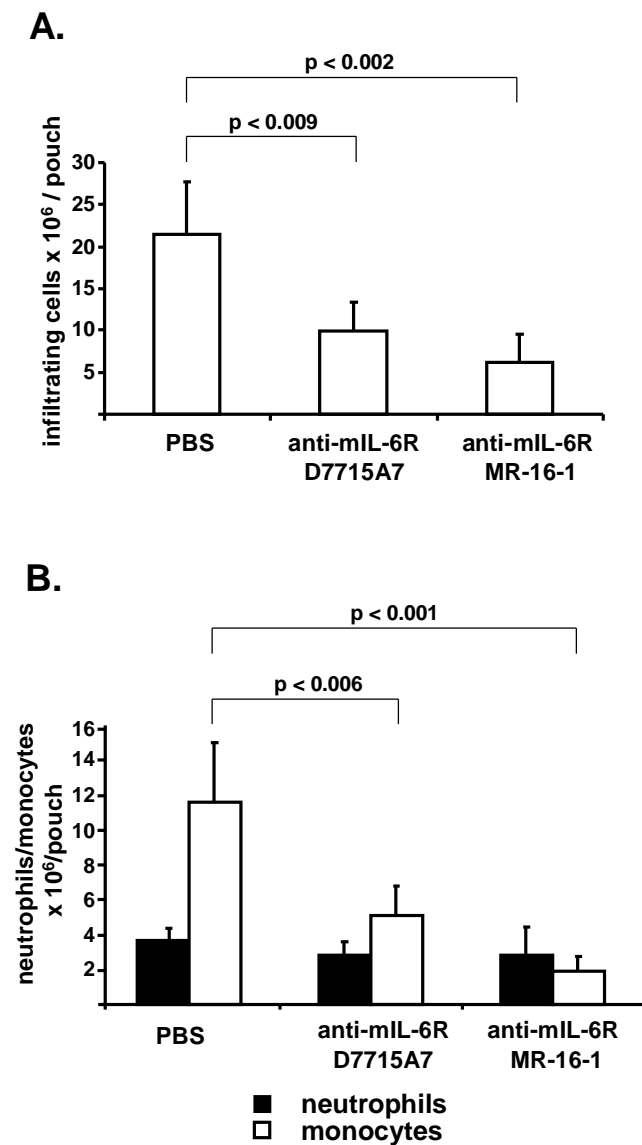


Figure 32: IL-6R signalling was important for monocyte infiltration into the inflamed air pouch.

A. Air pouches were formed on the back of C57Bl/6 wildtype mice (male, 8-10 weeks old) as described in Material and Methods. After 6 days the mice were injected i.p. with 400 μ l PBS, 100 μ g α -IL-6R D7715A7 or 100 μ g α -IL-6R MR-16-1, 6 hours before administration of 1 ml carrageenan solution (1 %). Each group contained 5 mice. 72 hours later the mice were sacrificed, the pouches were washed with 3 ml PBS and the total cell numbers were determined (neubauer cell chamber). Data are represented as mean values \pm SD.

B. 200,000 cells (pouch lavage) were stained with α -Ly6G (neutrophilic marker) and α -F4/80 (monocytic marker) and analyzed by flow cytometry. To obtain total numbers of infiltrated neutrophils and monocytes the percentages of each cell population which were determined by FACS analysis were multiplied with the total cell numbers. Data are represented as mean values \pm SD.

4.16 “Trans-signalling” rather than “classic signalling” is important for monocytic infiltration into the inflamed air pouch

Blocking IL-6-mediated signal transduction during acute inflammation by anti-murine IL-6R antibodies led to impaired monocytic infiltration into the inflamed area. The use of neutralizing antibodies against the IL-6R however blocked both, the classic signalling mediated by the membrane-bound IL-6R and the trans-signalling mediated by the soluble form of the IL-6R. To distinguish which pathway was important for leukocyte infiltration during acute inflammation, mice were challenged with recombinant-soluble gp130 protein fused to the Fc region of human IgG1 intraperitoneally before injection of the irritant carrageenan into the air pouch. It was showed in previous studies that sgp130 exclusively inhibited IL-6 responses mediated by the sIL-6R without interfering with responses mediated *via* the membrane-bound IL-6R or other cytokines of the IL-6 type family (73, 181).

8-10 weeks old male C57Bl/6 wildtype mice were challenged i.p. with 100 µg of sgp130-Fc protein 6 hours before injection of 1 % carrageenan solution into the air pouch. Cell numbers of neutrophils and monocytes were determined by flow cytometry, while levels of sgp130 were assessed by ELISA in the inflamed air pouches and in the serum 72 hours after induction of inflammation. High concentrations of circulating sgp130-Fc protein were detected in the serum of challenged mice indicating that the protein remained in a stable conformation during the entire experimental procedure. The serum concentration 72 hours after injection of sgp130-Fc was 17.4 µg/ml whereas approximately tenth part of the sgp130-Fc protein circulating in the bloodstream was transmitted to the air pouch cavity (3.5 µg/ml).

The number of total infiltrating cells was significantly reduced in sgp130-Fc challenged mice as compared to PBS control mice. Whereas the cell number in PBS control animals increased to 21×10^6 /pouch, the inflammatory reaction in the sgp130-Fc challenged mice was markedly suppressed to 8.7×10^6 cells/pouch. Additionally in the sgp130-Fc challenged mice the proportion of neutrophils and monocytes in the air pouch was strongly reduced. These results indicate that impaired leukocyte accumulation during acute inflammation was likely due to IL-6 trans-signalling, and not classical IL-6-signalling.

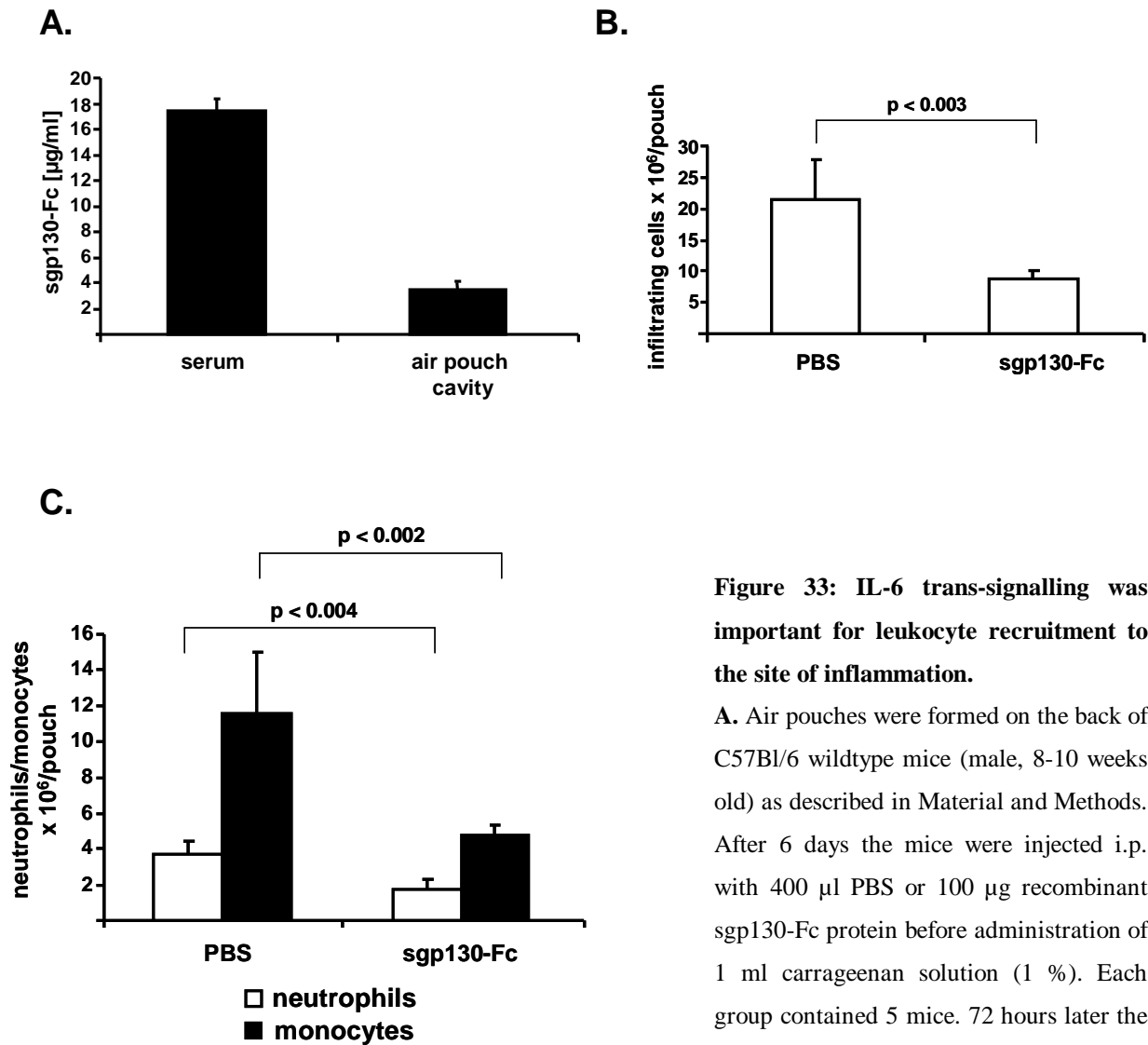


Figure 33: IL-6 trans-signalling was important for leukocyte recruitment to the site of inflammation.

A. Air pouches were formed on the back of C57Bl/6 wildtype mice (male, 8-10 weeks old) as described in Material and Methods. After 6 days the mice were injected i.p. with 400 μl PBS or 100 μg recombinant sgp130-Fc protein before administration of 1 ml carrageenan solution (1 %). Each group contained 5 mice. 72 hours later the mice were sacrificed, the pouches were washed with 3 ml PBS and the serum was

collected by heart puncture. Soluble gp130-Fc concentrations in the serum as well as in the pouch lavage samples were determined by a specific “sandwich”-ELISA for human gp130 (triplicates). Data are represented as mean values \pm SD.

B. Total cell numbers were determined in the pouch lavage (neubauer cell chamber). Data are represented as mean values \pm SD.

C. 200,000 cells (pouch lavage) were stained with α -Ly6G (neutrophilic marker) and α -F4/80 (monocytic marker) and analyzed by flow cytometry. To obtain total numbers of infiltrated neutrophils and monocytes the percentages of each cell population which were determined by FACS analysis were multiplied with the total cell numbers. Data are represented as mean values \pm SD.

4.17 Leukocyte recruitment during acute inflammation in IL-6-deficient mice

The air pouch model of acute inflammation was performed with IL-6-deficient (IL-6^{-/-}) mice. It was described before by Romano *et al.* that IL-6^{-/-} mice showed impaired leukocyte recruitment to the site of inflammation (176). However the experiments performed so far focus upon early time points of leukocyte recruitment during acute inflammation. Romano *et al.* used the air pouch model and demonstrated that 24 hours after carrageenan injection, IL-6^{-/-} mice recruit only half of the leukocytes compared to wild type control mice. At this time point it is very likely that the main cell population in the pouch cavity consist of infiltrated neutrophils. To investigate, if monocyte infiltration was impaired in IL-6^{-/-} mice, consistent with the data observed with sgp130-Fc protein and anti-IL-6R challenged mice, the air pouch model was performed and two different time points were analyzed: the 12 hours time point represented the early stage of inflammation and the 72 hours time point represented the late stage of inflammation. In line with already published data, the number of total infiltrating cells was significantly reduced in IL-6^{-/-} mice compared to the wildtype C57Bl/6 animals 12 hours after carrageenan injection. Further analysis of the infiltrating leukocytes revealed that IL-6^{-/-} mice harboured significantly less neutrophils in the air pouch cavity then the wildtype control animals (Figure 34).

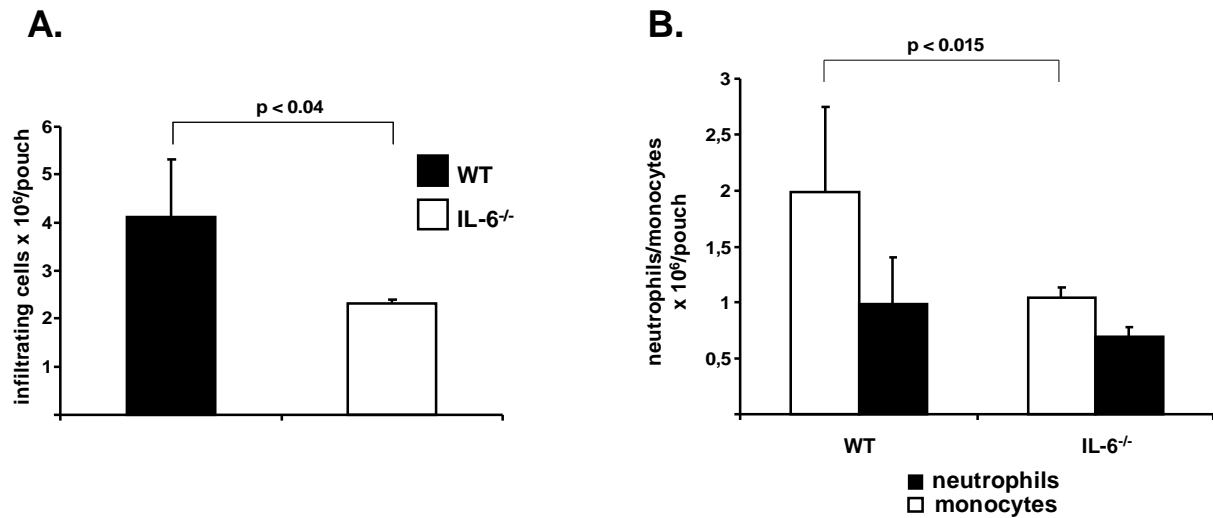


Figure 34: IL-6^{-/-} mice showed impaired leukocyte recruitment 12 hours after carrageenan injection.

A. Air pouches were formed on the back of C57Bl/6 wildtype mice (male, 8-10 weeks old, n=5) and C57Bl/6/IL-6^{-/-} mice (male, 8-10 weeks old, n=3) as described in Material and Methods. After 6 days the mice were challenged with 1 ml carrageenan solution (1 %). 12 hours later the mice were sacrificed, the pouches were washed with 3 ml PBS to obtain the pouch lavage. Total cell numbers were determined in the pouch lavage (neubauer cell chamber). Data are represented as mean values \pm SD (* p=0.04).

B. 200,000 cells (pouch lavage) were stained with α -Ly6G (neutrophilic marker) and α -F4/80 (monocytic marker) and analyzed by flow cytometry. To obtain total numbers of infiltrated neutrophils and monocytes the percentages of each cell population which were determined by FACS analysis were multiplied with the total cell numbers. Data are represented as mean values \pm SD.

Surprisingly, analysis of the infiltrating leukocytes 72 hours after induction of inflammation, revealed no significant differences between the IL-6^{-/-} mice and the wildtype control mice in terms of infiltrating neutrophils and monocytes. This outcome was not expected since the IL-6^{-/-} mice showed significantly impaired leukocyte recruitment during the onset of inflammation. These results indicate that IL-6 signalling is involved in leukocyte recruitment during onset of inflammation but can be compensated by other signal transduction pathways onward the inflammatory response.

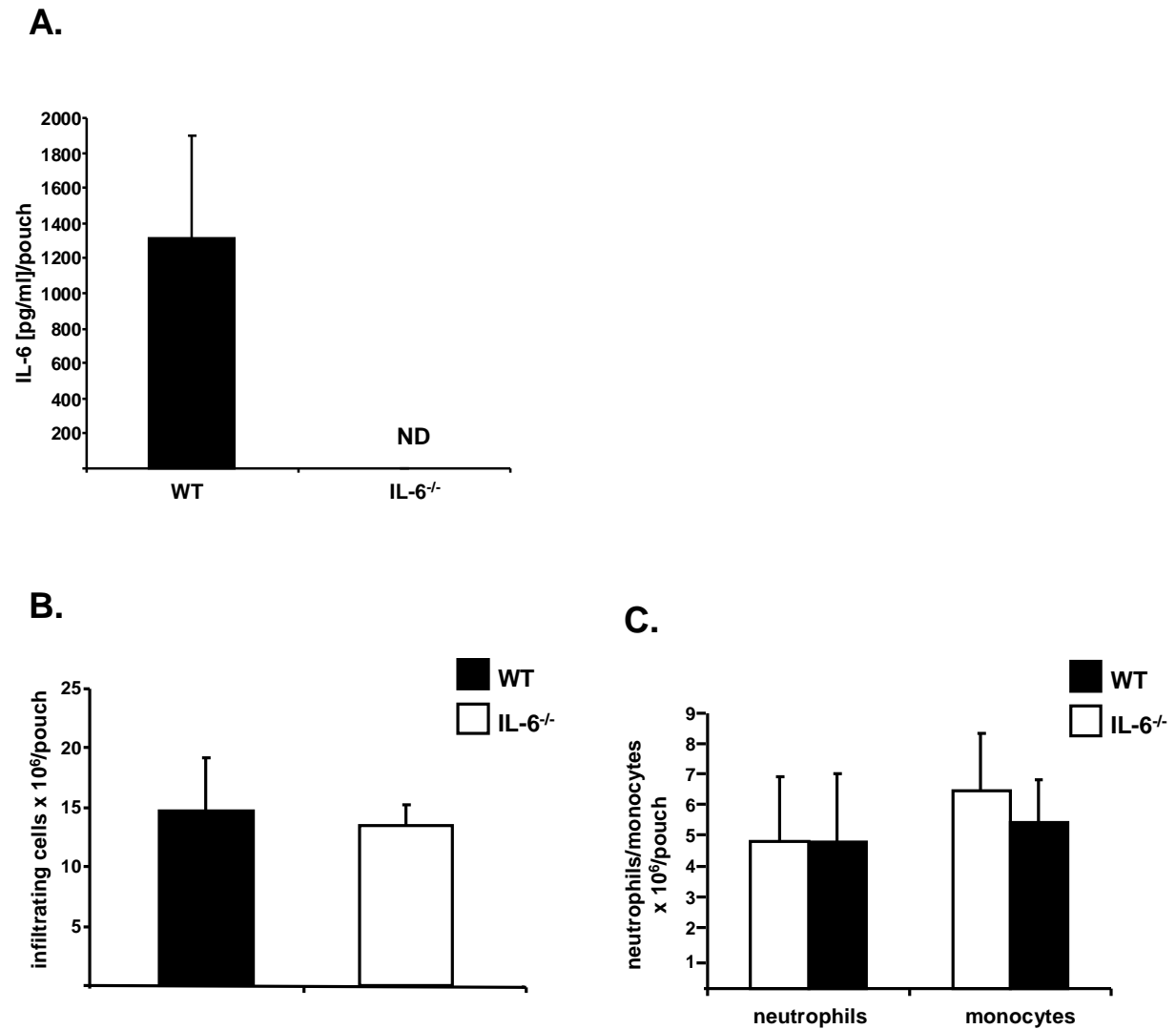


Figure 35: IL-6^{-/-} mice showed normal leukocyte recruitment 72 hours after carrageenan injection.

A. Air pouches were formed on the back of C57Bl/6 wildtype mice (male, 8-10 weeks old, n=7) and C57Bl/6/IL-6^{-/-} mice (male, 8-10 weeks old, n=7) as described in Material and Methods. After 6 days the mice were challenged with 1 ml carrageenan-solution (1 %). 72 hours later the mice were sacrificed, the pouches were washed with 3 ml PBS to obtain the pouch lavage. The murine IL-6 specific “sandwich”-ELISA was performed with the pouch lavages and data are represented as mean values \pm SD (ND: not detectable).

B+C. Total cell numbers as well as numbers of neutrophils and monocytes were determined as described in Figure 34.

5 Discussion

5.1 Molecular basis of ADAM 17 activation during apoptosis

Proteolytic processing is of prime importance for regulating the functional properties of cell surface proteins. Two large families of zinc-dependent metalloproteases have been described: the matrix metalloproteases and the ADAM proteases. ADAM17 (also referred to as TNF- α converting enzyme, TACE) cleaves a number of different cell surface proteins or receptors involved in a variety of biological processes. Among the numerous substrates of ADAM17 are several proteins which serve as inflammatory modulators like TNF- α , TNF receptors, L-selectin, fractalkine and the IL-6R. Proteolytic cleavage of the IL-6R occurs in a constitutive fashion and can be additionally stimulated by PMA-mediated PKC activation, treatment of cells with bacterial toxins, cholesterol depletion of cellular membranes and treatment of cells with C-reactive protein (CRP). Interestingly, all stimuli described so far trigger membrane alterations or perturbation (Figure 36). The phorbol ester PMA intercalates into the plasma membrane and potently activates PKC family members by recruiting them to the membrane, thus mimicking the mechanism of the natural activator, diacylglycerol. Thus, PKC activation is mediated by high-affinity binding to the membrane components diacylglycerol and phosphatidylserine (182). The acute phase protein CRP has a Ca^{2+} -dependent binding specificity for phosphorylcholine, the polar head group of two widely distributed lipids, lecithin (phosphatidylcholine, PC) and sphingomyelin (SM) (183, 184). A number of observations suggest that at least some of the biological activities of CRP depend on its interaction with phospholipids of cell membranes. Besides phospholipids CRP interacts also with the complement factor C1q and the immunoglobulin receptors (Fc γ R) (185). The bacterial toxins Streptolysin O and *Escherichia coli* Hemolysin A are pore-forming bacterial cytotoxins. Each is produced as a water-soluble single-chain polypeptide that inserts into target membranes to form aqueous transmembrane pores (186). Interestingly IL-6R shedding was not induced by a Streptolysin O mutant that retained cell membrane binding capacity but lacked pore-forming activity indicating that disruption of the plasma membrane is essential for ADAM activation (80). The exposure of living cells to cyclodextrins (e.g. methyl- β -cyclodextrins, m β CD) results in cholesterol removal from cell membranes into the

hydrophobic cavity of the m β CD molecule (187). Thus m β CD treatment leads to alteration of the plasma membrane composition by cholesterol efflux.

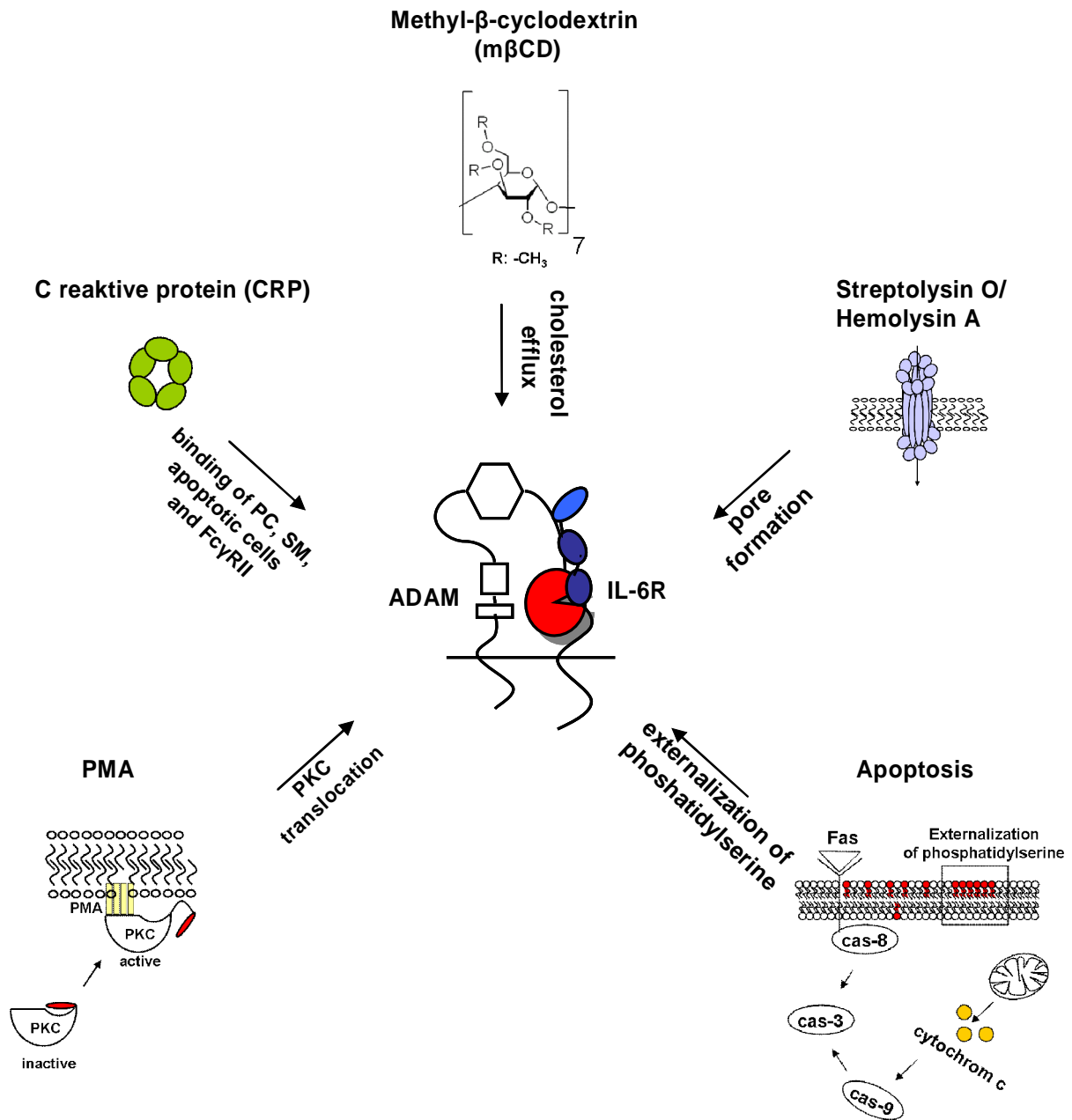


Figure 36: Stimuli involved in IL-6R shedding.

IL-6R shedding can be stimulated by the pentraxin family member CRP (C-reactive protein), Streptolysin O and Hemolysin A (bacterial pore forming proteins), m β CD (cholesterol depleting agent), PMA (phorbol ester) and during extrinsic and intrinsic apoptotic pathways. Note: PMA-induced PKC translocation from the cytosol to the plasma membrane leads to a conformational change of the protein. This conformational change results in removal of the autoinhibitory pseudosubstrate domain from the active site. Abbreviations: PC: phosphatidylcholine, SM: sphingomyelin, cas-8: caspase 8, cas-3: caspase 3, cas-9: caspase 9.

During apoptosis drastic membrane changes occur when phosphatidylserine is exposed to the exterior of the plasma membrane. Therefore the hypothesis was set up that apoptotic pathways might lead to an induction of IL-6R ectodomain shedding. Programmed cell death or apoptosis is essential in multi-cellular organisms for development, tissue turnover and host defense. In this study we show that the induction of intrinsic and extrinsic apoptotic pathways leads to an activation of the metalloproteinase ADAM17, which subsequently leads to IL-6R shedding. Therefore apoptotic pathways represent a physiological stimulus for induced IL-6R shedding.

During apoptosis the IL-6R is efficiently cleaved in Ba/F3 [gp130/IL-6] cells, HepG2 cells and primary human neutrophils. The soluble 65 kDa ectodomain of the IL-6R was released into the cell culture medium after induction of apoptosis by cytokine deprivation, doxorubicin, agonistic Fas antibody or UV treatment. The generation of the soluble IL-6R during apoptosis was efficiently blocked by GW280264X, a combined ADAM10 and ADAM17 inhibitor, whereas the specific ADAM10 inhibitor GI254023X did not prevent IL-6R shedding during apoptosis. Moreover transfection of a dominant-negative mutant of TACE decreased IL-6R shedding by 30 % in apoptotic HepG2 cells. Although shedding of the IL-6R is an early apoptotic process, blockade of ADAM17 did not inhibit apoptosis indicating that ADAM17 activity is not required for apoptosis. In this study it was demonstrated that most likely cleavage of the prodomain of ADAM17 is involved in ADAM17 activation, since the amount of processed ADAM17 protein increased during apoptosis. ADAM17 has been found to be transcriptionally up-regulated and to be translocated to the cell membrane during apoptosis (188, 189). Increased IL-6R shedding in apoptotic cells treated with the protein synthesis inhibitor cycloheximide was detected in this study. Therefore it was excluded that ADAM17 protein synthesis was needed for apoptosis-induced shedding of the IL-6R. Thus induction of ADAM17 activity appears to occur through an increase in the enzymatic activity of constitutively expressed ADAM17 molecules. Earlier studies with transfected COS-7 cells revealed that only a minor fraction of ADAM17 protein were present at the cell surface, with the majority being localized to a perinuclear region (190), and being translocated to the cell surface upon activation (191).

Induction of apoptosis requires a complex interplay of signaling molecules, receptors and enzymes. In the course of apoptosis the activation of caspases is the central step driving cells into the execution phase of programmed cell death. Activation of the caspase cascade comprising initiator caspases like caspase-8 and caspase-9 and executor caspases like caspase-

3, finally lead to morphological changes characterized by phosphatidylserine exposure, DNA-fragmentation and apoptotic body formation (192). This study demonstrates that ADAM17 activation is dependent on the combined activation of caspases-8, -9 and -3 but independent of PKC, a known mediator of PMA-induced shedding. Even though blocking of individual caspases did not significantly reduce IL-6R shedding, combined inhibition blocked shedding of the IL-6R. Although it is not possible to rule out non-specific effects of the individual caspase inhibitors, the results obtained in this study point to a common downstream target of caspases -3, -8, and -9 involved in governing ADAM17 activity.

How is ADAM17 activated during apoptosis finally leading to IL-6R shedding? Most cell stimuli that induce shedding of surface molecules appear to require the mitogen activated protein kinases (MAPK) or reactive oxygen species (ROS) generation. It was shown that Erk- and p38-MAPK are involved in ADAM17 activation during PMA and osmotic stress treatment. Moreover ADAM17 directly interacts with the Erk-MAPK after PMA treatment which leads to phosphorylation of ADAM17 at threonine₇₃₅ (108). Besides of the MAPK pathway it has been suggested that ADAM17 can be activated by ROS (e.g. H₂O₂). PMA treatment induces ROS generation and ROS scavengers attenuate PMA-induced ectodomain shedding (110, 193). During apoptosis proteins of the MAPK family are involved in the induction as well in the execution phase of programmed cell death pathways (194, 195). In this study we could show that IL-6R shedding during apoptosis is independent of MAPK activation. Induction of apoptosis in the presence of specific inhibitors for the p38-MAPK as well as for the Erk1/2-MAPK did not block IL-6R shedding. Apoptotic stimuli like UV treatment, Fas stimulation and doxorubicin treatment are well known inducer of ROS. Therefore we analyzed next the effect of ROS generation on the shedding of the IL-6R during apoptosis. Preincubation of HepG2 cells with the ROS-scavengers nPG and DMTU as well as the NADPH oxidase inhibitor DPI did not result in inhibition of IL-6R shedding during apoptosis. In summary, the molecular mechanism of ADAM17 activation during apoptosis is caspase dependent since combined inhibition of caspase-3, -8 and -9 results in diminished IL-6R shedding. Although well known ADAM17 activators, like proteins belonging to the PKC and MAPK family, are either downstream targets of caspases or are activated during apoptotic pathways, they do not seem to be involved in ADAM17 activation. ROS can activate latent proforms of metalloproteinases. However, ROS did not activate ADAM17 mediated IL-6R-shedding during apoptosis. Interestingly, a recent study demonstrates that ADAM10 is the sheddase responsible for releasing CD46 from apoptotic cells. In contrast to our findings regarding ADAM17 activation, Hakulinen et al. could show that ADAM10 activity during

apoptosis is ROS dependent (196). Thus besides ADAM17 the close related sheddase ADAM10 is activated during apoptosis by a different molecular pathway involving ROS generation.

In a previous study Gómez-Gavero et al. could show that L-selectin shedding on human neutrophils is induced by several nonsteroidal anti-inflammatory drugs (NSAIDs) which lead to reduction of intracellular ATP concentration. In line with this finding L-selectin shedding was also induced by the metabolic blockers azide and 2-deoxy-D-glucose. The authors claim that maintenance of L-selectin on the cell surface requires energy consumption which suggests that L-selectin is shed in default of intracellular ATP concentration (111). Similar studies regarding the regulating of IL-6R shedding during ATP depleting conditions were not performed so far. Nevertheless it is unlikely that cellular ATP reduction is the molecular mechanism which induces ADAM17 activation during apoptosis since a high concentration of ATP is required for cells to undergo programmed cell death. Moreover levels of intracellular ATP determine whether cells die by apoptosis or necrosis. In contrast to apoptosis which is an ATP-dependent process, necrosis does not require intracellular ATP.

5.2 The physiologic role of IL-6R shedding during apoptosis

IL-6 mediated signal transduction is involved in induction of growth, differentiation and pro-survival pathways in different cell types. IL-6 effectively protects gastric cancer cells from apoptosis induced by hydrogen peroxide (H₂O₂) and serves as a growth factor for multiple myeloma cells and renal cell carcinoma cells (12, 13, 197). Moreover IL-6 is involved in extended neutrophil survival during pathological conditions and serves as major growth regulator in the liver following toxic damage, hepatitis and surgical resection (198, 199). The anti-apoptotic effect of IL-6 is cooperatively mediated by the PI3K/Akt and STAT3 pathways. The signaling pathway, from PI3-kinase to the serine/threonine protein kinase Akt/protein kinase B (PKB), results in induced *mcl-1* gene expression. Mcl-1 belongs to the anti-apoptotic Bcl-2 protein family and exerts together with Bcl-2 and Bcl-X_L a central role in regulating apoptosis (200). The STAT3 pathway regulates growth-promoting genes (*cyclin D* and *c-myc*) as well as anti-apoptotic genes (*survivin* and *bcl-xl*) (201-203).

Due to the major biological properties of IL-6 to induce cell proliferation and survival it is reasonable to argue that IL-6R shedding during apoptosis is important for regulating the survival decision of cells undergoing programmed cell death. Shedding of the IL-6R would accord to unresponsiveness towards IL-6 during apoptosis. Surprisingly, blocking IL6R

shedding from apoptotic cells with the metalloprotease-inhibitor marimastat did not alter the STAT3 phosphorylation in the presence of IL-6. During onset of apoptosis Ba/F3 [gp130/IL-6R] cells became unresponsive to IL-6 in absence or presence of the IL-6R. This result indicates that IL-6 mediated signal transduction is terminated during apoptosis by other pathways than IL-6R shedding. This was further highlighted by the finding that during apoptosis, the mRNA of the negative signalling protein SOCS3 was slightly up-regulated in neutrophils and gp130 was down-regulated in hepatocytes, indicating the induction of a negative feedback loop for gp130 signalling (204). In addition Hideshima et al. demonstrate that the cytoplasmic tail of gp130 is a substrate for caspases. Caspase-mediated cleavage of the intracellular part of gp130 results in a signal-transduction defective receptor (205).

It is reported that IL-6 attenuates spontaneous neutrophil apoptosis (198). Findings in this study revealed that IL-6-mediated signalling did not necessarily play a role in the survival decision of induced neutrophil apoptosis. The extent of apoptosis of neutrophils after Fas stimulation was not altered in the presence of IL-6 or the fusion protein Hyper-IL-6 a complex of the IL-6/sIL-6R. It is possible that IL-6 exerts its pro-survival properties only on neutrophils undergoing spontaneous apoptosis. Unlike many other cell types, neutrophils undergo spontaneous apoptosis without any need for apparent external inductive stimuli. However the signal-transduction pathways involved in spontaneous apoptosis remain elusive and could probably differ from the pathways involved in induced programmed cell death, like Fas ligation or UV treatment. Therefore our finding that IL-6 signalling is rather not involved in inhibition of Fas-induced neutrophil apoptosis does not necessarily conflict with previous reports.

IL-6 can elicit responses directly in cells expressing IL-6R/gp130 or, alternatively, a soluble form of the IL-6R (sIL-6R) can bind IL-6 and the complex can be recognized by cells expressing gp130 alone. This process is known as trans-signalling (50, 51). Because the role of IL-6R shedding was not termination of IL-6 signalling the hypothesis was set up that IL-6R shedding during apoptosis was important to stimulate surrounding non-apoptotic cells via IL-6. Indeed the sIL-6R generated during apoptosis was biologically active and could promote IL-6 trans-signalling in Ba/F3 [gp130] cells. Therefore apoptotic cells may represent the source of sIL-6R in normal as well as in inflammatory and pathologic conditions.

5.3 IL-6R shedding during neutrophil apoptosis: Implication during acute inflammation

The sIL-6R is present in the plasma of healthy individuals (25-35 ng/ml) and elevated levels of this soluble receptor have been detected in numerous disease states. The confined cellular expression of the IL-6R narrow the cell types down to neutrophils, macrophages, B-cells, subpopulation of T-cells and hepatocytes, which could represent the source of shed sIL-6R *in vivo*. Neutrophils have been used in this study for several reasons (1) it has been shown in previous studies that neutrophils express both the IL-6R and ADAM17 (174, 188), (2) neutrophils have the shortest life span of the various leukocytes and die rapidly via apoptosis *in vivo* and *in vitro*, (3) IL-6R shedding from neutrophils has been associated with activation by C-reactive protein, chemokines and other chemotactic agents (53, 78, 175, 206).

Consistent with the data obtained with HepG2 and Ba/F3 [gp130/IL-6R] cells, human primary neutrophils shed the IL-6R upon induction of apoptosis in an ADAM17-dependent manner. Interestingly recent studies by Walcheck et al. demonstrate that L-selectin is also shed from the cell surface by neutrophils undergoing apoptosis indicating that during programmed cell death several proteins are cleaved by metalloprotease activity (188). It has been reported that in apoptotic neutrophils ADAM17 expression was up-regulated and that airway neutrophils are activated by bacteria leading to the release of sIL-6R possibly via ADAM17 activation (174). The data obtained in this study suggest that induction of apoptosis, irrespective of the activation stimuli, will lead to activation of the metalloproteinase ADAM17 resulting in enhanced IL-6R shedding from the neutrophil surface.

Soluble IL-6R is found in the serum of healthy individuals. It was shown in previous studies that both IL-6R isoforms, the differential mRNA spliced as well as the proteolytically cleaved, were circulating in blood obtained from normal healthy individuals (207). Thus it is tempting to speculate that apoptotic neutrophils contribute to the circulating sIL-6R level due to approximate 10^{11} short-lived neutrophils are delivered to the blood each day.

The inflammatory response is characterized largely by influx of neutrophils. These phagocytes possess microbicidal capacity and are thus efficient at killing invading microorganisms. Although the inflammatory response is highly beneficial to the host, coordinated termination is critical to limit tissue damage (208). To avoid tissue damage, neutrophils undergo apoptosis following phagocytosis as a mechanism to promote resolution of inflammation. The resolution process includes switching from neutrophil to mononuclear leukocyte recruitment and mononuclear leukocytes are responsible for removal of apoptotic

neutrophils. Appropriate control of the inflammatory infiltrate is reliant upon the coordinated regulation of inflammatory chemokines together with a balanced apoptotic clearance of immune cells. The switch between the initial neutrophilic stage of inflammation and the later, more sustained influx of mononuclear cells involves IL-6 trans-signalling but a trigger for this process has remained elusive (209).

Previously, it was shown that IL-6 trans-signaling in stromal cells including endothelial cells, mesothelial cells, smooth muscle cells and fibroblasts differentially regulates the expression of inflammatory chemokines including the neutrophil attracting chemokines CXCL8/IL-8 and the monocyte attracting chemokines CCL2/MCP1 (210-212). Through clinical evaluation of local sIL-6R levels in various inflammatory conditions, it is evident that a close association exists between the number of infiltrating neutrophils and sIL-6R levels (175). In this context, IL-6R shedding from neutrophils has been associated with activation by C-reactive protein, chemokines and other chemotactic agents (53, 78, 175, 206) whereas gp130 is not subject to proteolysis by ADAM proteases (213). In this present study, an alternative mechanism is offered, whereby apoptosis-induced shedding of IL-6R from the neutrophil surface facilitates formation of an IL-6/sIL-6R complex and directs IL-6 trans-signaling presumably on endothelial cells to promote recruitment of monocytic cells involved in the nonphlogistic removal of apoptotic neutrophils. Thus shedding processes in apoptotic neutrophils may have profound effects on the outcome of the inflammatory response. Notably, such a cascade of neutrophils and mononuclear cells has been shown to be non-functional in IL-6^{-/-} mice (175, 214). In this study the air pouch model of acute inflammation was used to analyze leukocyte migration during inflammation under various experimental conditions. Injection of the irritant carrageenan into dorsal air pouches of mice resulted in a local inflammatory reaction. Infiltrating leukocytes were analyzed after a period of 72 hours. The studies revealed that IL-6 signalling and precisely IL-6 trans-signalling were important for recruitment of mononuclear cells into the center of inflammation. Soluble gp130-Fc (inhibitor of trans-signalling but not classic signalling) and neutralizing antibodies against the IL-6R (inhibitor of classic signalling and trans-signalling) block signalling pathways which are involved in recruitment of mononuclear cells. The control animals show 72 hours after injection of the irritant high amounts of infiltrated mononuclear cells in the air pouch cavity. In the sgp130-Fc as well as in the neutralizing IL-6R-antibody treated mice the mononuclear cell infiltration was strongly reduced. Further studies will be needed to analyze which exact molecular pathway is impaired in absence of IL-6 trans-signalling. Notably application of sgp130-Fc also reduced the amount of infiltrated neutrophils into the inflamed air pouches suggesting that IL-6 trans-signalling is

not only important for monocytic but also for neutrophilic attraction during inflammatory responses. In previous studies Romano et al. used the air pouch model of acute inflammation to analyze leukocyte infiltration in IL-6-deficient (IL-6^{-/-}) mice. The studies revealed that IL-6^{-/-} mice harboured significantly less leukocytes in the inflamed air pouch compared to the wildtype littermates 24 hours after injection of the irritant carrageenan (176). The air-pouch experiments performed in the present work with the IL-6^{-/-} mice revealed similar results concerning the infiltrating leukocytes in the initial phase of inflammation (12 hours after injection of carrageenan). Surprisingly, in the advanced phase of inflammation (72 hours after injection of carrageenan) the IL-6^{-/-} mice showed no significant impairment in leukocyte migration compared to age-matched wildtype animals. This observation indicates that IL-6-mediated signal transduction is indispensable during onset of inflammation in agreement with previous reports but at later time points leukocyte infiltration is restored by a yet unknown mechanism in IL-6^{-/-} mice. It is very likely that the lack of IL-6 is probably compensated by the redundancy within the IL-6 system. IL-6 is only one member of a large IL-6 family that includes e.g. LIF, CT-1, OSM, CNTF, IL-11 and NNT-1, which share the common receptor subunit gp130 for signalling. Further studies are needed to investigate if and which factor is responsible for the compensation of IL-6 in IL-6^{-/-} mice during the advanced phase of acute inflammation. In previous studies it has been shown that IL-6^{-/-} mice exert severe deficiency in several aspects of the acute host response after turpentine treatment, including the liver acute phase reaction, anorexia, loss of body weight, and hypoglycaemia. However, the same responses were only slightly modified after LPS treatment. The finding that IL-6 was not required to generate an inflammatory response to LPS was surprising, as IL-6 is produced in large quantities upon LPS injection. The authors speculate that functional redundancy between different cytokines, in particular IL-1 and TNF- α , can compensate for IL-6 loss of function (215).

In summary, administration of neutralizing antibodies against the IL-6R as well as sgp130-Fc lead to impaired attraction of monocytes to the inflamed area. The results obtained in this study support already published observations where administration of blocking antibodies against the IL-6R or recombinant sgp130-Fc have proved to moderate leukocyte infiltration during pathological conditions like rheumatoid arthritis and peritonitis (175, 210). Therefore, the IL-6R system is a likely target for new therapeutics designed to treat inflammatory disorder.

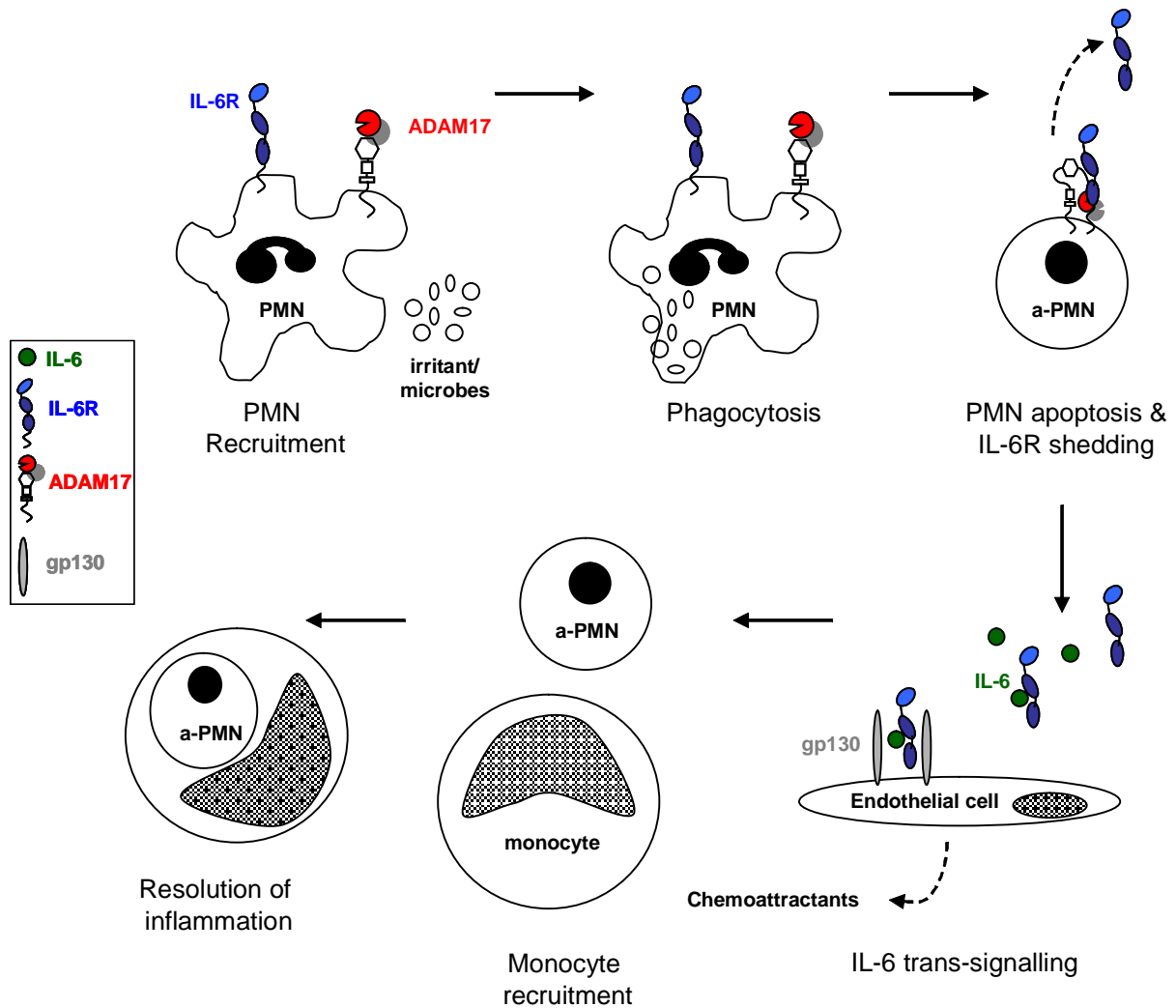


Figure 37: IL-6 trans-signalling in the switch from neutrophil to mononuclear leukocyte recruitment during the resolution of inflammation.

The inflammatory response involves influx of polymorphonuclear leukocytes (PMNs or neutrophils). Phagocytosis of microbes and cell activation ultimately lead to PMN apoptosis (a-PMN), during which ADAM17 is activated to cleave the IL-6R from the cell surface (shedding). IL-6 and soluble IL-6R derived from apoptotic neutrophils activate signal transduction pathways which lead to recruitment of mononuclear phagocytes via IL-6 trans-signalling, possibly through endothelial cells. Phagocytosis of apoptotic neutrophils by mononuclear phagocytes, typically macrophages, is a key step in the resolution of acute inflammation. Adopted from (216).

5.4 Outlook

In this work extrinsic and intrinsic apoptotic pathways were identified as physiological stimuli for induced IL-6R shedding *in vitro*. The sheddase which mediates IL-6R ectodomain cleavage during programmed cell death was identified as ADAM17. Although ADAM17 activation was caspase dependent, the exact molecular mechanism leading to activation of the sheddase was not identified in this work. It is a challenge for future studies to identify the molecular mechanism which leads to ADAM17 activation during apoptosis. In this work already described stimuli, like MAPKs or reactive oxygen species (ROS), were excluded to be involved in ADAM17 activation during apoptosis by application of widely used inhibitors.

Since ADAM17 is responsible not only for shedding of the IL-6R but has also been implicated in the cleavage of, for example, TNF α , TGF- α , and various adhesion molecules as well as of some cytokine and growth factor receptors (213), it will be interesting to analyze whether all these substrates are also shed upon induction of apoptosis. Therefore, further experiments will be needed to fully understand the importance of this metalloprotease activation step for the progress and outcome of immune responses. Such consequences might include altered adhesion, rolling and attraction of neutrophils as well as changes in the activation pattern of other immune and non-immune cells.

The observation that primary human neutrophils shed the IL-6R upon induction of apoptosis makes it tempting to speculate that this cell type is the major provider of shed IL-6R *in vivo*. Neutrophils are short live cells, which undergo spontaneous apoptosis during normal conditions. During inflammation neutrophils constitute the “first line of defence” against all classes of infectious agents but, paradoxically, they are also involved in the pathology of various inflammatory conditions. It would be interesting to investigate if the amount of sIL-6R correlates with the number of circulating or infiltrating neutrophils during normal and pathological conditions. If neutrophils represent the major source of shed IL-6R, then the level of this protein should be drastic reduced in patients suffering from neutropenia (e.g., after chemotherapy). Future experiments with neutrophils deficient in ADAM17 expression, will reveal more information about the role of soluble IL-6R, derived from ectodomain shedding on neutrophils, during pathological and inflammatory conditions.

6 Summary

Interleukin-6 (IL-6) trans-signalling has emerged as a prominent regulator of immune responses during both innate and acquired immunity. Regulation of IL-6 trans-signalling is reliant upon the release of soluble IL-6R (sIL-6R), which binds IL-6 to create an agonistic IL-6/sIL-6R complex capable of activating cell types that would normally not respond to IL-6 alone. Soluble IL-6R is generated by proteolytic cleavage of the membrane-anchored precursor (shedding) or from alternative spliced mRNA. Several inducers of IL-6R shedding such as bacterial pore forming toxins, bacterial metalloproteases, the phorbol ester PMA, cholesterol depleting agents and C-reactive protein have been identified in previous studies. IL-6R shedding induced by PMA and cholesterol depletion is dependent on the metalloprotease ADAM17 (A Disintegrin And Metalloprotease), and to a lesser extent on the related sheddase ADAM10.

In this study apoptosis was identified as a natural stimulus of IL-6R shedding. Apoptosis, or programmed cell death, plays an important role in regulating growth, tissue homeostasis, development and immune responses. The induction of apoptosis is mediated by extrinsic and intrinsic pathways which require the cooperation of a series of molecules including signal molecules and receptors, enzymes and gene regulating proteins. Among them, the caspase-cascade signalling system is crucial for induction, transduction and amplification of intracellular apoptotic signals. This study demonstrates that intrinsic and extrinsic apoptotic stimulation of cells by DNA-damage, cytokine deprivation, UV irradiation and Fas ligation promotes shedding of the IL-6R from the cell surface thereby generating sIL-6R. Apoptosis-induced shedding of the IL-6R was caspase dependent but PKC, MAPK and ROS independent. Inhibition of ADAM17 during apoptosis by small pharmacological inhibitors or a dominant-negative ADAM17 variant resulted in prevention of IL-6R shedding. The sIL-6R generated during apoptosis was biological active and formed complexes with IL-6 thereby facilitating IL-6 trans-signalling in nonapoptotic cells.

Neutrophils have a short life span and die rapidly *via* apoptosis *in vivo* and *in vitro*. In this study neutrophils were used as a cellular model. Induction of apoptosis by Fas-ligation or UV irradiation of primary human neutrophils promoted IL-6R shedding thereby resulting in a two-fold increase of sIL-6R release. Neutrophils represent the first cell population infiltrating inflamed areas and play a crucial role during inflammatory responses due to their extraordinary microbial capacity. Following phagocytosis of invaded microorganisms

neutrophils undergo apoptosis as a mechanism to promote resolution of inflammation. The second cell population which migrates into the inflamed area consists mostly of mononuclear phagocytes (monocytes) which are responsible for the clearance of apoptotic neutrophils thus leading to resolution of the inflammatory reaction. Findings in this study indicate that apoptosis-induced shedding of the IL-6R from the neutrophils surface facilitates formation of an [IL-6/sIL-6R] complex which directs IL-6 trans-signalling presumably on endothelial cells to promote recruitment of mononuclear phagocytic cells involved in the nonphlogistic removal of apoptotic neutrophils. Using a mouse model of acute inflammation, it was demonstrated in this study that blocking IL-6R-mediated signal transduction by neutralizing antibodies or soluble gp130-Fc during acute inflammation resulted in a normal influx of neutrophils but a severely impaired influx of monocytes into the inflamed area. Therefore, IL-6R shedding and subsequent IL-6 trans-signalling represent important steps for the resolution of inflammatory responses by controlling the recruitment of mononuclear phagocytes. Thus, shedding of the IL-6R during neutrophil apoptosis may have profound effects on the outcome of the inflammatory response.

7 Zusammenfassung

Interleukin-6 (IL-6) vermitteltes *trans-signalling* ist ein wichtiger regulatorischer Signalweg für die Steuerung der angeborenen und erworbenen Immunität. IL-6 *trans-signalling* wird durch die Freisetzung vom löslichen Interleukin-6-Rezeptor (sIL-6R) moduliert; dieser bindet an IL-6, um einen IL-6/sIL-6R Komplex zu bilden. Der Komplex aus IL-6 und sIL-6R kann dann Zellen stimulieren, die lediglich gp130 exprimieren und normalerweise nicht in der Lage sind auf IL-6 zu reagieren, da ihnen die ligandenbindende Untereinheit (IL-6R) fehlt. Die lösliche Form des IL-6Rs kann entweder durch limitierte Proteolyse des membranständigen Rezeptors oder durch alternatives Spleißen der IL-6R mRNA generiert werden. In vorherigen Arbeiten konnte bereits gezeigt werden, dass die limitierte Proteolyse des IL-6Rs (*Shedding*) durch bakterielle porenformende Toxine, bakterielle Metalloproteasen, den Phorbolster PMA, Cholesterinentzug und C-reaktivem Protein induziert werden kann. Shedding des IL-6Rs durch Phorbolster und Cholesterinentzug wird hauptsächlich durch die Metalloprotease ADAM17 (*A Disintegrin And Metalloprotease 17*) und zum geringen Teil von der verwandten Protease ADAM10 vermittelt.

Im Rahmen dieser Arbeit konnte gezeigt werden, dass apoptotische Zellen vermehrt den IL-6R spalten; demnach stellen apoptotische Prozesse einen physiologischen Stimulus für induzierte IL-6R Proteolyse dar. Apoptose wird auch als programmierter Zelltod bezeichnet und spielt in der Regulation von Zellwachstum, Gewebemöostase und Immunreaktionen eine entscheidende Rolle. Apoptose kann abhängig von der Art des auslösenden Reizes auf verschiedene Wege eingeleitet werden; zum einen durch Aktivierung von Todesrezeptoren auf der Zellmembran und zum anderen durch mitochondrial vermittelte Signalwege. Hauptmerkmal beider Apoptosewege sind Caspasen (Cysteinproteasen), welche die morphologischen und biochemischen Merkmale der Apoptose durch Spaltung von zellulären Bestandteilen hervorrufen.

Im Rahmen dieser Arbeit konnte gezeigt werden, dass sowohl todesrezeptoren- als auch mitochondrialvermittelte Apoptose zu vermehrter Proteolyse des IL-6Rs führt. Dabei wurde zelluläre Apoptose durch verschiedene Wege induziert, wie zum Beispiel durch toxische Substanzen, die zur Schädigung des genetischen Materials führen, UV-Bestrahlung, Aktivierung des Todesrezeptors CD95 (Fas) oder Entzug von Überlebensfaktoren. Das durch Apoptose induzierte IL-6R Shedding war Caspase-abhängig jedoch PKC-, MAPK- und ROS-unabhängig. Des Weiteren führte eine Inhibition von ADAM17 durch kleine

pharmakologische Inhibitoren oder durch eine dominant-negative ADAM17 Variante während des programmierten Zelltodes zur kompletten Unterbindung von apoptosevermitteltem IL-6R Shedding. Der lösliche IL-6R, welcher während der Apoptose vermehrt gebildet wurde, war biologisch aktiv und konnte im Komplex mit IL-6 in nicht-apoptotischen gp130 exprimierenden Zellen *trans-signalling* auslösen.

Polymorphkernige Neutrophile sind kurzlebige Zellen mit einer Lebensdauer von 6-8 Stunden; danach sterben Neutrophile durch Apoptose. Im Rahmen dieser Arbeit wurden Neutrophile als zelluläres System verwendet. CD95 (Fas) Aktivierung und UV-Bestrahlung lösten in primären humanen Neutrophilen Apoptose aus, welche mit erhöhtem *Shedding* des IL-6Rs einherging. Bei Entzündungsprozessen stellen Neutrophile die erste Verteidigungslinie gegen Mikroorganismen dar. Neutrophile phagozytieren Mikroorganismen und töten diese durch vermehrte Produktion von Sauerstoffradikalen ab. Um die inflammatorische Reaktion zu beenden, müssen die aktivierten Neutrophilen eliminiert werden. Dies passiert durch die Einleitung von Apoptose in aktivierten Neutrophilen und anschließender Phagozytose durch mononukleäre Immunzellen (Monocyten), welche als zweite Zellpopulation in den Entzündungsort einwandern. Ergebnisse in dieser Arbeit zeigen, dass apoptotische Neutrophile verstärkt den IL-6R spalten. Dieser bildet einen Komplex mit IL-6. Der Komplex aus sIL-6R/IL-6 stimuliert daraufhin endotheliale Zellen, Mediatoren auszuschütten, die an der Rekrutierung von Monocyten beteiligt sind. Mit Hilfe eines murinen Krankheitsmodells (*Air-pouch*-Modell) konnte gezeigt werden, dass Blockierung von sIL-6R-vermittelten Signalwegen durch neutralisierende Antikörper oder rekombinantem löslichen gp130-Fc zu einer stark verminderten Akkumulation von Monocyten in den Entzündungsherd führt. Demnach wird der sIL-6R von apoptotischen Neutrophilen freigesetzt und beeinflusst bei entzündlichen Prozessen die Einwanderung von Monocyten, welche für das Beenden der inflammatorischen Reaktion verantwortlich sind.

8 References

1. **Hirano, T., K. Yasukawa, H. Harada, T. Taga, Y. Watanabe, T. Matsuda, S. Kashiwamura, K. Nakajima, K. Koyama, A. Iwamatsu, S. Tsunasawa, F. Sakiyama, H. Matsui, Y. Takahara, T. Taniguchi, and T. Kishimoto.** 1986. Complementary DNA for a novel human interleukin (BSF-2) that induces B lymphocytes to produce immunoglobulin. *Nature*. 324:73-76.
2. **Muraguchi, A., T. Hirano, B. Tang, T. Matsuda, Y. Horii, K. Nakajima, and T. Kishimoto.** 1988. The essential role of B cell stimulatory factor 2 (BSF-2/IL-6) for the terminal differentiation of B cells. *J. Exp. Med.* 167:332-344.
3. **Kishimoto, T., S. Akira, M. Narazaki, and T. Taga.** 1995. Interleukin-6 family of cytokines and gp130. *Blood*. 86:1243-1254.
4. **Gauldie, J., C. Richards, D. Harnish, P. Lansdorp, and H. Baumann.** 1987. Interferon beta 2/B-cell stimulatory factor type 2 shares identity with monocyte-derived hepatocyte-stimulating factor and regulates the major acute phase protein response in liver cells. *PNAS*. 84:7251-7255.
5. **Okada, M., M. Kitahara, S. Kishimoto, T. Matsuda, T. Hirano, and T. Kishimoto.** 1988. IL-6/BSF-2 functions as a killer helper factor in the in vitro induction of cytotoxic T cells. *J. Immunol.* 141:1543-1549.
6. **Nicola, N.A., D. Metcalf, M. Matsumoto and G.R. Johnson.** 1983. Purification of a factor inducing differentiation in murine myelomonocytic leukemia cells. Identification as granulocyte colony-stimulating factor. *J. Biol. Chem.* 258:9017-9023.
7. **Ishibashi, T., H. Kimura, T. Uchida, S. Kariyone, P. Friese, and S. A. Burstein.** 1989. Human interleukin 6 is a direct promoter of maturation of megakaryocytes in vitro. *PNAS*. 86:5953-5957.
8. **Ulich, T., J. d. Castillo, and K. Guo.** 1989. In vivo hematologic effects of recombinant interleukin-6 on hematopoiesis and circulating numbers of RBCs and WBCs. *Blood*. 73:108-110.
9. **Chen, Q., D. T. Fisher, K. A. Clancy, J. M. Gauguet, W. C. Wang, E. Unger, S. Rose-John, U. H. von Andrian, H. Baumann, and S. S. Evans.** 2006. Fever-range thermal stress promotes lymphocyte trafficking across high endothelial venules via an interleukin 6 trans-signaling mechanism. *Nat. Immunol.* 12:1299-1308.
10. **Chung, Y. C., and Y. F. Chang.** 2003. Serum interleukin-6 levels reflect the disease status of colorectal cancer. *J. Surg. Oncol.* 83:222-226.
11. **Becker, C., M. C. Fantini, S. Wirtz, A. Nikolaev, H. A. Lehr, P. R. Galle, S. Rose-John, and M. F. Neurath.** 2005. IL-6 signaling promotes tumor growth in colorectal cancer. *Cell Cycle*. 4:217-220.
12. **Kawano, M., T. Hirano, T. Matsuda, T. Taga, Y. Horii, K. Iwato, H. Asaoku, B. Tang, O. Tanabe, H. Tanaka, A. Kuramoto, and T. Kishimoto.** 1988. Autocrine

- generation and requirement of BSF-2/IL-6 for human multiple myelomas. *Nature*. 332:83-85.
13. **Miki, S., M. Iwano, Y. Miki, M. Yamamoto, B. Tang, K. Yokokawa, T. Sonoda, T. Hirano, and T. Kishimoto.** 1989. Interleukin-6 (IL-6) functions as an in vitro autocrine growth factor in renal cell carcinomas. *FEBS Lett.* 250:607-610.
 14. **Kopf, M., H. Baumann, G. Freer, M. Freudenberg, M. Lamers, T. Kishimoto, R. Zinkernagel, H. Bluethmann, and G. Kohler.** 1994. Impaired immune and acute-phase responses in interleukin-6-deficient mice. *Nature*. 368:339-342.
 15. **Alonzi, T., E. Fattori, D. Lazzaro, P. Costa, L. Probert, G. Kollias, F. De Benedetti, V. Poli, and G. Ciliberto.** 1998. Interleukin 6 is required for the development of collagen-induced arthritis. *J. Exp. Med.* 187:461-468.
 16. **Okuda, Y., S. Sakoda, C. C. Bernard, H. Fujimura, Y. Saeki, T. Kishimoto, and T. Yanagihara.** 1998. IL-6-deficient mice are resistant to the induction of experimental autoimmune encephalomyelitis provoked by myelin oligodendrocyte glycoprotein. *Int. Immunol.* 10:703-708.
 17. **Hirano, T., T. Matsuda, and K. Nakajima.** 1994. Signal transduction through gp130 that is shared among the receptors for the interleukin 6 related cytokine subfamily. *Stem Cells Dayt.* 12:262-277.
 18. **Bravo, J., and J. K. Heath.** 2000. Receptor recognition by gp130 cytokines. *EMBO J.* 19:2399-2411.
 19. **Giese, B., C. Roderburg, M. Sommerauer, S. B. Wortmann, S. Metz, P. C. Heinrich, and G. Muller-Newen.** 2005. Dimerization of the cytokine receptors gp130 and LIFR analysed in single cells. *J. Cell. Sci.* 118:5129-5140.
 20. **Taga, T., and T. Kishimoto.** 1997. gp130 and the Interleukin-6 Family of Cytokines. *Annu. Rev. Immunol.* 15:797-819.
 21. **Pflanz, S., L. Hibbert, J. Mattson, R. Rosales, E. Vaisberg, J. F. Bazan, J. H. Phillips, T. K. McClanahan, R. de Waal Malefyt, and R. A. Kastelein.** 2004. WSX-1 and glycoprotein 130 constitute a signal-transducing receptor for IL-27. *J. Immunol.* 172:2225-2231.
 22. **Pennica, D., V. Arce, T. A. Swanson, R. Vejsada, R. A. Pollock, M. Armanini, K. Dudley, H. S. Phillips, A. Rosenthal, A. C. Kato, and C. E. Henderson.** 1996. Cardiotrophin-1, a cytokine present in embryonic muscle, supports long-term survival of spinal motoneurons. *Neuron*. 17:63-74.
 23. **Elson, G. C., E. Lelievre, C. Guillet, S. Chevalier, H. Plun-Favreau, J. Froger, I. Suard, A. B. de Coignac, Y. Delneste, J. Y. Bonnefoy, J. F. Gauchat, and H. Gascan.** 2000. CLF associates with CLC to form a functional heteromeric ligand for the CNTF receptor complex. *Nat. Neurosci.* 3:867-872.

24. **Plun-Favreau, H., G. Elson, M. Chabbert, J. Froger, O. deLapeyriere, E. Lelievre, C. Guillet, J. Hermann, J. F. Gauchat, H. Gascan, and S. Chevalier.** 2001. The ciliary neurotrophic factor receptor alpha component induces the secretion of and is required for functional responses to cardiotrophin-like cytokine. *EMBO J.* 20:1692-1703.
25. **Guschin, D., N. Rogers, J. Briscoe, B. Witthuhn, D. Watling, F. Horn, S. Pellegrini, K. Yasukawa, P. Heinrich, G. R. Stark, J. N. Ihle, and I. A. Kerr.** 1995. A major role for the protein tyrosine kinase JAK1 in the JAK/STAT signal transduction pathway in response to interleukin-6. *EMBO J.* 14:1421-1429.
26. **Gerhartz, C., B. Heesel, J. Sasse, U. Hemmann, C. Landgraf, J. Schneider Mergener, F. Horn, P. C. Heinrich, and L. Graeve.** 1996. Differential activation of acute phase response factor/STAT3 and STAT1 via the cytoplasmic domain of the interleukin 6 signal transducer gp130. I. Definition of a novel phosphotyrosine motif mediating STAT1 activation. *J. Biol. Chem.* 271:12991-12998.
27. **Zhong, Z., Z. Wen, and J. E. J. Darnell.** 1994. Stat3: a STAT family member activated by tyrosine phosphorylation in response to epidermal growth factor and interleukin-6. *Science.* 264:95-98.
28. **Heinrich, P. C., I. Behrmann, G. Muller Newen, F. Schaper, and L. Graeve.** 1998. Interleukin-6-type cytokine signalling through the gp130/Jak/STAT pathway. *Biochem. J.* 334:297-314.
29. **Sekimoto, T., N. Imamoto, K. Nakajima, T. Hirano, and Y. Yoneda.** 1997. Extracellular signal-dependent nuclear import of Stat1 is mediated by nuclear pore-targeting complex formation with NP-1, but not Rch1. *EMBO J.* 16:7067-7077.
30. **Wegenka, U. M., J. Buschmann, C. Lütticken, P. C. Heinrich, and F. Horn.** 1993. Acute-phase response factor, a nuclear factor binding to acute-phase response elements, is rapidly activated by interleukin-6 at the posttranslational level. *Mol. Cell. Biol.* 13:276-288.
31. **Kordula, T., R. E. Rydel, E. F. Brigham, F. Horn, P. C. Heinrich, and J. Travis.** 1998. Oncostatin M and the interleukin-6 and soluble interleukin-6 receptor complex regulate alpha1-antichymotrypsin expression in human cortical astrocytes. *J. Biol. Chem.* 273:4112-4118.
32. **Schumann, R. R., C. J. Kirschning, A. Unbehauen, H. P. Aberle, H. P. Knope, N. Lamping, R. J. Ulevitch, and F. Herrmann.** 1996. The lipopolysaccharide-binding protein is a secretory class 1 acute-phase protein whose gene is transcriptionally activated by APRF/STAT/3 and other cytokine-inducible nuclear proteins. *Mol. Cell. Biol.* 16:3490-3503.
33. **Coffer, P., C. Lutticken, A. van Puijenbroek, M. Klop-de Jonge, F. Horn, and W. Kruijer.** 1995. Transcriptional regulation of the junB promoter: analysis of STAT-mediated signal transduction. *Oncogene.* 10:985-994.

34. **Hill, C. S., and R. Treisman.** 1995. Differential activation of c-fos promoter elements by serum, lysophosphatidic acid, G proteins and polypeptide growth factors. *EMBO J.* 14:5037-5047.
35. **Harroch, S., M. Revel, and J. Chebath.** 1994. Induction by interleukin-6 of interferon regulatory factor 1 (IRF-1) gene expression through the palindromic interferon response element pIRE and cell type-dependent control of IRF-1 binding to DNA. *EMBO J.* 13:1942-1949.
36. **Yamada, T., K. Tobita, S. Osada, T. Nishihara, and M. Imagawa.** 1997. CCAAT/Enhancer-Binding Protein {delta} Gene Expression Is Mediated by APRF/STAT3. *J. Biochem.* 121:731-738.
37. **Haspel, R. L., M. Salditt Georgieff, and J. E. Darnell, Jr.** 1996. The rapid inactivation of nuclear tyrosine phosphorylated Stat1 depends upon a protein tyrosine phosphatase. *EMBO J.* 15:6262-6268.
38. **Chung, C. D., J. Liao, B. Liu, X. Rao, P. Jay, P. Berta, and K. Shuai.** 1997. Specific inhibition of Stat3 signal transduction by PIAS3. *Science.* 278:1803-1805.
39. **Starr, R., T. A. Willson, E. M. Viney, L. J. Murray, J. R. Rayner, B. J. Jenkins, T. J. Gonda, W. S. Alexander, D. Metcalf, N. A. Nicola, and D. J. Hilton.** 1997. A family of cytokine-inducible inhibitors of signalling. *Nature.* 387:917-921.
40. **Endo, T. A., M. Masuhara, M. Yokouchi, R. Suzuki, H. Sakamoto, K. Mitsui, A. Matsumoto, S. Tanimura, M. Ohtsubo, H. Misawa, T. Miyazaki, N. Leonor, T. Taniguchi, T. Fujita, Y. Kanakura, S. Komiya, and A. Yoshimura.** 1997. A new protein containing an SH2 domain that inhibits JAK kinases. *Nature.* 287:921-924.
41. **Stahl, N., T. J. Farruggella, T. G. Boulton, Z. Zhong, J. E. Darnell, Jr., and G. D. Yancopoulos.** 1995. Choice of STATs and other substrates specified by modular tyrosine-based motifs in cytokine receptors. *Science.* 267:1349-1353.
42. **Fukada, T., M. Hibi, Y. Yamanaka, M. Takahashi Tezuka, Y. Fujitani, T. Yamaguchi, K. Nakajima, and T. Hirano.** 1996. Two signals are necessary for cell proliferation induced by a cytokine receptor gp130: involvement of STAT3 in anti-apoptosis. *Immunity.* 5:449-460.
43. **Saito, M., K. Yoshida, M. Hibi, T. Taga, and T. Kishimoto.** 1992. Molecular cloning of a murine IL-6 receptor-associated signal transducer, gp130, and its regulated expression in vivo. *J. Immunol.* 148:4066-4071.
44. **Sprecher, C., F. Grant, and J. Baumgartner.** 1998. Cloning and characterization of a novel class I cytokine receptor. *Biochem. Biophys. Res. Commun.* 246:82-90.
45. **Martens, A. S., J. G. Bode, P. C. Heinrich, and L. Graeve.** 2000. The cytoplasmic domain of the interleukin-6 receptor gp80 mediates its basolateral sorting in polarized madin-darby canine kidney cells. *J. Cell Sci.* 113:3593-3602.
46. **Rose-John, S., M. Ehlers, J. Grötzinger, and J. Müllberg.** 1995. The soluble interleukin-6 receptor. *Ann. N. Y. Acad. Sci.* 762:207-220; discussion 220-201.

47. **Honda, M., S. Yamamoto, M. Cheng, K. Yasukawa, H. Suzuki, T. Saito, Y. Osugi, T. Tokunaga, and T. Kishimoto.** 1992. Human soluble IL-6 receptor: its detection and enhanced release by HIV infection. *J. Immunol.* 148:2175-2180.
48. **Müller-Newen, G., C. Kohne, R. Keul, U. Hemmann, W. Muller-Esterl, J. Wijdenes, J. P. Brakenhoff, M. H. Hart, and P. C. Heinrich.** 1996. Purification and characterization of the soluble interleukin-6 receptor from human plasma and identification of an isoform generated through alternative splicing. *Eur. J. Biochem.* 236:837-842.
49. **Yasukawa, K., K. Futatsugi, T. Saito, H. Yawata, M. Narazaki, H. Suzuki, T. Taga, and T. Kishimoto.** 1992. Association of recombinant soluble IL-6-signal transducer, gp130, with a complex of IL 6 and soluble IL-6 receptor, and establishment of an ELISA for soluble gp130. *Immunol. Lett.* 31:123-130.
50. **Rose-John, S., and P. C. Heinrich.** 1994. Soluble receptors for cytokines and growth factors: generation and biological function. *Biochem. J.* 300:281-290.
51. **Peters, M., A. Müller, and S. Rose-John.** 1998. Interleukin-6 and soluble Interleukin-6 Receptor: Direct Stimulation of gp130 and Hematopoiesis. *Blood.* 92:3495-3504.
52. **Horiuchi, S., Y. Koyanagi, Y. Zhou, H. Miyamoto, Y. Tanaka, M. Waki, A. Matsumoto, M. Yamamoto, and N. Yamamoto.** 1994. Soluble interleukin-6 receptors released from T cell or granulocyte/macrophage cell lines and human peripheral blood mononuclear cells are generated through an alternative splicing mechanism. *Eur. J. Immunol.* 24:1945-1948.
53. **Müllberg, J., E. Dittrich, L. Graeve, C. Gerhartz, K. Yasukawa, T. Taga, T. Kishimoto, P. C. Heinrich, and S. Rose-John.** 1993. Differential shedding of the two subunits of the interleukin-6 receptor. *FEBS Lett.* 332:174-178.
54. **Montero-Julian, F. A.** 2001. The soluble IL-6 receptors: serum levels and biological function. *Cell Mol. Biol.* 47:583-597.
55. **Müller-Newen, G., A. Küster, U. Hemmann, R. Keul, U. Horsten, A. Martens, L. Graeve, J. Wijdenes, and P. C. Heinrich.** 1998. Soluble IL-6 receptor potentiates the antagonistic activity of soluble gp130 on IL-6 responses. *J. Immunol.* 161:6347-6355.
56. **Narazaki, M., K. Yasukawa, T. Saito, Y. Ohsugi, H. Fukui, Y. Koishihara, G. D. Yancopoulos, T. Taga, and T. Kishimoto.** 1993. Soluble forms of the interleukin-6 signal-transducing receptor component gp130 in human serum possessing a potential to inhibit signals through membrane-anchored gp130. *Blood.* 82:1120-1126.
57. **Müllberg, J., F. H. Durie, C. Otten Evans, M. R. Alderson, S. Rose-John, D. Cosman, R. A. Black, and K. M. Mohler.** 1995. A metalloprotease inhibitor blocks shedding of the IL-6 receptor and the p60 TNF receptor. *J. Immunol.* 155:5198-5205.

58. **Orlando, S., M. Sironi, G. Bianchi, A. H. Drummond, D. Boraschi, D. Yabes, and A. Mantovani.** 1997. Role of metalloproteases in the release of the IL-1 type II decoy receptor. *J. Biol. Chem.* 272:31764-31769.
59. **Mohler, K. M., P. R. Sleath, J. N. Fitzner, D. P. Cerretti, M. Alderson, S. S. Kerwar, D. S. Torrance, C. Otten Evans, T. Greenstreet, K. Weerawarna, S. R. Kronheim, M. Petersen, M. Gerhart, C. J. Kozlosky, C. J. March, and R. A. Black.** 1994. Protection against a lethal dose of endotoxin by an inhibitor of tumour necrosis factor processing. *Nature.* 370:218-220.
60. **Jones, S., and S. Rose-John.** 2002. The role of soluble receptors in cytokine biology: The agonistic properties of the sIL-6R/IL-6 complex. *Biochim. Biophys. Acta.* 1592:251-264.
61. **Feldmann, M., F. M. Brennan, and R. N. Maini.** 1996. Role of Cytokines in Rheumatoid Arthritis. *Annu. Rev. Immunol.* 14:397-440.
62. **Yoshizaki, K., N. Nishimoto, M. Mihara, and T. Kishimoto.** 1998. Therapy of rheumatoid arthritis by blocking IL-6 signal transduction with a humanized anti-IL-6 receptor antibody. *Springer Semin Immunopathol.* 20:247-259.
63. **Robak, T., A. Gladalska, H. Stepien, and E. Robak.** 1998. Serum levels of interleukin-6 type cytokines and soluble interleukin-6 receptor in patients with rheumatoid arthritis. *Mediators Inflamm.* 7:347-353.
64. **Kotake, S., K. Sato, K. J. Kim, N. Takahashi, N. Udagawa, I. Nakamura, A. Yamaguchi, T. Kishimoto, T. Suda, and S. Kashiwazaki.** 1996. Interleukin-6 and soluble interleukin-6 receptors in the synovial fluids from rheumatoid arthritis patients are responsible for osteoclast-like cell formation. *J. Bone. Miner. Res.* 11:88-95.
65. **Choy, E. H., D. A. Isenberg, S. Farrow, T. Garrood, Y. Ioannou, H. Bird, N. Cheung, B. D. Williams, B. Hazlemau, R. Price, T. Kishimoto, and G. S. Panayi.** 2001. A double-blind, randomized, placebo-controlled trial of anti-interleukin-6 (IL-6) receptor monoclonal antibody in rheumatoid arthritis (RA). *Arthritis Rheum.* 44:S84.
66. **Desgeorges, A., C. Gabay, P. Silacci, D. Novick, P. Roux-Lombard, G. Grau, J. M. Dayer, T. Vischer, and P. A. Guerne.** 1997. Concentrations and origins of soluble interleukin 6 receptor-alpha in serum and synovial fluid. *J. Rheumatol.* 24:1510-1516.
67. **Ohtani, K., H. Ninomiya, Y. Hasegawa, T. Kobayashi, H. Kojima, T. Nagasawa, and T. Abe.** 1995. Clinical significance of elevated soluble interleukin-6 receptor levels in the sera of patients with plasma cell dyscrasias. *Br. J. Haematol.* 91:116-120.
68. **Pulkki, K., T. T. Pelliniemi, A. Rajamaki, A. Tienhaara, M. Laakso, and R. Lahtinen.** 1996. Soluble interleukin-6 receptor as a prognostic factor in multiple myeloma. Finnish Leukaemia Group. *Br. J. Haematol.* 92:370-374.
69. **Kyriakou, D., H. Papadaki, A. G. Eliopoulos, A. Foudoulakis, M. Alexandrakis, and G. D. Eliopoulos.** 1997. Serum soluble IL-6 receptor concentrations correlate

- with stages of multiple myeloma defined by serum beta 2-microglobulin and C-reactive protein. *Int. J. Hematol.* 66:367-371.
70. **Gaillard, J.-P., J. Liautard, B. Klein, and J. Brochier.** 1997. Major role of the soluble interleukin-6/interleukin-6 receptor complex for the proliferation of interleukin-6-dependent human myeloma cell lines. *Eur. J. Immunol.* 27:3332-3340.
 71. **Mitsuyama, K., A. Toyonaga, E. Sasaki, O. Ishida, H. Ikeda, O. Tsuruta, K. Harada, H. Tateishi, T. Nishiyama, and K. Tanikawa.** 1995. Soluble interleukin-6 receptors in inflammatory bowel disease: relation to circulating interleukin-6. *Gut.* 36:45-49.
 72. **Atreya, R., J. Mudter, S. Finotto, J. Müllberg, T. Jostock, S. Wirtz, M. Schütz, B. Bartsch, M. Holtmann, C. Becker, D. Strand, J. Czaja, J. F. Schlaak, H. A. Lehr, F. Autschbach, G. Schürmann, N. Nishimoto, K. Yoshizaki, H. Ito, T. Kishimoto, P. R. Galle, S. Rose-John, and M. F. Neurath.** 2000. Blockade of IL-6 transsignaling abrogates established experimental colitis in mice by suppression of the antiapoptotic resistance of lamina propria T cells. *Nat. Med.* 6:583-588.
 73. **Jostock, T., J. Müllberg, S. Özbek, R. Atreya, G. Blinn, N. Voltz, M. Fischer, M. F. Neurath, and S. Rose-John.** 2001. Soluble gp130 is the natural inhibitor of soluble IL-6R transsignaling responses. *Eur. J. Biochem.* 268:160-167.
 74. **Peters, M., S. Jacobs, M. Ehlers, P. Vollmer, J. Müllberg, E. Wolf, G. Brem, K. H. Meyer zum Büschenfelde, and S. Rose-John.** 1996. The function of the soluble interleukin 6 (IL-6) receptor in vivo: sensitization of human soluble IL-6 receptor transgenic mice towards IL-6 and prolongation of the plasma half-life of IL-6. *J. Exp. Med.* 183:1399-1406.
 75. **Jones, S. A., S. Horiuchi, N. Topley, N. Yamamoto, and G. M. Fuller.** 2001. The soluble interleukin 6 receptor: mechanisms of production and implications in disease. *FASEB J.* 15:43-58.
 76. **Hooper, N. M., E. H. Karran, and A. J. Turner.** 1997. Membrane protein secretases. *Biochem. J.* 321:265-279.
 77. **Matthews, V., B. Schuster, S. Schütze, I. Bussmeyer, A. Ludwig, C. Hundhausen, T. Sadowski, P. Saftig, D. Hartmann, K. J. Kallen, and S. Rose-John.** 2003. Cholesterol depletion of the plasma membrane triggers shedding of the human interleukin-6 receptor by TACE and independently of PKC. *J. Biol. Chem.* 278:38829-38839.
 78. **Jones, S. A., D. Novick, S. Horiuchi, N. Yamamoto, A. J. Szalai, and G. M. Fuller.** 1999. C-reactive protein: a physiological activator of interleukin 6 receptor shedding. *J. Exp. Med.* 189:599-604.
 79. **Franchimont, N., C. Lambert, P. Huynen, C. Ribbens, B. Relic, A. Chariot, V. Bours, J. Piette, M. Merville, and M. Malaise.** 2005. Interleukin-6 receptor shedding is enhanced by interleukin-1beta and tumor necrosis factor alpha and is partially mediated by tumor necrosis factor alpha-converting enzyme in osteoblast-like cells. *Arthritis Rheum.* 52:84-93.

80. **Walev, I., P. Vollmer, M. Palmer, S. Bhakdi, and S. Rose-John.** 1996. Pore-forming toxins trigger shedding of receptors for interleukin 6 and lipopolysaccharide. *PNAS*. 93:7882-7887.
81. **Vollmer, P., I. Walev, S. Rose-John, and S. Bhakdi.** 1996. Novel pathogenic mechanism of microbial metalloproteinases: liberation of membrane-anchored molecules in biologically active form exemplified by studies with the human interleukin-6 receptor. *Infect. Immun.* 64:3646-3651.
82. **Bank, U., D. Reinhold, C. Schneemilch, D. Kunz, H. J. Synowitz, and S. Ansorge.** 1999. Selective proteolytic cleavage of IL-2 receptor and IL-6 receptor ligand binding chains by neutrophil-derived serine proteases at foci of inflammation. *J. Interferon. Cytokine. Res.* 19:1277-1287.
83. **Black, R. A., C. T. Rauch, C. J. Kozlosky, J. J. Peschon, J. L. Slack, M. F. Wolfson, B. J. Castner, K. L. Stocking, P. Reddy, S. Srinivasan, N. Nelson, N. Boiani, K. A. Schooley, M. Gerhart, R. Davis, J. N. Fitzner, R. S. Johnson, R. J. Paxton, C. J. March, and D. P. Cerretti.** 1997. A metalloproteinase disintegrin that releases tumour-necrosis factor-alpha from cells. *Nature*. 385:729-733.
84. **Moss, M. L., S. L. Jin, M. E. Milla, D. M. Bickett, W. Burkhart, H. L. Carter, W. J. Chen, W. C. Clay, J. R. Didsbury, D. Hassler, C. R. Hoffman, T. A. Kost, M. H. Lambert, M. A. Leesnitzer, P. McCauley, G. McGeehan, J. Mitchell, M. Moyer, G. Pahel, W. Rocque, L. K. Overton, F. Schoenen, T. Seaton, J. L. Su, J. Warner, D. Willard, and J. D. Becherer.** 1997. Cloning of a disintegrin metalloproteinase that processes precursor tumour-necrosis factor-alpha. *Nature*. 385:733-736.
85. **Leann Hinkle, C., S. W. Sunnarborg, D. Loisel, C. E. Parker, M. Stevenson, W. E. Russell, and D. C. Lee.** 2004. Selective roles for Tumor Necrosis Factor alpha-converting enzyme/ADAM17 in the shedding of the Epidermal Growth Factor receptor ligand family. *J. Biol. Chem.* 279:24179-24188.
86. **Sahin, U., G. Weskamp, K. Kelly, H. Zhou, S. Higashiyama, J. Peschon, D. Hartmann, P. Saftig, and C. Blobel.** 2004. Distinct roles for ADAM10 and ADAM17 in ectodomain shedding of six EGFR ligands. *J. Cell. Biol.* 164:769-779.
87. **Schäfer, B., B. Marg, A. Gschwind, and A. Ullrich.** 2004. Distinct ADAM metalloproteinases regulate G protein coupled receptor-induced cell proliferation and survival. *J. Biol. Chem.* 279:47929-47938.
88. **Montero, J. C., L. Yuste, E. Díaz-Rodríguez, A. Esparís-Ogando, and A. Pandiella.** 2000. Differential Shedding of Transmembrane Neuregulin Isoforms by the Tumor Necrosis Factor- α -Converting Enzyme. *Mol. Cell. Neurosci.* 16:631-648.
89. **Diaz-Rodriguez, E., J. C. Montero, A. Esparis-Ogando, L. Yuste, and A. Pandiella.** 2002. Extracellular signal-regulated kinase phosphorylates tumor necrosis factor alpha-converting enzyme at threonine 735: a potential role in regulated shedding. *Mol. Biol. Cell.* 13:2031-2044.

90. **Zang, Y., J. Jiang, R. A. Black, G. Baumann, and S. J. Frank.** 2000. Tumor Necrosis Factor- α Converting Enzyme (TACE) is a Growth Hormone Binding Protein (GHBP) Sheddase: The Metalloprotease TACE/ADAM-17 Is Critical for (PMA-Induced) GH Receptor Proteolysis and GHBP Generation. *J. Biol. Chem.* 141:4342–4348.
91. **Brou, C., F. Logeat, N. Gupta, C. Bessia, O. LeBail, J. Doedens, A. Cumano, P. Roux, R. Black, and A. Israël.** 2003. A Novel Proteolytic Cleavage Involved in Notch Signaling. The Role of the Disintegrin-Metalloprotease TACE. *Molecular Cell.* 5:207-216.
92. **Reddy, P., J. L. Slack, R. Davis, D. P. Cerretti, C. J. Kozlosky, R. A. Blanton, D. Shows, J. J. Peschon, and R. A. Black.** 2000. Functional analysis of the domain structure of tumor necrosis factor- α converting enzyme. *J. Biol. Chem.* 275:14608-14614.
93. **Preece, G., G. Murphy, and A. Ager.** 1996. Metalloproteinase-mediated regulation of L-selectin levels on leukocytes. *J. Biol. Chem.* 271:11634-11640.
94. **Müllberg, J., H. Schooltink, T. Stoyan, M. Gunther, L. Graeve, G. Buse, A. Mackiewicz, P. C. Heinrich, and S. Rose-John.** 1993. The soluble interleukin-6 receptor is generated by shedding. *Eur. J. Immunol.* 23:473-480.
95. **Garton, K. J., P. J. Gough, C. P. Blobel, G. Murphy, D. R. Greaves, P. J. Dempsey, and E. W. Raines.** 2001. TACE (ADAM17) mediates the cleavage and shedding of Fractalkine (CX3CL1). *J. Biol. Chem.* 276:37993-38001.
96. **Colotta, F., S. Orlando, E. J. Fadlon, S. Sozzani, C. Matteucci, and A. Mantovani.** 1995. Chemoattractants induce rapid release of the interleukin 1 type II decoy receptor in human polymorphonuclear cells. *J. Exp. Med.* 181:2181-2186.
97. **Rovida, E., A. Paccagnini, M. Del Rosso, J. Peschon, and P. Dello Sbarba.** 2001. TNF- α -converting enzyme cleaves the macrophage colony-stimulating factor receptor in macrophages undergoing activation. *J. Immunol.* 166:1583-1589.
98. **Bulanova, E., V. Budagian, E. Duitman, Z. Orinska, H. Krause, R. Rückert, N. Reiling, and S. Bulfone-Paus.** 2007. Soluble Interleukin IL-15 α is generated by alternative splicing or proteolytic cleavage and forms functional complexes with IL-15. *J. Biol. Chem.* 282:13167-13179.
99. **Buxbaum, J. D., K. N. Liu, Y. Luo, J. L. Slack, K. L. Stocking, J. J. Peschon, R. S. Johnson, B. J. Castner, D. P. Cerretti, and R. A. Black.** 1998. Evidence that tumor necrosis factor α converting enzyme is involved in regulated α -secretase cleavage of the Alzheimer amyloid protein precursor. *J. Biol. Chem.* 273:27765-27767.
100. **Parkin, E. T., N. T. Watt, A. J. Turner, and N. M. Hooper.** 2004. Dual mechanisms for shedding of the cellular prion protein. *J. Biol. Chem.* 279:11170-11178.

101. Thathiah, A., C. P. Blobel, and D. D. Carson. 2003. Tumor necrosis factor-alpha converting enzyme (TACE)/ADAM 17 mediates MUC1 shedding. *J. Biol. Chem.* 278:3386-3394.
102. **Franzke, C. W., K. Tasanen, H. Schäcke, Z. Zhou, K. Tryggvason, C. Mauch, P. Zigrino, S. Sunnarborg, D. C. Lee, F. Fahrenholz, and L. Bruckner-Tuderman.** 2002. Transmembrane collagen XVII, an epithelial adhesion protein, is shed from the cell surface by ADAMs. *EMBO J.* 21 5026–5035, :5026–5035.
103. **Mezyk, R., M. Bzowska, and J. Bereta.** 2003. Structure and functions of tumor necrosis factor-alpha converting enzyme. *Acta Biochem. Pol.* 50:625-645.
104. **Stöcker, W., F. Grams, U. Baumann, P. Reinemer, F. X. Gomis-Ruth, D. B. McKay, and W. Bode.** 1995. The metzincins--topological and sequential relations between the astacins, adamalysins, serralysins, and matrixins (collagenases) define a superfamily of zinc-peptidases. *Protein Sci.* 4:823-840.
105. **Blobel, C. P.** 1997. Metalloprotease-disintegrins: links to cell adhesion and cleavage of TNF alpha and Notch. *Cell.* 90:589-592.
106. **Black, R. A., and J. M. White.** 1998. ADAMs: focus on the protease domain. *Curr. Opin. Cell Biol.* 10:654-659.
107. **Gechtman, Z., A. J.L., G. Raab, D. E. Ingber, and M. Klagsbrun.** 1999. The shedding of membrane-anchored heparin-binding epidermal-like growth factor is regulated by the Raf/Mitogen-activated protein kinase cascade and by cell adhesion and spreading. *J. Biol. Chem.* 274:28828-28835.
108. **Diaz-Rodriguez, E., N. Cabrera, A. Esparis-Ogando, J. C. Montero, and A. Pandiella.** 1999. Cleavage of the TrkA neurotrophin receptor by multiple metalloproteases generates signalling-competent truncated forms. *Eur. J. Neuroscience.* 11:1421-1430.
109. **Zhang, Q., S. M. Thomas, V. W. Y. Lui, S. Xi, Y. M. Siegfried, H. Fan, T. E. Smithgall, G. B. Mills, and J. R. Grandis.** 2006. Phosphorylation of TNF- α converting enzyme by gastrin-releasing peptide induces amphiregulin release and EGF receptor activation. *PNAS.* 103:6901-6906.
110. **Zhang, Z., P. Oliver, J. J. R. Lancaster, P. O. Schwarzenberger, M. S. Joshi, and J. Cork.** 2001. Reactive oxygen species mediate tumor necrosis factor alpha-converting, enzyme-dependent ectodomain shedding induced by phorbol myristate acetate. *FASEB J.* 2:303-305.
111. **Gomez-Gavero, M. V., I. Gonzales-Alvaro, C. Dominguez-Jimenez, J. Peschon, R. A. Black, F. Sanchez-Madrid, and F. Diaz-Gonzales.** 2002. Structure-Function Relationship and Role of Tumor Necrosis Factor-alpha -converting Enzyme in the Down-regulation of L-selectin by Non-steroidal Anti-inflammatory Drugs. *J. Biol. Chem.* 277:38212-38221.

112. **Steinhusen, U., J. Weiske, V. Badock, R. Tauber, K. Bommert, and O. Huber.** 2001. Cleavage and Shedding of E-cadherin after Induction of Apoptosis. *J. Biol. Chem.* 276:4972-4980.
113. **Bleackley, R. C., and J. A. Heibein.** 2001. Enzymatic control of apoptosis. *Nat. Prod. Rep.* 18:431-440.
114. **Wyllie, A. H., J. F. Kerr, and A. R. Currie.** 1980. Cell death: the significance of apoptosis. *Int. Rev. Cytol.* 68:251-306.
115. **Perfettini, J. L., and G. Kroemer.** 2003. Caspase activation is not death. *Nat. Immunol.* 4:308-310.
116. **Balasubramanian, K., and A. J. Schroit.** 2003. Aminophospholipid asymmetry: A matter of life and death. *Annu. Rev. Physiol.* 65:701-734.
117. **Alneri, E. S.** 1996. Human ICE/CED-3 protease nomenclature. *Cell* 87:171.
118. **Thornberry, N. A.** 1997. A combinatorial approach defines specificities of members of the caspase family and granzyme B. Functional relationships established for key mediators of apoptosis. *J. Biol. Chem.* 272:17907-17911.
119. **Budihardjo, I., H. Oliver, M. Lutter, X. Luo, and X. Wang.** 1999. Biochemical pathways of caspase activation during apoptosis. *Annu. Rev. Cell Dev. Biol.* 15:269-290.
120. **Cikala, M., B. Wilm, E. Hobmayer, A. Bottger, and C. N. David.** 1999. Identification of caspases and apoptosis in the simple metazoan Hydra. *Curr. Biol.* 9:959-962.
121. **Earnshaw, W. C., L. M. Martins, and S. H. Kaufmann.** 1999. Mammalian caspases: structure, activation, substrates, and functions during apoptosis. *Annu. Rev. Biochem.* 68:383-424
122. **Earnshaw, W. C., L. M. Martins, and S. H. Kaufmann.** 1999. Mammalian caspases: structure, activation, substrates, and functions during apoptosis. *Annu. Rev. Biochem.* 68:383-424.
123. **Kaufmann, S. H., S. Desnoyers, Y. Ottaviano, N. E. Davidson, and G. Poirier.** 1993. Specific proteolytic cleavage of poly(ADP-ribose) polymerase: an early marker of chemotherapy-induced apoptosis. *Cancer Res.* 53:3976-3985.
124. **Lazebnik, Y. A., A. Takahashi, G. G. Poirier, S. H. Kaufmann, and W. C. Earnshaw.** 1995. Characterization of the execution phase of apoptosis in vitro using extracts from condemned-phase cells. *J. Cell Sci. Suppl.* 19:41-49.
125. **Mashima, T., M. Naito, K. Noguchi, D. K. Miller, D. W. Nicholson, and T. Tsuruo.** 1997. Actin cleavage by CPP-32/apopain during the development of apoptosis. *Oncogene.* 14:1007-1012.

126. **Martin, S. J., G. A. O'Brien, W. K. Nishioka, A. J. McGahon, A. Mahboubi, T. C. Saido, and D. R. Green.** 1995. Proteolysis of fodrin (non-erythroid spectrin) during apoptosis. *J. Biol. Chem.* 270:6425-6428.
127. **Emoto, Y., Y. Manome, G. Meinhardt, H. Kisaki, S. Kharbanda, M. Robertson, T. Ghayur, W. W. Wong, R. Kamen, and R. Weichselbaum.** 1995. Proteolytic activation of protein kinase C delta by an ICE-like protease in apoptotic cells. *EMBO J.* 14:6148-6156.
128. **Jänicke, R. U., P. A. Walker, X. Y. Lin, and A. G. Porter.** 1996. Specific cleavage of the retinoblastoma protein by an ICE-like protease in apoptosis. *EMBO J.* 15:6969-6978.
129. **Boldin, M. P., I. L. Mett, E. E. Varfolomeev, I. Chumakov, Y. Shemer-Avni, J. H. Camonis, and D. Wallach.** 1995. Self-association of the "death domains" of the p55 tumor necrosis factor (TNF) receptor and Fas/APO1 prompts signaling for TNF and Fas/APO1 effects. *J. Biol. Chem.* 270:7795-7798.
130. **Liu, X., C. N. Kim, J. Yang, R. Jemmerson, and X. Wang.** 1996. Induction of apoptotic program in cell-free extracts: requirement for dATP and cytochrome c. *Cell.* 86:147-157.
131. **Zou, H., W. J. Henzel, X. Liu, A. Lutschg, and X. Wang.** 1997. Apaf-1, a human protein homologous to *C. elegans* CED-4, participates in cytochrome c-dependent activation of caspase-3. *Cell.* 90:405-413.
132. **Hua, Z., L. Yuchen, L. Xuesong, and W. Xiaodong.** 1999. An APAF-1-Cytochrome c Multimeric Complex Is a Functional Apoptosome That Activates Procaspase-9. *J. Biol. Chem.* 274:11549-11556.
133. **Finucane, D. M., E. Bossy-Wetzel, N. J. Waterhouse, T. G. Cotter, and D. R. Green.** 1999. Bax-induced caspase activation and apoptosis via cytochrome c release from mitochondria is inhibitable by Bcl-xL. *J. Biol. Chem.* 274:2225-2233.
134. **Gajkowska, B., U. Wojewodzka, and J. Gajda.** 2004. Bid to mitochondria, endoplasmic reticulum and nuclear envelope: possible control points in apoptosis. *J. Mol. Histol.* 35:11-19.
135. **Huang, D. C., and A. Strasser.** 2000. BH3-only proteins-essential initiators of apoptotic cell death. *Cell.* 103:839-842.
136. **Adams, J. M., and S. Cory.** 1998. The Bcl-2 protein family: arbiters of cell survival. *Science.* 281:1322-1326.
137. **Gajkowska, B., U. Wojewodzka, and J. Gajda.** 2004. Translocation of Bax and Bid to mitochondria, endoplasmic reticulum and nuclear envelope: possible control points in apoptosis. *J. Mol. Histol.* 35:11-19.
138. **Lithgow, T., R. van Driel, J. F. Bertram, and A. Strasser.** 1994. The protein product of the oncogene bcl-2 is a component of the nuclear envelope, the

- endoplasmic reticulum, and the outer mitochondrial membrane. *Cell. Growth. Differ.* 5:411-417.
139. **Zong, W. X., C. Li, G. Hatzivassiliou, T. Lindsten, Q. C. Yu, J. Yuan, and C. B. Thompson.** 2003. Bax and Bak can localize to the endoplasmic reticulum to initiate apoptosis. *J. Cell Biol.* 162:59-69.
140. **Oda, E., R. Ohki, H. Murasawa, J. Nemoto, T. Shibue, T. Yamashita, T. Tokino, T. Taniguchi, and T. N.** 2000. Noxa, a BH3-only member of the Bcl-2 family and candidate mediator of p53-induced apoptosis. *Science.* 288:1053-1058.
141. **Zha, J., H. Harada, E. Yang, J. Jockel, and S. J. Korsmeyer.** 1996. Serine phosphorylation of death agonist BAD in response to survival factor results in binding to 14-3-3 not BCL-XL. *Cell.* 87:619-628.
142. **Chen, M., H. He, S. Zhan, S. Krajewski, J. C. Reed, and R. A. Gottlieb.** 2001. Bid is cleaved by calpain to an active fragment in vitro and during myocardial ischemia/reperfusion. *J. Biol. Chem.* 276:30724-30728.
143. **Li, H., H. Zhu, C. J. Xu, and J. Yuan.** 1998. Cleavage of BID by caspase 8 mediates the mitochondrial damage in the Fas pathway of apoptosis. *Cell.* 94:491-501.
144. **Mandic, A., K. Viktorsson, L. Strandberg, T. Heiden, J. Hansson, S. Linder, and M. C. Shoshan.** 2002. Calpain-mediated Bid cleavage and calpain-independent Bak modulation: two separate pathways in cisplatin-induced apoptosis. *Mol. Cell Biol.* 22:3003-3013.
145. **Sedlak, T. W., Z. N. Oltvai, E. Yang, K. Wang, L. H. Boise, C. B. Thompson, and S. J. Korsmeyer.** 1995. Multiple Bcl-2 family members demonstrate selective dimerizations with Bax. *PNAS.* 92:7834-7838.
146. **Willis, S. N., L. Chen, G. Dewson, A. Wei, E. Naik, J. I. Fletcher, J. M. Adams, and D. C. Huang.** 2005. Proapoptotic Bak is sequestered by Mcl-1 and Bcl-xL, but not Bcl-2, until displaced by BH3-only proteins. *Genes Dev.* 19:1294-1305.
147. **Cheng, E. H., T. V. Sheiko, J. K. Fisher, W. J. Craigen, and S. J. Korsmeyer.** 2003. VDAC2 inhibits BAK activation and mitochondrial apoptosis. *Science.* 301:513-517.
148. **Palacios, R., and M. Steinmetz.** 1985. Il-3-dependent mouse clones that express B-220 surface antigen, contain Ig genes in germ-line configuration, and generate B lymphocytes in vivo. *Cell.* 41:727-734.
149. **Gearing, D. P., S. F. Ziegler, M. R. Comeau, D. Friend, B. Thoma, D. Cosman, L. Park, and B. Mosley.** 1994. Proliferative responses and binding properties of hematopoietic cells transfected with low-affinity receptors for leukemia inhibitory factor, oncostatin M, and ciliary neurotrophic factor. *PNAS.* 91:1119-1123.
150. **Stoyan, T., U. Michaelis, H. Schooltink, M. Van Dam, R. Rudolph, P. C. Heinrich, and S. Rose-John.** 1993. Recombinant soluble human interleukin-6

- receptor. Expression in *Escherichia coli*, renaturation and purification. *Eur. J. Biochem.* 216:239-245.
151. **van Dam, M., J. Müllberg, H. Schooltink, T. Stoyan, J. P. Brakenhoff, L. Graeve, P. C. Heinrich, and S. Rose-John.** 1993. Structure-function analysis of interleukin-6 utilizing human/murine chimeric molecules. Involvement of two separate domains in receptor binding. *J. Biol. Chem.* 268:15285-15290.
152. **Fischer, M., J. Goldschmitt, C. Peschel, J. Brakenhoff, K. Kallen, A. Wollmer, J. Grotzinger, and S. Rose-John.** 1997. A bioactive designer cytokine for human hematopoietic progenitor cell expansion. *Nat. Biotechnol.* 15:142-145.
153. **Sambrook, J., E. F. Fritsch, and T. Maniatis.** 1989. *Molecular Cloning: A laboratory manual.* Cold Spring Harbor Laboratory Press, Cold Spring Harbor, NY.
154. **Samland, H., J. Tilgner, P. März, U. Otten, S. Rose-John, and B. Volk.** 1998. Investigation of the potential neuroprotective effect of the new designer cytokine H-IL-6 on NMDA-induced neurotoxicity in rat brain. In *26th Göttingen Neurobiology Conference.* N. Elsner, and R. Wehner, eds. Georg Thieme Verlag, Göttingen. 722.
155. **Laemmli, U. K.** 1970. Cleavage of structural proteins during the assembly of the head of bacteriophage T4. *Nature.* 227:680-685.
156. **Edwards, J. C., A. D. Sedgwick, and D. A. Willoughby.** 1981. The formation of a structure with the features of synovial lining by subcutaneous injection of air: an in vivo tissue culture system. *J. Pathol.* 134:147-156.
157. **Sedgwick, A. D., Y. M. Sin, J. C. Edwards, and D. A. Willoughby.** 1983. Increased inflammatory reactivity in newly formed lining tissue. *J. Pathol.* 141:483-495.
158. **Dawson, J., A. D. Sedgwick, J. C. Edwards, and P. Lees.** 1991. A comparative study of the cellular, exudative and histological responses to carrageenan, dextran and zymosan in the mouse. *Int. J. Tissue. React.* 13:171-185.
159. **Fischer, M., J. Goldschmitt, C. Peschel, K. J. Kallen, J. P. J. Brakenhoff, A. Wollmer, J. Grötzinger, and S. Rose-John.** 1997. A designer cytokine with high activity on human hematopoietic progenitor cells. *Nat. Biotechnol.* 15:142-145.
160. **Schroers, A., O. Hecht, K. J. Kallen, M. Pachta, S. Rose-John, and J. Grotzinger.** 2005. Dynamics of the gp130 cytokine complex: a model for assembly on the cellular membrane. *Protein Sci.* 14:783-790.
161. **Ludwig, A., C. Hundhausen, M. H. Lambert, N. Broadway, R. C. Andrews, D. M. Bickett, M. A. Leesnitzer, and J. D. Becherer.** 2005. Metalloproteinase inhibitors for the disintegrin-like metalloproteinases ADAM10 and ADAM17 that differentially block constitutive and phorbol ester-inducible shedding of cell surface molecules. *Comb. Chem. High Throughput Screen.* 8:161-171.
162. **Hundhausen, C., D. Misztela, T. A. Berkhout, N. Broadway, P. Saftig, K. Reiss, D. Hartmann, F. Fahrenholz, R. Postina, V. Matthews, K. J. Kallen, S. Rose-John, and A. Ludwig.** 2003. The disintegrin-like metalloproteinase ADAM10 is

- involved in constitutive cleavage of CX3CL1 (fractalkine) and regulates CX3CL1-mediated cell-cell adhesion. *Blood*. 102:1186-1195.
163. **Solomon, K. A., N. Pesti, G. Wu, and N. R. C.** 1999. Cutting edge: a dominant negative form of TNF-alpha converting enzyme inhibits proTNF and TNFRII secretion. *J. Immunol.* 163:4105-4108.
164. **Toker, A.** 1998. Signaling through protein kinase C. *Frontiers Biosci.* 3:1134-1147.
165. **Mellor, H., and P. Parker.** 1998. The extended protein kinase C superfamily. *Biochem. J.* 332:281-292.
166. **Thabard, W., M. Collette, R. Bataille, and M. Amiot.** 2001. Protein kinase C delta and ieta isoenzymes control the shedding of the interleukin 6 receptor alpha in myeloma cells. *Biochem. J.* 358:193-200.
167. **Ghayur, T., M. Hugunin, R. V. Talanian, S. Ratnofsky, C. Quinlan, Y. Emoto, P. Pandey, R. Datta, Y. Huang, S. Kharbanda, H. Allen, R. Kamen, W. Wong, and D. Kufe.** 1996. Proteolytic Activation of Protein Kinase C delta by an ICE/CED 3-like Protease Induces Characteristics of Apoptosis. *J. Exp. Med.* 184:2399-3404.
168. **Fan, H.** 2003. Characterization of growth factor-induced serine phosphorylation of tumor necrosis factor- α converting enzyme and of an alternatively translated polypeptide. *J. Biol. Chem.* 278:18617-18627.
169. **Weskamp, G., J. Schlöndorff, L. Lum, T. W. Kim, P. Saftig, D. Hartmann, G. Murphy, and C. P. Blobel.** 2004. Evidence for a Critical Role of the Tumor Necrosis Factor α Convertase (TACE) in Ectodomain Shedding of the p75 Neurotrophin Receptor (p75NTR). *J. Biol. Chem.* 279:4241-4249
170. **Fischer, O. M., S. Hart, A. Gschwind, N. Prenzel, and A. Ullrich.** 2004. Oxidative and Osmotic Stress Signaling in Tumor Cells Is Mediated by ADAM Proteases and Heparin-Binding Epidermal Growth Factor. *Mol. Cell Biol.* 24:5172-5183.
171. **Lee, Y. S., Y. S. Kang, S. H. Lee, and J. A. Kim.** 2000. Role of NAD(P)H oxidase in the tamoxifen-induced generation of reactive oxygen species and apoptosis in HepG2 human hepatoblastoma cells. *Cell Death Differ.* 7:925-932.
172. **Kim, J. A., Y. S. Kang, S. H. Park, H. W. Kim, S. Y. Cho, and Y. S. Lee.** 2001. Role of reactive oxygen species in apoptosis induced by N-ethylmaleimide in HepG2 human hepatoblastoma cells. *Eur. J. Pharmacol.* 7:925-932
173. **Lindemann, S. W., C. C. Yost, M. M. Denis, T. M. McIntyre, A. S. Weyrich, and G. A. Zimmerman.** 2004. Neutrophils alter the inflammatory milieu by signal-dependent translation of constitutive messenger RNAs. *PNAS.* 101:7076-7081.
174. **Modur, V., Y. Li, G. A. Zimmerman, S. M. Prescott, and T. M. McIntyre.** 1997. Retrograde inflammatory signaling from neutrophils to endothelial cells by soluble interleukin-6 receptor alpha. *J. Clin. Invest.* 100:2752-2756.
175. **Hurst, S. M., T. S. Wilkinson, R. M. McLoughlin, S. Jones, S. Horiuchi, N. Yamamoto, S. Rose-John, G. M. Fuller, N. Topley, and S. A. Jones.** 2001. Control

- of leukocyte infiltration during inflammation: IL-6 and its soluble receptor orchestrate a temporal switch in the pattern of leukocyte recruitment. *Immunity*. 14:705-714.
176. **Romano, M., M. Sironi, C. Toniatti, N. Polentarutti, P. Fruscella, P. Ghezzi, R. Faggioni, W. Luini, V. van Hinsbergh, S. Sozzani, F. Bussolino, V. Poli, G. Ciliberto, and A. Mantovani.** 1997. Role of IL-6 and its soluble receptor in induction of chemokines and leukocyte recruitment. *Immunity*. 6:315-325.
177. **Romano, M., R. Faggioni, M. Sironi, S. Sacco, B. Echtenacher, E. Di Santo, M. Salmona, and P. Ghezzi.** 1997. Carrageenan-induced acute inflammation in the mouse air pouch synovial model. Role of tumour necrosis factor. *Mediators of Inflammation*. 6:32-38.
178. **Becker, C., M. C. Fantini, C. Schramm, H. A. Lehr, S. Wirtz, A. Nikolaev, J. Burg, S. Strand, R. Kiesslich, S. Huber, H. Ito, N. Nishimoto, K. Yoshizaki, T. Kishimoto, P. R. Galle, M. Blessing, S. Rose-John, and M. F. Neurath.** 2004. TGF-beta suppresses tumor progression in colon cancer by inhibition of IL-6 trans-signaling. *Immunity*. 21:491-501.
179. **Koizumi, N., T. Yamaguchi, K. Kawabata, F. Sakurai, T. Sasaki, Y. Watanabe, T. Hayakawa, and H. Hayakawa.** 2007. Fiber-Modified Adenovirus Vectors Decrease Liver Toxicity through Reduced IL-6 Production. *J. of Immunol.* 178:1767-1773.
180. **Weigert, C., A. M. Hennige, R. Lehmann, K. Brodbeck, B. F., M. Schäuble, H. U. Häring, and E. D. Schleicher.** Direct Cross-talk of Interleukin-6 and Insulin Signal Transduction via Insulin Receptor Substrate-1 in Skeletal Muscle Cells. *J. Biol. Chem.* 281:7060-7067.
181. **Scheller, J., B. Schuster, C. Holscher, T. Yoshimoto, and S. Rose-John.** 2005. No inhibition of IL-27 signaling by soluble gp130. *Biochem. Biophys. Res. Commun.* 326:724-728.
182. **Kraft, A. S., and W. B. Anderson.** Phorbol esters increase the amount of Ca²⁺, phospholipid-dependent protein kinase associated with plasma membrane. *Nature*. 301:621-623.
183. **Volanakis, J. E., and M. H. Kaplan.** 1971. Specificity of C-reactive protein for choline phosphate residues of Pneumococcal C-polysaccharide. *PNAS*. 236:612-614.
184. **Volanakis, J. E., and K. W. A. Wirtz.** 1974. Interaction of C-reactive protein with artificial phosphatidylcholine bilayers. *Nature*. 281:155-157.
185. **Bharadwaja, D., M. P. Steina, M. Volzera, C. Mold, and T. W. Du Closa.** 1999. The Major Receptor for C-Reactive Protein on Leukocytes Is Fc-gamma Receptor II. *J. Exp. Med.* 190:585-590.
186. **Bhakdi, S., H. Bayley, A. Valeva, I. Walev, B. Walker, M. Kehoe, and M. Palmer.** 1996. Staphylococcal alpha-toxin, streptolysin-O, and Escherichia coli hemolysin: prototypes of pore-forming bacterial cytolysins. *Arch. Microbiol.* 165:73-79.

187. **Christian, A. E., M. P. Haynes, M. C. Phillips, and G. H. Rothblat.** 1997. Use of cyclodextrins for manipulating cellular cholesterol content. *J. Lipid Res.* 38:2264-2272.
188. **Walcheck, B., A. H. Herrera, C. St Hill, P. E. Mattila, A. R. Whitney, and F. R. Deleo.** 2006. ADAM17 activity during human neutrophil activation and apoptosis. *Eur. J. Biochem.* 36:968-974.
189. **Schlondorff, J., J. D. Becherer, and C. P. Blobel.** 2000. Intracellular maturation and localization of the tumor necrosis factor alpha convertase (TACE). *Biochem. J.* 347:131-138.
190. **Soond, S. M., B. Everson, D. W. Riches, and G. Murphy.** 2005. ERK-mediated phosphorylation of Thr735 in TNFalpha-converting enzyme and its potential role in TACE protein trafficking. *J. Cell Sci.* 118:2371-2380.
191. **Colotta, F., F. Re, N. Polentarutti, S. Sozzani, and A. Mantovani.** 1992. Modulation of granulocyte survival and programmed cell death by cytokines and bacterial products. *Blood.* 80:2012-2020.
192. **Jacobson, M. D., M. Weil, and M. C. Raff.** 1997. Programmed cell death in animal development. *Cell.* 88:347-354.
193. **Matt, X., G. Shao, and N. J.A.** 2005. Dual oxidase 1-dependent MUC5AC mucin expression in cultured human airway epithelial cells. *PNAS.* 102:767-772.
194. **Aoshiba, K., S. Yasui, M. Hayashi, J. Takaoki, and A. Nagai.** 1999. Role of p38-Mitogen-Activated Protein Kinase in Spontaneous Apoptosis of Human Neutrophils. *J. Immunol.* 162:1692-1700.
195. **Cross, T. G., D. Scheel-Toellner, N. V. Henriquez, E. Deacon, M. Salmon, and J. M. Lord.** 2000. Serine/Threonine protein kinases and apoptosis. *Exp. Cell Res.* 256:34-41.
196. **Hakulinen, J., and J. Keski-Oja.** 2006. ADAM10-mediated Release of Complement Membrane Cofactor Protein during Apoptosis of Epithelial Cells. *J. Biol. Chem.* 281:21369-21376.
197. **Ito, R., W. Yasui, H. Kuniyasu, H. Yokozaki, and E. Tahara.** 1997. Expression of interleukin-6 and its effects on the cell growth of gastric carcinoma cell lines. *Jpn. J. Cancer Res.* 88:953-958.
198. **Asensi, V., E. Valle, A. Meana, J. Fierer, A. Celada, V. Alvarez, J. Paz, E. Coto, J. A. Carton, J. A. Maradona, A. Dieguez, J. Sarasúa, M. G. Ocaña, and J. M. Arribas.** 2004. In Vivo Interleukin-6 Protects Neutrophils from Apoptosis in Osteomyelitis. *Infect. Immun.* 72:3823-3828.
199. **Kovalovich, K., W. Li, R. DeAngelis, L. E. Greenbaum, G. Ciliberto, and R. Taub.** 2001. Interleukin-6 protects against Fas-mediated death by establishing a critical level of anti-apoptotic hepatic proteins FLIP, Bcl-2, and Bcl-xL. *J. Biol. Chem.* 276:26605-26613.

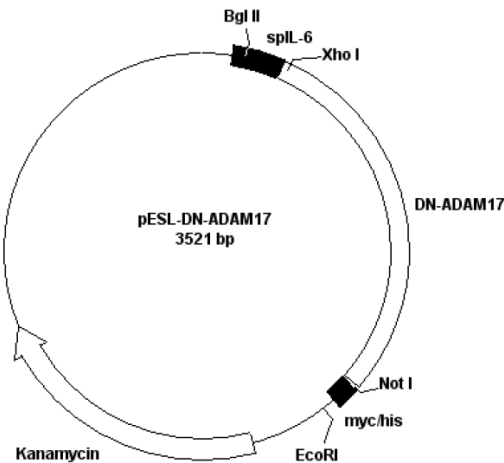
200. **Kuo, M. L., S. E. Chuang, M. T. Lin, and S. Y. Yang.** 2001. The involvement of PI 3-K/Akt-dependent up-regulation of Mcl-1 in the prevention of apoptosis of Hep3B cells by interleukin-6. *Oncogene*. 20:677-685.
201. **Bowman, T., M. A. Broome, and D. Sinibaldi.** 2001. Stat3-mediated Myc expression is required for Src transformation and PDGF-induced mitogenesis. *PNAS*. 98:7319-7324.
202. **Sinibaldi, D., W. Wharton, J. Turkson, T. Bowman, W. J. Pledger, and R. Jove.** 2000. Induction of p21WAF1/CIP1 and cyclin D1 expression by the Src oncoprotein in mouse fibroblasts: role of activated STAT3 signaling. *Oncogene*. 19:5419-5427.
203. **Catlett-Falcone, R., T. H. Landowski, M. M. Oshiro, J. Turkson, A. Levitzki, R. Savino, G. Ciliberto, L. Moscinski, J. L. Fernandez-Luna, G. Nunez, W. S. Dalton, and R. Jove.** 1999. Constitutive activation of Stat3 signaling confers resistance to apoptosis in human U266 myeloma cells. *Immunity*. 10:105-115.
204. **Zychlinsky, A., and P. Sansonetti.** 1997. Perspectives series: host/pathogen interactions: apoptosis in bacterial pathogenesis. *J. Clin. Invest.* 420:846-852.
205. **Hideshima, T., D. Chauhan, T. Hayashi, M. Akiyama, N. Mitsiades, C. Mitsiadis, K. Podar, N. C. Munshi, P. G. Richardson, and K. C. Anderson.** 2003. Proteasome inhibitor PS-341 abrogates IL-6 triggered signaling cascades via caspase-dependent downregulation of gp130 in multiple myeloma. *Oncogene*: 36: 8386-8393.
206. **McLoughlin, R. M., S. M. Hurst, and M. A. Nowell.** 2004. Differential regulation of neutrophil-activating chemokines by IL-6 and its soluble receptor isoforms. *J. Immunol.* 172:5676-5683.
207. **Müller-Newen, G., C. Kohne, R. Keul, U. Hemmann, W. Muller Esterl, J. Wijdenes, J. P. Brakenhoff, M. H. Hart, and P. C. Heinrich.** 1996. Purification and characterization of the soluble interleukin-6 receptor from human plasma and identification of an isoform generated through alternative splicing. *Eur. J. Biochem.* 236:837-842.
208. **McLoughlin, R. M., J. Witowski, R. L. Robson, T. S. Wilkinson, S. M. Hurst, A. S. Williams, J. D. Williams, S. Rose-John, S. A. Jones, and N. Topley.** 2003. Interplay between IFN-gamma and IL-6 signaling governs neutrophil trafficking and apoptosis during acute inflammation. *J. Clin. Invest.* 112:598-607.
209. **Gomez, M. I., S. H. Sokol, A. B. Muir, G. Soong, J. Bastien, and A. S. Prince.** 2005. Bacterial induction of TNF-alpha converting enzyme expression and IL-6/Ralpha shedding regulates airway inflammatory signaling. *J. Immunol.* 175:1930-1936.
210. **Nowell, M. A., P. J. Richards, S. Horiuchi, N. Yamamoto, S. Rose-John, N. Topley, A. S. Williams, and S. A. Jones.** 2003. Soluble IL-6 receptor governs IL-6 activity in experimental arthritis: blockade of arthritis severity by soluble glycoprotein 130. *J. Immunol.* 171:3202-3209.

211. **Klouche, M., S. Bhakdi, M. Hemmes, and S. Rose-John.** 1999. Novel Path of activation of primary human smooth muscle cells: upregulation of gp130 creates an autocrine activation loop by IL-6 and its soluble receptor. *J Immunol* 163:4583-4589.
212. **Marin, V., F. A. Montero-Julian, S. Gres, V. Boulay, P. Bongrand, C. Farnarier, and K. G.** 2001. The IL-6-soluble IL-6Ralpha autocrine loop of endothelial activation as an intermediate between acute and chronic inflammation: an experimental model involving thrombin. *J. Immunol.* 167:3435-3442.
213. **Müllberg, J., K. Althoff, T. Jostock, and S. Rose-John.** 2000. The Importance of Shedding of Membrane Proteins for Cytokine Biology. *Eur. Cyt. Netw.* 11:27-38.
214. **Rabe, B., A. Chalaris, D. Seegert, S. Rose-John, and J. Scheller.** 2007. Blocking IL-6-transsignaling in vivo effects in abrogation of inflammation. *Submitted.*
215. **Fattori, E., M. Cappelletti, P. Costa, C. Sellitto, L. Cantoni, M. Carelli, R. Faggioni, G. Fantuzzi, P. Ghezzi, and V. Poli.** 1994. Defective inflammatory response in interleukin 6-deficient mice. *J. Exp. Med.* 180:1243-1250.
216. **De Leo, F. R.** 2007. Attractive shedding. *Blood* 110:1711.

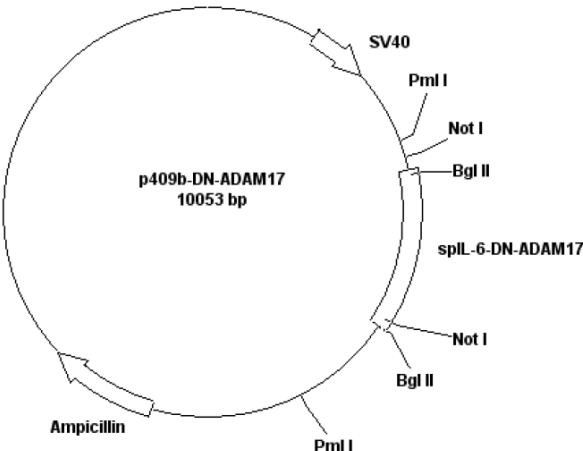
9 Appendix

9.1 Vector maps

A. pESL-DN-ADAM17



B. p409b-DN-ADAM17



9.2 Oligonucleotides

Nr.	Primer	Sequence (5`-3`)	Remarks
1	D-ADAM17-up	AGCAATAAAGTTTGTGGG	
2	D-ADAM17-dn	CAGT <u>GCGGCCGCGC</u> ACTTTGTTTCTTTGCTG	Not-I site

9.3 Accession numbers

Protein	Organism	Accession number
ADAM17	<i>human</i>	NM_003183
IL-6R	<i>human</i>	NM_000565

9.4 Abbreviations

A

A	Adenine
ADAM	A Disintegrin And Metalloprotease
APAF1	Apoptotic Protease Activating Factor 1
APC	Allophycocyanin
APS	Ammoniumperoxodisulfate
ATCC	<i>American Type Culture Collection</i>
ATP	Adenosine 5'-Triphosphate

B

BCA	Bicinchoninic Acid
bp	Base Pairs
BSA	Bovine Serum Albumine

C

C	Cytosine
CBM	Cytokine Binding Module
CD	Cluster of Differentiation
cDNA	Complementary DNA
CHX	Cycloheximide
CIAP	Calf Intestine Alkaline Phosphatase
CLC	Cardiotrophin-Like Cytokine
CNTF	Ciliary Neurotrophic Factor
CRP	C-Reactive Protein
CT-1	Cardiothropin-1

D

DEAE-Dextran	Diethylaminoethyl-Dextran
DISC	Death-Inducing Signaling Complex
DMEM	Dulbeccos Modified Eagle Medium
DMSO	Dimethylsulfoxide
DMTU	1,3-Dimethyl-2-Thiourea

DNA	Deoxyribonucleic Acid
dNTP	2'-Desoxyribonucleotide-5'-Triphosphate
DPI	Diphenyleneiodonium Chloride

E

EDTA	Ethylenediaminetetraacetic Acid
EGFP	Enhanced Green Fluorescent Protein
EGF	Epidermal Growth Factor
ELISA	Enzyme Linked Immunosorbent Assay
ERK	Extracellular Signal Regulated Kinase

F

FACS	Fluorescence Activated Cell Sorter
FADD	Fas-Associated Death Domain
FCS	Fetal Calf Serum
FITC	Fluorescein Isothiocyanate
FN III	Fibronectin Type III

G

x g	g-force
G	Guanosine
gp130	Glycoprotein 130
GPCR	G-protein Coupled Receptors
Grb2	Growth Factor Receptor Bound Protein 2

H

HB-EGF	Heparin Binding-Epidermal Growth Factor
HIL-6	Hyper-IL-6
HlyA	Hemolysin A

I

Ig-domain	Immunoglobulin-Domain
i.p.-injection	Intraperitoneal-Injection
IVC	Individually Ventilated Cages

J

JRA Juvenile Rheumatoid Arthritis

L

LB Lysogeny Broth

LIF Leukaemia Inhibitory Factor

M

MAPK Mitogen-Activated Protein Kinase

m β CD Methyl- β -Cyclodextrin

mg Milligram

μ g Microgram

N

NADPH Nicotinamide Adenine Dinucleotide Phosphate

NP Neuropoietin

nPG n-Propyl-Galleate

NSAID Non-Steroidal Anti-Inflammatory Drug

O

OD Optic Density

OSM Oncostatin M

P

PARP Poly ADP ribose polymerase

PBS Phosphate Buffered Saline

PC Phosphatidylcholine

PCR Polymerase Chain Reaction

PDK1 3-Phosphoinositide-Dependent Protein Kinase 1

PIAS Protein Inhibitors of Activated STAT

PKC Protein Kinase C

PMA Phorbol 12-Myristate 13-Acetate

PMN	Polymorphonuclear cells
PMSF	Phenylmethylsulfonylfluoride
p-STAT3	Phospho-STAT3
PVDF	Polyvinylidene Fluoride

R

RA	Rheumatoid Arthritis
RNA	Ribonucleic Acid
ROS	Reactive Oxygen Species
Rpm	Rounds Per Minute
RT-PCR	Reverse Transcriptase PCR

S

SD	Standard Deviation
SDS	Sodium Dodecyl Sulfate
SDS-PAGE	SDS-Polyacrylamide Gel Electrophoresis
sgp130	Soluble gp130
SH2-domain	Src Homology-2 Domain
SHP-2	Src homology protein 2 tyrosine phosphatase-2
sIL-6R	soluble IL-6R
SLO	Streptolysin O
SM	Sphingomyelin
SOCS	Suppressors Of Cytokine Signalling
SOS	Son Of Sevenless
STAT	Signal Transducers and Activators of Transcription
SVMP	Snake Venom Metalloproteinase

T

T	Thymine
TACE	Tumor Necrosis Factor-Alpha Converting Enzyme
TAPI	N-(R)-[2-(Hydroxyaminocarbonyl)Methyl]-4-Methylpentanoyl-L-t-Butyl-Alanyl-L-Alanine, 2-Aminoethyl Amide
TBE	Tris Borat EDTA
TBS	Tris Buffered Saline

Appendix

TEMED	N,N,N',N'-Tetramethylethylenediamine
TGF	Transforming Growth Factor
T _M	Melting Temperature
TNF	Tumor necrosis factor
U	
U	Units
UV	Ultraviolet
V	
v/v	Volume per Volume
vIL-6	Viral interleukin-6
VDAC	Voltage-Dependent Anion Channel
W	
w/v	Weight per Volume
WT	Wildtype

9.5 Publications

Chalaris, A., Rabe, B., Paliga, K., Lange, H., Laskay, T., Fielding, C.A., Jones, S.A., Rose-John, S. and J. Scheller. Apoptosis is a natural stimulus of IL6R shedding and contributes to the pro-inflammatory trans-signaling function of neutrophils, *Blood*, 2007, 110(6):1748-55

Rabe, B., **Chalaris, A.**, Seegert, D., Rose-John, S. and J. Scheller. Blocking IL-6-transsignaling *in vivo* effects in abrogation of inflammation, 2007, submitted

Stuhlmann-Laisz, C., Lang, S., **Chalaris, A.**, Sudarman, E., Eichler, J., Klingmüller, U., Samuel, M., Ernst, M., Rose-John, S. and J. Scheller. Forced dimerization of gp130 leads to constitutive STAT3 activation, cytokine independent growth and blockade of differentiation of embryonic stem cells, *Mol Biol Cell*, 2006, 17(7):2986-95

9.6 Curriculum vitae

Name:	Athena Chalaris
Geburtstag:	05.03.1979
Geburtsort:	Hamburg
Staatsangehörigkeit:	deutsch
2004 – 2007	Anfertigung der vorliegenden Arbeit in der Arbeitsgruppe von Prof. Dr. Rose-John am Biochemischen Institut der Christian-Albrechts-Universität zu Kiel
2003 – 2004	Diplomarbeit im Zentrum für Molekulare Neurobiologie Hamburg (ZMNH): „Suche und Charakterisierung von intrazellulären Bindungspartnern des multiplen PDZ-Domänen Proteins MUPP1“
2003	Diplomprüfungen im Studiengang Biologie an der Universität Hamburg in den Fächern Genetik/Molekularbiologie, Biochemie und Pharmazeutische Biologie.
2001–2003	Studienortswechsel an die Universität Hamburg
2000	Vordiplom im Studiengang Biologie an der Universität Kiel
1998 – 2000	Beginn des Biologiestudiums an der Christian-Albrechts-Universität zu Kiel
1994-1998	Übergang zum Dörpheld-Gymnasium in Athen, Abitur 1998
1989-1998	Übergang zum Humboldt-Gymnasium in Kiel
1979 – 1983	Einschulung in Kiel

Danksagung

Sehr herzlich bedanken möchte ich mich bei Herrn Professor Rose-John, der mich während meiner Zeit in Seinem Institut fachlich wie auch persönlich sehr unterstützt und gefördert hat. Außerdem möchte ich Ihn für die Freiheit bei der Ausgestaltung dieser Arbeit und Seinen zügig vorgenommenen Korrekturen danken.

Besonderer Dank gilt auch Herrn Dr. Jürgen Scheller für die Betreuung dieser Promotion und die interessanten wie auch unterhaltsamen und intensiven Diskussionen. Nicht zu vergessen ist die schnelle und hilfreiche Korrektur und Durchsicht dieser Arbeit.

Besonders möchte ich mich auch bei Herrn Professor Schulz-Friedrich bedanken für die Übernahme des Zweitgutachtens dieser externen Promotion.

Bei Krzysztof Paliga und Ulrich Klostermeyer (Ulle) bedanke ich mich für die ausgesprochen kreative Zusammenarbeit.

Bei meinen Laborkollegen Björn Rabe, Jessica Gewiese, Claudia Drücker, Jan Suthaus, Michaela Jahn, Marc Schulte, Andrea Rittger und Alex Schneede möchte ich mich für die freundschaftliche und lustige Zusammenarbeit im Labor bedanken, ohne die manches sicherlich wesentlich schwerer zu ertragen gewesen wäre. Ich bin wirklich froh, dass es euch gibt. Bei meinen Ex-Laborkollegen Björn Schuster, Alex Schulte, Marina Kovaleva und Ingo Bußmeyer möchte ich mich für die intensive Starthilfe bedanken.

Bedanken möchte ich mich außerdem bei Radek Sedlacek sowie Inken Beck für die wertvollen Tipps zum Umgang mit Mäusen und die netten Feiern (Hoch die Tassen).

Danke Moktsch (Michael Schwarz).

Vielen, vielen, vielen Dank Georgios für Deine Unterstützung und Liebe in den letzten drei Jahren. Dich laß ich nicht mehr los.

Paola, Mama, Omi, Papa, Dolce; Ihr seid dieGrößten. Vielen Dank für Alles.

Eidesstattliche Erklärung

Hiermit versichere ich, Athena Chalaris, an Eides statt, dass ich die vorliegende Arbeit selbstständig und nur mit Hilfe der angegebenen Hilfsmittel und Quellen unter Anleitung meiner akademischen Lehrer angefertigt habe.

Diese Dissertation wurde bisher an keiner anderen Fakultät vorgelegt.

Ich erkläre, kein anderes Promotionsverfahren ohne Erfolg beendet zu haben und dass keine Aberkennung eines bereits erworbenen Doktorgrades vorliegt.

Kiel, den 23.10.2007

Athena Chalaris